Auswirkungen einer Immuntherapie auf die Angiogenese in Tumoren und Psoriasis

Effects of immune therapy on angiogenesis in tumours and psoriasis

DISSERTATION

der Fakultät für Chemie und Pharmazie

der Eberhard-Karls-Universität Tübingen

zur Erlangung des Grades eines Doktors

der Naturwissenschaften

2008

vorgelegt von

Alexandra Ziegler

Tag der mündlichen Prüfung: 28.05.2008

Dekan:	Prof. Dr. L. Wesemann
1. Berichterstatter:	Prof. Dr. med. M. Röcken
2. Berichterstatter:	Prof. Dr. S. Stevanovic

To my mother

Acknowledgments

I would like to thank:

Prof. Dr. Martin Röcken for giving me the opportunity to work in his laboratory and the financial and scientific support to write my dissertation. The very interesting research field, the good working conditions, and the high degree of trust made this work possible.

Dr. Regina Heidenreich, head of the project group, for her scientific support, advice, and discussions throughout my thesis.

Prof. Stefan Stevanovic for being my supervisor at the faculty of chemistry at the university of Tübingen. His support enabled this external dissertation.

Prof. Dr. Hartwig Wolburg for performing the electron microscopy analysis.

All the people in the lab which were always helpful in matters of discussing problems of every description and giving a hand in the lab: Susanne Weidemann, Ivana Glocova, Jeanette Wagener, York Kamenisch, Koming Chen, Katrin Schaak, Dr. Günther Weindl, Dr. Heidi Braumüller, Dr. Kamran Ghoreschi, Dr. Susanne Kaessler and Dr. Thomas Volz.

Dr. Jürgen Brück for helping me with everything accumulating in everyday life, resulting in long-lasting discussions in several locations, long nights out, and finally in reading the manuscript of the thesis.

Maria Junginger, Martin Judenhofer, and Dr. Winfried Schuller for looking through the manuscript and giving me a lot of advice.

My mother and my partner Markus Eitel who were backing me all the way and kept faith with me, most notably during all the time I was ill and in hospital. I am very thankful for their patience and understandig, especially lately.

Finally, all my friends outside the lab I always can rely on.

Table of contents

Abbreviations

A	Ampere
ABC	Avidin-biotin complex
ACT	Adoptive T cell therapy
ADCC	Antibody-dependent cellular cytotoxity
AEC	3-Amino-9-ethyl carbazole
Ang	Angiopoietin
APC	Antigen presenting cells; Allophycocyanin
bFGF	Basic fibroblast growth factor
BM	Bone marrow
Bp	Base pairs
BrdU	5-Bromo-2'-deoxyuridine
BSA	Bovine serum albumin
CAM	Chick choreoallantoic membrane
CD	Cluster of differentiation
$CD4^+$	CD4 positive T cell
$CD8^+$	CD8 positive T cell
cDNA	Complementary DNA
CIA	Collagen-induced arthritis
CMV	Cytomegalovirus
Cp	Crossing point
CpG	Cytosine-phosphorothioate-guanine
CTL	Cytotoxic T lymphocytes
CTLA	Cytotoxic T lymphocyte-associated antigen
Da	Dalton
DAB	3,3'-Diaminobenzidine
DABCO	Triethylendiamine; 1,4-Diazabicyclo[2.2.2]octane
DC	Dendritic cells
DMEM	Dulbecco's modified Eagles Media
DMF	Dimethylfumarate
DMSO	Dimethyl sulfoxide
DNA	Deoxyribonucleic acid
dNTPs	Deoxyribonucleoside triphosphates
dsDNA	Double-stranded DNA

DTHR	Delayed type hypersensitivity reaction
DTT	Dithiothreitol
EAE	Experimental autoimmune encephalomyelitis
Ebi3	EBV-induced gene
EBV	Epstein-Barr virus
EC	Endothelial cells
ECGS	Endothelial cell growth supplement
ECM	Extracellular matrix
EDTA	Ethylene diamine tetraacetate
ELISA	Enzyme-linked immunosorbent assay
EpCAM	Epithelial cell adhesion molecule
ERK	Extracellular signal-regulated kinase
ESAF	Endothelial cell stimulating angiogenesis factor
FACS	Fluorescence activated cell sorting
FAE	Fumaric acid esters
FCS	Fetal calf serum (heat-inactivated)
FITC	Fluorescein isothiocyanate
Flk-1	Fetal liver kinase-1
Flt	Fms-like tyrosine kinase
g	Gravity
GAPDH	Glyceralehyde-3-phosphate dehydrogenase
GPx-1	Glutathione peroxidase-1
GSH	Glutathione
GSH-OEt	Glutathione monoethyl-glycyl ester
Gy	Gray
h	Hour(s)
Her2/neu	Human epidermal growth factor receptor
HIF	Hypoxia-inducible factor
HIV	Human immunodeficiency virus
HLMEC	Human lung-derived microvascular endothelial cells
HPRT	Hypoxanthine-guanine phosphoribosyltransferase
HRPO	Horseradish peroxidase
HUVEC	Human umbilical vein endothelial cells
Hz	Hertz
ICAM	Intracellular adhesion molecule

IF	Immunofluorescence
IFN	Interferon
Ig	Immunoglobulin
IHC	Immunohistochemistry
IL	Interleukin
IP-10/CXCL10	Interferon-inducible protein
kb	Kilo bases
KDR	Kinase insert domain receptor
KLH	Keyhole limpet hemocyanin
l	Litre
LN	Lymphnode
M	Molar
mAb	monoclonal antibody
MAPK	Mitogen-activated protein kinase
MAR	Mouse anti-rat antibody
MCA	Methylcholanthrene
MHC	Major Histocompatibility Complex
MHF	Methylhydrogenfumarate
Mig/CXCL9	Monokine-induced by IFN-γ
min	Minute
MMP	Matrix metalloproteinase
Moviol	Polyvinylalcohol 4-88
NAC	N-Acetylcysteine
NADPH	Nicotinamide adenine dinucleotide phosphate
NFκB	Nuclear factor-kappa B
NK	Natural killer
NO	Nitric oxide
NOS	Nitric oxide synthase
OD	Optical density
ODN	Oligodeoxynucleotides
OVA	Ovalbumin
p	Passage
PAGE	Polyacrylamide gel elektrophoresis
PAI-1	Plasminogen activator inhibitor-1
PBS	Phosphate buffered saline

PBST	Phosphate buffered saline containing Tween 20
PCR	Polymerase chain reaction
PDGF	Platelet-derived growth factor
PE	Phycoerythrin
PECAM-1	Platelet endothelial cell adhesion molecule (CD31 antigen)
Pen/Strep	Penicillin/Streptomycin
PFA	Paraformaldehyde
PI	Propidium iodide
PI3K	Phosphoinositide 3 kinase
PIGF	Placental growth factor
PMA	Phorbol 12-myristate 13-acetate
PMSF	Phenylmethanesulfonyl fluoride
PS	Phospholipid phoshatidyl serine
PVDF	Polyvinylidene difluoride
RNA	Ribonucleic acid
ROS	Reactive oxygen species
rpm	Revolutions per minute
RT	Room temperature; reverse transcriptase
RT-PCR	Real-time polymerase chain reaction
SAPK	Stress-activated protein kinase
SD	Standard deviation
SDS	Sodium dodecyl sulfate
SEM	Standard error of the mean
SOD	Superoxide dismutase
T_{reg}	Regulatory T cells
TAA	Tumour-associated antigen
TAE	Tris acetate EDTA-buffer
TCR	T cell receptor
TEMED	*N,N,N',N'*-tetramethyl-ethane-1,2-diamine
TGF-β	Transforming growth factor-β
Th	T helper
Tie	Tyrosine kinase with immunoglobulin-like and EGF-like domains
TLR	Toll-like receptor
TNF	Tumour necrosis factor

Tris	Trishydroxymethylaminomethane; 2-Amino-2-hydroxymethyl-propane-1,3-diol
TSP-1	Thrombospondin-1
Tween 20	Polysorbate 20; Polyoxyethylene (20) sorbitan monolaurate
U	Unit
uPA	Urokinase plasminogen activator
UV	Ultraviolet
V	Volt
VCAM	Vascular cell adhesion molecule
VE-cadherin	Vascular endothelial cadherin
VEGF	Vascular endothelial growth factor
VEGFR	Vascular endothelial growth factor receptor
VEGI	Vascular endothelial growth inhibitor
WT	Wildtype
% (v/v)	Percent by volume
% (w/v)	Percent by weight

1 Introduction

1.1 Angiogenesis

During embryonic development new blood vessels are formed by vasculogenesis and angiogenesis as the growing embryo requires oxygen and the transport of nutrients and waste [1-4]. During vasculogenesis a primitive vascular network develops in the embryo by *in situ* differentiation of endothelial cells (EC) from endothelial precursor cells (angioblasts), proliferation, and the assembly of EC into blood vessels including the aorta and major veins [1, 5]. Subsequent formation of new capillaries by sprouting or splitting from their vessel of origin (angiogenesis and intussusception) and remodeling are finally leading to a mature cardiovascular system, the first functional organ system in the embryo [1, 2, 4, 6, 7].

In the adult, vessels arise mainly through angiogenesis, describing the development of new capillaries from pre-existing blood vessels [2, 3, 8]. Physiologically, angiogenesis only occurs in the female reproductive system, hair growth, and wound healing [9, 10]. Under pathological situations such as chronic inflammatory processes the quiescent vasculature is activated and new capillaries grow [2, 8, 11]. Abnormal vascular growth contributes to cancer and numerous non-neoplastic disorders such as psoriasis, rheumatoid arthritis and retinopathies, or may result from tissue ischemia [6, 9, 12].

Several steps in angiogenesis have been determined (Fig. 1): 1) Proteolytic degradation of the extracellular matrix (ECM), 2) chemotactic migration and proliferation of EC, 3) formation of vascular tube structures and functional remodelling of the endothelium [2, 13]. In the following, these steps are described more in detail.

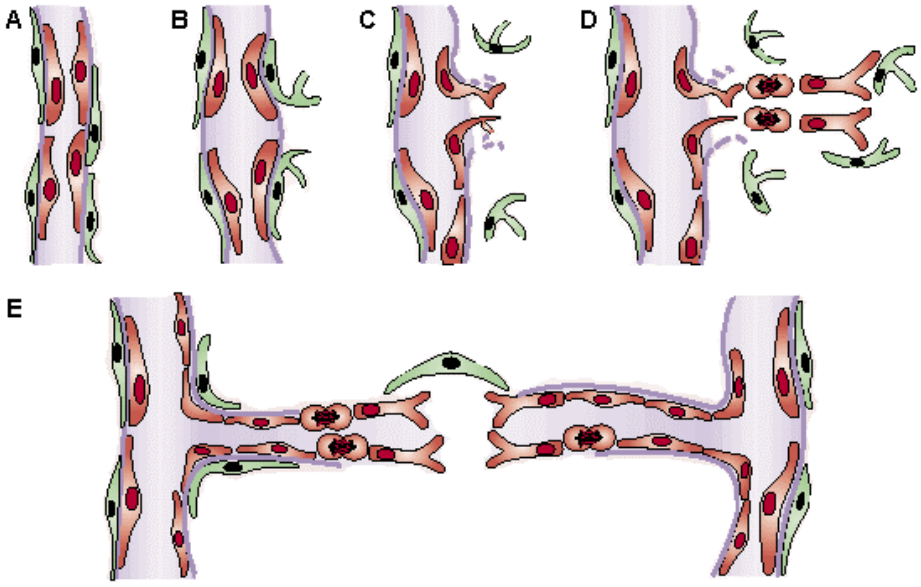

Figure 1. New blood vessel formation. A, During angiogenesis blood vessels arise from pre-existing capillaries or post-capillary venules. B, Pericytes (green) detach and blood vessels dilate before proteolytic degradation of the extracellular matrix. C, Chemotactic migration of endothelial cells (red) towards angiogenic stimuli into the perivascular space is facilitated. D, Endothelial cells proliferate, loosely following each other. E, Endothelial cells adhere to each other, create a lumen, and build a new circulatory system. Finally, blood vessels need to be functionally remodelled (modified from Bergers [13]).

1.1.1 The VEGF and angiopoietin family

Mechanistically, the vascular endothelial growth factor (VEGF)/VEGF receptor system is required for embryonic development [7, 12, 14-18] and together with the angiopoietin (Ang)/Ang receptor system continues to play a critical role during subsequent angiogenesis [19-23].

The VEGF family of growth factors consists of several homologues in mammals: VEGF-A [24], VEGF-B [25], VEGF-C [26], VEGF-D [27], and the placental growth factor (PIGF) [28]. Another homologous polypeptide has been found in the genome of the orf virus, a parapoxvirus, named VEGF-E [29]. The VEGFs mediate cellular responses by different high-affinity endothelial receptor tyrosine kinases: VEGF receptor (VEGFR)-1/fms-like tyrosine kinase (Flt)-1 [30], VEGFR-2/fetal liver kinase (Flk)-1 in mice [31], respectively kinase insert domain receptor (KDR) in human [32], VEGFR-3/Flt-4 [33] and the collapsin/ semaphorin receptors neuropilin-1 and neuropilin-2 (co-receptors of VEGFR-2)

[34, 35]. The most important receptor of angiogenesis is VEGFR-2 which is activated by VEGF-A and VEGF-B [24].

The second family of growth factors are the angiopoietins. Three members have been discovered in mice, Ang-1 to Ang-3, and additionally Ang-4 in humans [12, 20, 36]. Ang-1 and Ang-2 differ in their expression pattern during vasculogenesis [19, 21] and angiogenesis [2] and bind primarily to the receptor tyrosine kinase with immunoglobulin-like and EGF-like domains (Tie)-2 [14]. Ligands for the highly homologous receptor Tie1 have not yet been identified [23, 37].

1.1.2 Degradation of the extracellular matrix

Before EC can migrate from their pre-existing site, mature vessels need to be destabilised to become sensitive for the activity of growth and survival signals [3]. Therefore, VEGF induces phosphorylation of the junctional molecule vascular endothelial (VE)-cadherin [38], weakening interendothelial cell contacts. Moreover, periendothelial cells and smooth muscle cells are detached from the vessel. Ang-2 may be involved in this process [3, 19]. Vasodilation and increased vascular permeability in response to VEGF enable the extravasation of plasma proteins which form a matrix for migration of activated EC [3, 39]. Moreover, platelet endothelial cell adhesion molecule (PECAM)-1 (CD31) [40] and VE-Cadherin [38] are redistributed and fenestrations and ‘vesiculo-vacuolar organelles’ are formed, contributing to the increase in vascular permeability [3]. Then, the ECM is proteolytically degraded by proteinases of the chymase or heparanase families, the urokinase plasminogen activator (uPA), and matrix metalloproteinases (MMP) [3, 15, 41]. MMPs can degrade most components of the vascular basement membrane and the interstitial matrix such as collagen, laminin, fibronectin, and elastin [42]. This contributes to the release of growth factors sequestered within the ECM, promoting angiogenesis [43]. At the same time, activated EC secrete proteinase inhibitors such as plasminogen activator inhibitor-1 (PAI-1) to locally define this degradation [41, 44].

1.1.3 Endothelial cell proliferation and migration

Once the ECM has been degraded and a perivascular space is created, EC proliferate, elongate, and migrate towards angiogenic stimuli such as VEGF-A [45]. Moreover, angiogenic sprouting is activated by Ang-1 which furthermore potentiates VEGF [22, 46]. αvß3 integrin, a cell-matrix receptor for ECM constituents such as vitronectin, fibronectin, fibrinogen, or osteopontin, mediates adhesion of EC to ECM to enable migration and cell spreading [6, 47-49]. A balance of activators and inhibitors controls angiogenic sprouting [3, 13]. Thus, angiogenic inhibitors such as angiostatin (an internal fragment of plasminogen) [50] or endostatin (a fragment of collagen XVIII) [51] can restrain the proliferation and/or migration of EC [3].

Furthermore, the VEGF-induced EC proliferation requires mitogen-activated protein kinase (MAPK)- and phosphoinositide 3 kinase (PI3K)-dependent signals [52]. MAPKs are a widely conserved family of serine/threonine protein kinases that regulate multiple cellular activities such as cell differentiation, proliferation, migration, and death. For example, the extracellular signal-regulated kinase (ERK)1/2 or (p44/p42)-MAPK signalling pathways control the expression of cell-cycle regulated genes and responds to several distinct extracellular stimuli including cytokines, growth factors, and mitogens [53, 54]. The p38 MAPK or stress-activated protein kinase (SAPK)-2 is activated by phosphorylation and acts in a signalling cascade that controls cellular responses to inflammatory cytokines and environmental stress such as ultraviolet (UV) light and osmotic shock [53, 55]. Another key role in regulating cell growth and proliferation plays the PI3K target mTOR, a serine/threonine protein kinase which also acts as a sensor of nutrient levels [56-58].

1.1.4 Vascular tube formation and functional remodelling

The EC form a migration column and adhere to each other to form a lumen and loops [13]. Continued proliferation of EC leads to an increase of vessel diameter and length which is induced by Ang-1 in combination with VEGF [3, 13, 22, 59]. Integrins such as αvβ3 support this lumen formation [48], whereas thrombospondin (TSP)-1 is an endogenous inhibitor [3]. If capillaries merge or additional EC join existing vessels, this process is called intercalated growth or

non-sprouting angiogenesis [7]. This process was first described in the embryonic lung [60] and is important for vessel growth in the heart and during healing of endothelial wounds [7, 15]. If vessels are split by pillars of the capillary wall, this process of blood vessel formation is called intussusceptive growth [2, 60, 61].

All vessels formed are initially immature and must further develop [12]. For stability, vessels get surrounded by pericytes or smooth muscle cells which stimulate the re-establishment of the ECM [3, 62]. Proteinase inhibitors (for example PAI-1) prevent degradation of the provisional ECM around developing vessels [6]. Signalling by transforming growth factor-β1 (TGF-β1) and Ang-1/Tie2 stabilises the interaction between endothelial and smooth muscle cells and therefore protects vessels against damage [6, 22, 62]. After the onset of blood circulation, smooth muscle cells provide blood vessels with viscoelastic and vasomotor properties that are important to adapt to changes in the blood pressure [3, 7].

1.1.5 Endothelial cell survival

EC become quiescent once they are integrated in new vessels and survive for years [3], as they are among the longest-living cells in the body aside cells of the central nervous system [11]. In the adult, under normal physiological conditions, EC have a low turnover [63, 64] and only 0.01% of EC are undergoing division [6, 11]. Nevertheless, vessel regression which occurs in the retina and ovary after birth is caused by endothelial apoptosis [3, 65]. The lack of nutrients or survival signals, the increase of nitric oxide (NO) and reactive oxygen species (ROS), a blocked lumen, and angiogenic inhibitors such as angiostatin and vascular endothelial growth inhibitor (VEGI) can all induce endothelial apoptosis [2, 3, 17, 65]. VEGF, depending on the interaction between VEGFR-2, β-catenin and VE-cadherin [66], and Ang-1 act, whereas Ang-2 counteracts, as endothelial survival factors [3, 14, 59]. αvβ3 is a survival factor for angiogenic but not quiescent EC as it is only expressed in proliferative cells [3, 7, 47, 67].

1.2 Tumour angiogenesis

Already 100 years ago, angiogenesis was observed around tumours [68, 69]. Like normal tissue, tumours require oxygen and nutrients for their survival and therefore need blood vessel structures with capillaries at a mean distance of 100 to 200 µm - the diffusion limit for oxygen. Blood vessels enable tumours to grow beyond a critical size and to metastasise to another organ such as lung and liver [6, 70].

There are two distinct concepts of early tumour vascularization which have provoked significant debates, the avascular growth of tumours and the co-option concept, both outlined below (Fig. 2) [71].

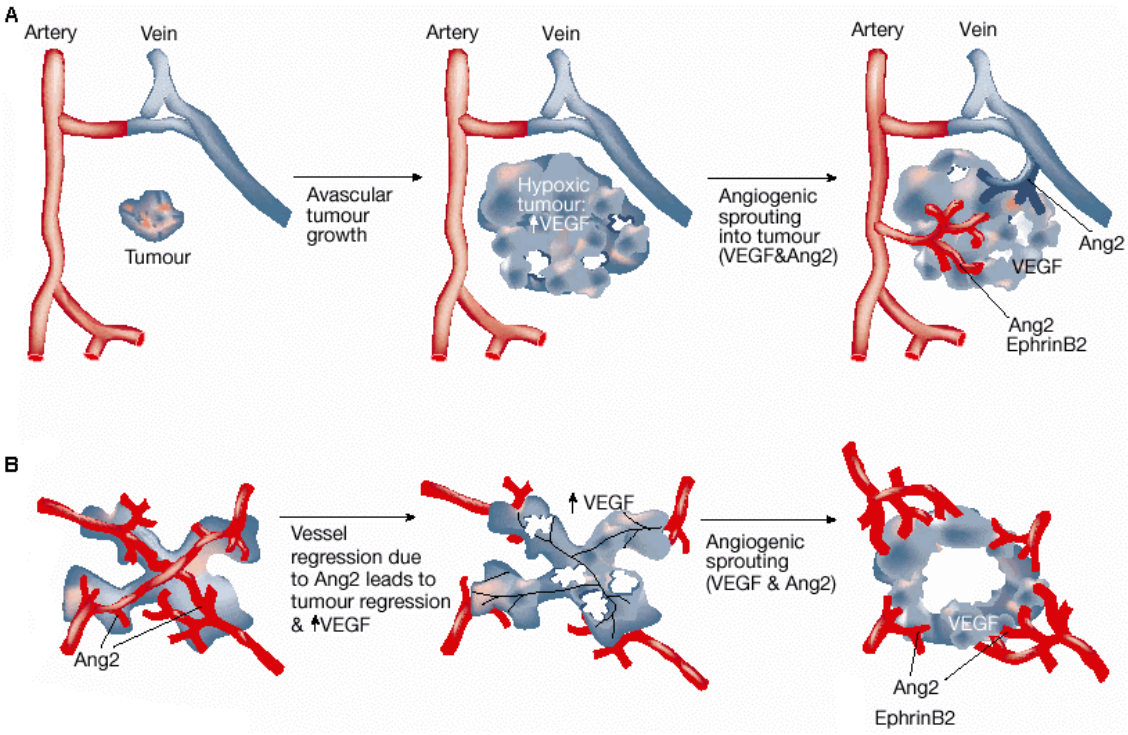

Figure 2. Models of tumour angiogenesis. A, Model of avascular tumour initiation. B, Tumour initiation involving host vessel co-option (according to Yancopoulos [12]).

The avascular tumour initiation has become widely accepted, as many primary tumours and metastases arise avascularly and only later induce their vascularization [11, 12, 72, 73]. This principle has been confirmed in many model systems, whereby tumour cells were injected in a subcutaneous pouch or in another avascular site such as the cornea pocket [11, 74], thus requiring angiogenesis for further growth. Through these experiments it has been

considered that the critical size at which tumours switch to an angiogenic phenotype is 1-2 mm [13, 41, 73]. Through the fast tumour growth local tissue hypoxia is induced. This is leading to an upregulation of VEGF expression in tumour cells and stroma which in turn stimulates, together with Ang-2, the growth of blood vessels by sprouting or intussusception [75-78].

The other concept describes that tumours initiate vascularly without inducing angiogenesis as they co-opt preexisting host blood vessels [12, 73]. Then, host vessels start to express high autocrine levels of Ang-2 and the co-opted vessels get apoptotic so that the tumour becomes secondarily avascular and hypoxic [12, 79, 80]. Hence, tumour-derived VEGF is induced and angiogenesis is stimulated, allowing further tumour growth [12, 79, 80].

1.2.1 The angiogenic switch

Cancer cells begin to promote angiogenesis early in tumourigenesis by producing a ‘diffusible angiogenic substance’ later defined as VEGF [6, 81, 82] and hence, tumour growth and metastasis have been proposed to be ‘angiogenesis-dependent’ [6, 72]. Activation of angiogenesis occurs in a process called the angiogenic switch which is associated with an imbalance of pro- and antiangiogenic molecules (Fig. 3) [11, 71]. On the one hand, proangiogenic factors such as VEGF, basic fibroblast growth factor (bFGF), interleukin-8 (IL-8), or PIGF are upregulated. On the other hand, angiogenesis suppressors such as TSP-1 are downregulated [11, 83]. Further signals triggering this switch include immune/inflammatory response mechanisms, mechanical and metabolic stress such as pressure or low pO_2, and genetic mutations [6, 13].

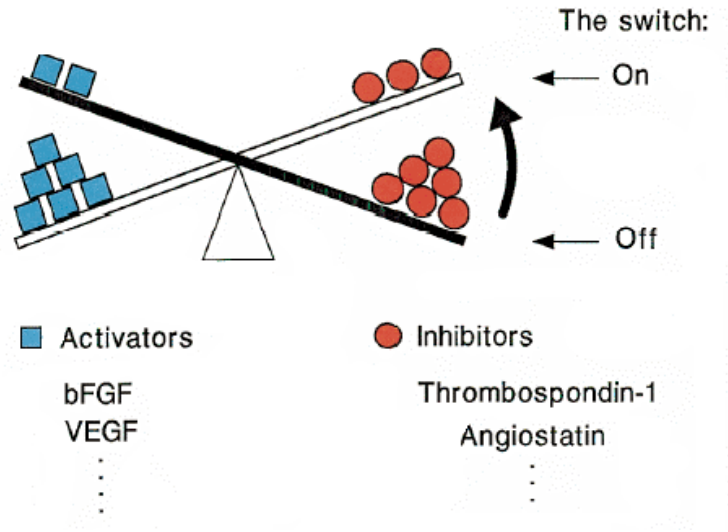

Figure 3. The balance hypothesis for the angiogenic switch. Angiogenesis is activated by an angiogenic switch mechanism which is associated with an imbalance of pro- and antiangiogenic molecules. The switch may be kept off through the absence of angiogenesis inducers while in others higher levels of angiogenesis inhibitors retain the effects of angiogenesis inducers. Thus, either increasing the activator levels (e.g. induction of VEGF by hypoxia) or reducing the inhibitor concentration (e.g. of TSP-1) can change the balance and activate the angiogenic switch leading to the growth of new blood vessels (according to Hanahan [11]).

1.2.2 Structure and function of tumour vessels

In contrast to the normal, organised vessel network, tumour vasculature is unstructured, dilated, and leaky as tumour vessels mostly lack a protective coat of perivascular cells and smooth muscle cells, have widened interendothelial junctions and numerous ‘openings’ [6, 13, 39, 84, 85]. Moreover, vessels are tortuous and have an unsteady diameter, leading to an irregular blood flow, resulting in hypoxic and acidic regions in the tumour [6, 13]. In addition, vessels may be lined by multiple layers of EC [6, 13] and cancer cells can be integrated into the vessel wall (‘vasculogenic mimicry’) [86-89].

1.3 Angiogenesis in non-neoplastic diseases

Hypoxia and inflammation contribute to angiogenesis in non-neoplastic diseases such as psoriasis or diabetes, in that vessels do not grow but rather abnormally remodel [6, 90, 91].

1.3.1 Hypoxia-induced angiogenesis

Hypoxia is a strong stimulus for angiogenesis in numerous disorders such as wounds or atherosclerotic plaques, diabetes, Alzheimer's disease, and asthma [6, 90]. Hypoxia-inducible factor (HIF)-1 is a transcription complex which is composed of HIF-1α and HIF-1β subunits. During normoxia the von Hippel-Lindau tumour suppressor gene product regulates the HIF system by oxygen dependent degradation of HIF-1α [3]. Once hypoxia occurs, the degradation of HIF-1α is interrupted, HIF translocates into the nucleus and upregulates the expression of VEGF, VEGFR-1, VEGFR-2, neuropilin-1, Ang-2, nitric oxide synthase (NOS), tumour necrosis factor (TNF), TGF-β1, IL-8, and other target genes [3, 6, 90].

1.3.2 Inflammation-induced angiogenesis

Prolonged and excessive angiogenesis is a distinct feature of chronic inflammatory disorders in many organs such as rheumatoid arthritis, asthma, psoriasis of the skin and joints, and also in cancer [6, 91, 92]. Several leukocytes including monocytes, macrophages, mast cells, and others release a variety of angiogenic factors including VEGF, Ang-1, TGF-α/β, TNF-α or platelet-derived growth factor (PDGF), various interleukins such as IL-1, IL-6, and IL-8, and cytotoxic mediators including ROS and proteinases [4, 6, 93, 94]. Wound cells such as endothelial and smooth muscle cells, fibroblasts, leukocytes, or platelets are attracted by some of these factors and produce additional angiogenic factors [6]. Morever, during inflammation, but in the absence of angiogenesis, vasodilation and increased permeability can be strong pathogenic mechanisms [6].

1.4 Immunotherapy

Generation of a protective immunity against different diseases is the classical aim of immunotherapy. In active immunotherapy, therapeutic immunity is triggered by antigen administration using adjuvants such as immunostimulatory cytosine-phosphorothioate-guanine (CpG) containing DNA or the keyhole limpet hemocyanin (KLH) [95]. In passive immunotherapy, *ex vivo* generated, specific T cells are adoptively transferred [95, 96]. Moreover, monoclonal antibodies directed against cell surface antigens such as the human epidermal growth factor receptor (Her)2/neu, the human epithelial cell adhesion molecule EpCAM (CD326), or other target antigens are applied in immunotherapy [95, 97]. These antibodies directly target cancer cells by complement mediated cytolysis and can be conjugated with toxins, radionuclides or chemotherapeutic drugs [98]. Moreover, the antibody-dependent cellular cytotoxity (ADCC) mediated by natural killer (NK) cells results in apoptosis of cancer cells [98].

1.4.1 Active immunotherapy

Active immunisation or vaccination with major histocompatibility complex (MHC) class I-restricted tumour antigens is used in tumour immune therapy of mice and humans, but still, the therapeutic effect is limited [99-101]. It has been described that vaccination efficiency can be improved by tumour antigen-loaded dendritic antigen presenting cells (APC) and genetically modified tumour cells [99, 100, 102]. Moreover, stimulating T cells through CD28/CTLA-4 (cytotoxic T lymphocyte antigen-4) or increasing $CD4^+$ T helper (Th) cell activity can increase vaccination effectiveness, but altogether these approaches raise the risk that autoimmune disease may occur [99]. Moreover, vaccination with tumour antigens following an adoptive cell transfer may enhance therapeutic efficiency in mouse models of tumour therapy [103, 104].

1.4.2 Passive cellular immunotherapy

At the moment, adoptive T cell therapy (ACT) is studied for the treatment of both, infectious (cytomegalovirus (CMV), human immunodeficiency virus (HIV), Epstein-Barr virus (EBV)) and malignant (melanoma, leukemia) diseases in

humans [95, 105-111]. In mouse models, tumour-specific T cells, after *ex vivo* activation, expansion, and selection, are adoptively transferred into tumour bearing mice for the treatment of established experimental tumours [106]. This approach has been extensively analysed and was shown to be very successful in tumour therapy [95, 103, 104, 106, 112-115]. Through therapy of transplanted syngeneic tumours with splenocytes from immunised mice in early ACT studies, the characteristics of transferred T cells were defined [106]. Nowadays, most studies use T cell receptor (TCR)-transgenic mouse models in order to study the exact mechanisms by which T cells eliminate large established tumours [96, 103, 106, 116, 117].

1.4.3 $CD4^+$ and $CD8^+$ T cells in ACT

$CD4^+$ and $CD8^+$ T cells detect tumour cells through the recognition of MHC-I and MHC-II-restricted tumour-specific antigens by the TCR [118, 119]. Through changes in the cell metabolism, multiple tumour-associated antigens are expressed during the development of malignant tumours [118, 119].

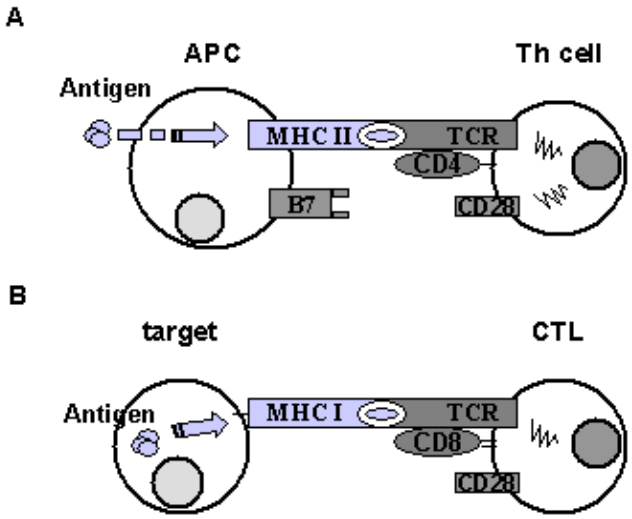

Figure 4. Activation of T effector cells. A, Th cells express the T cell receptor and the CD4 co-receptor and recognize antigens which are presented on MHC class II molecules on the cell surface of antigen presenting cells. A second signal for activation of Th cells is provided by the co-stimulatory molecules CD28 and B7 (CD80/CD86). B, Cytotoxic T lymphocytes (CTL) express the TCR and the CD8 co-receptor. They recognize target cells which present cytosolic antigens on their surface MHC class I molecules (modified from Janeway [120] and Jung [121]).

1.4.3.1 Immunotherapy with CD8$^+$ T cells

CD8$^+$ T cells recognize target antigens from intracellular proteins presented in an MHC class I-restricted manner and thus may activate tumour-specific CD8$^+$ T cells [118, 122]. Exogenous antigens may also be presented by MHC class I molecules on bone marrow (BM)-derived APC a process that is called crosspresentation [122, 123]. Moreover, CD8$^+$ cytotoxic T lymphocytes (CTL) have the ability to lyse tumour cells by direct cell-to-cell contact [122, 124]. Accordingly, it has been shown that CTL are effective in rejecting implanted tumours, even in the absence of CD4$^+$ T cells [111, 125-128]. Surprisingly, most transfer experiments with TCR transgeneic CD8$^+$ T cells were ineffective without the addition of other help mechanisms [125, 128-132]. Nevertheless, most adoptive transfer studies keep on focusing on tumour-specific CD8$^+$ T cells [129].

1.4.3.2 Immunotherapy with CD4$^+$ T cells

Antigens presented by MHC class II molecules on APC are recognized by CD4$^+$ T cells [118, 122]. Although many class II peptides could be characterised from primary solid tumours, so far, only a few MHC class II-restricted tumour-specific antigens have been identified as highly immunogenic peptides [133-136]. CD4$^+$ T cells can directly lyse tumour cells expressing MHC class II in the rare case of lymphomas [99, 137]. Yet, most tumours are MHC class II negative [134]. Nevertheless, over the last 30 years several experiments have shown that CD4$^+$ T cells themselves can control tumours in a dose dependent manner and almost completely independently of CD8$^+$ T cells [99, 115, 117, 122, 129, 138-140]. Surprisingly, it was demonstrated that CD4$^+$ T cells are even more effective than CD8$^+$ T cells in eliminating several different tumours, even when the lytic activity of CD4$^+$ T cells against tumour cells *in vitro* or *in vivo* was very low and tumour cells lacked MHC expression [129, 141, 142]. Although the CD4$^+$ T cells could act independently of CD8$^+$ T cells [129], it was essential that they did interact with other host cells, in particular with NK cells [99, 117, 141] or macrophages [117, 129, 139, 143, 144]. These data suggest that CD4$^+$ T cells may be potent effector cells that are able to reject a broad range of tumours. However, current studies keep on analysing tumour-specific CD4$^+$ T cells mainly for their role in helping CTL to kill tumour cells [123, 129, 140, 145].

1.4.3.3 $CD4^+$ T cells in the antitumour immune response

$CD4^+$ T cells have several functions in the development of an antitumour response but it still remains elusive how $CD4^+$ T cells control tumour growth [117, 122]. During the priming phase of an immune response $CD4^+$ T cells provide costimulatory signals for the priming of MHC class I-restricted $CD8^+$ CTL and help CTL to develop [122, 145]. APC may present tumour antigens in the context of MHC class II molecules to tumour-specific $CD4^+$ T cells leading to a reciprocal activation of APC and T cells by CD40/CD40L interactions what is necessary for further CTL crosspriming [117, 122, 140, 146, 147].

Moreover, $CD4^+$ T cells are required in the effector phase of an antitumour immune response [122]. This was shown by depletion studies [113, 122, 139] and by adoptive transfer experiments [138, 139], demonstrating that tumour rejection required $CD4^+$ T cells. It has been proposed that memory $CD4^+$ T cells are activated by APC and induce a delayed type hypersensitivity reaction (DTHR) [148]. Consequently, through the release of cytokines, $CD4^+$ T cells recruit and activate inflammatory cells such as macrophages, granulocytes, or NK cells to mediate antitumour effects [113, 122, 139, 149].

Furthermore, $CD4^+$ T cells secrete cytokines such as IL-2 which are necessary for the proliferation and survival of CTL [105, 122, 150, 151]. Accordingly, it was shown that after the transfer of mixed $CD4^+$/$CD8^+$ T cell lines in the treatment of EBV-induced lymphoma, the viability of transferred EBV-specific $CD8^+$ CTL was maintained for many months [95, 122]. Interferon (IFN)-γ (see 1.4.4.1.1) provided by $CD4^+$ Th1 cells inhibits tumour angiogenesis and is crucial for tumour rejection [122, 142, 152].

1.4.3.4 T cell subpopulations

$CD4^+$ T cells play a significant role in orchestrating antitumour immunity [99, 152] and can be divided into Th1, Th2, Th17 cells, and regulatory T cells (T_{reg}) based on the profile of transcription factors and secreted cytokines [139, 148, 153, 154]. Th1 cells mainly produce high levels of the proinflammatory cytokines IFN-γ and IL-2 [148, 152]. The Th1 commitment depends on activation of T-bet by locally produced IL-12 (see 1.4.4.1.2) [155].

Th2 cells mainly produce IL-4, IL-5, IL-10, and IL-13 after TCR stimulation and activation of GATA3 by IL-4 [148, 153]. Both, Th1 and Th2 cells, are derived from a common precursor [156]. Th1 cells activate APC, secrete cytokines which are important for the eradication of intracellular pathogens, and mediate DTHR whereas Th2 cells play a predominant role in humoral responses [148, 157]. In contrast to Th2 cells, Th1 cells promote the generation of memory responses against intracellular pathogens [152, 155, 158]. So, specifically directing the Th1 cell responses against a tumour antigen could be a safe and effective approach to immune based tumour therapies [158].

Recently, a new distinct subset, unrelated to Th1 and Th2 cells, has been called Th17 [159-162]. Th17 cells produce mainly IL-17A (IL-17) and IL-17F (see 1.4.4.1.3), develop from naïve $CD4^+$ T cells when stimulated in the presence of TGF-β and IL-6, and require IL-23 (see 1.4.4.1.2) for population expansion and as survival factor [163-165]. The orphan nuclear receptor RORγt has been identified to direct the Th17 generation [166]. Th17 cells have been associated with many inflammatory autoimmune diseases such as asthma [167], psoriasis [168], and experimental autoimmune encephalomyelitis (EAE) [169], but also with the inhibition of tumour growth mediated by the production of IL-17 [170]. Therefore, Th17 cells might also be useful for immunotherapy of cancer.

1.4.4 Other factors relevant for tumour rejection

Recent evidence suggests that a potent tumour antigen, together with activated T cells, is not sufficient for tumour rejection and that tumour immunity cannot entirely depend on direct tumour cell killing [122, 171]. Actually, it is very likely that cytokines produced by effector $CD4^+$ T cells and a permissive tumour microenvironment are required to achieve a successful therapy [171, 172]. Indeed, experimental studies showed the 'interdependence of $CD4^+$/$CD8^+$ T cell-mediated immunity and cytokine-driven innate immune responses', anti-angiogenesis, and the host environment [122, 132, 142, 152, 173-178].

1.4.4.1 Cytokines involved in tumour rejection

1.4.4.1.1 Interferon-γ

It has been proposed that *in vivo* IFN-γ secretion by $CD4^+$ T cells is important to allow subsequent tumour rejection [142, 179-182]. Evidence came from experiments showing that the generation of a T cell dependent tumour immunity is reduced in IFN-γ-deficient (IFN-$\gamma^{-/-}$) [130, 132, 139] and IFN-γ-receptor-deficient (IFN-$\gamma R^{-/-}$) mice [122, 131, 176]. Besides Th1 cells, mainly $CD8^+$ T cells and NK cells produce IFN-γ which is an important effector molecule in cell-mediated immunity and necessary for Th1 development [148, 183-185]. As the IFN-γR is expressed on almost every cell type, IFN-γ exerts various biological activities on different cell types [122, 176, 183, 186]. IFN-γ, together with TNF-α released from activated macrophages, shows cytotoxic effects on tumour cells [122, 187] and inhibits tumour cell proliferation [188]. Moreover, IFN-γ enhances MHC class I and II expression, resulting in increased tumour cell recognition and killing [122, 180, 189, 190]. Additionally, IFN-γ activates innate immune cells such as macrophages, mast cells, dendritic cells (DC), and NK cells within the tumour stroma to mediate tumour rejection [122, 173, 191]. By inhibiting the production of immunosuppressive molecules such as TGF-β, IFN-γ may also exert immunomodulatory effects [122, 152]. Tumour angiogenesis can also be inhibited through IFN-γ secretion by $CD4^+$ T cells as IFN-γ induces the expression of angiogenesis inhibitors such as the chemokines Interferon-inducible protein 10 (IP-10 or CXCL10) and monokine-induced by IFN-γ (Mig or CXCL9) in tumour cells and macrophages [192-195].

1.4.4.1.2 IL-6 cytokine family: IL-12, IL-23, IL-27

These type I cytokines are a superfamily of immunomodulators [196]. IL-12 was initially identified as a NK cell stimulatory factor [197] and cytotoxic lymphocyte maturation factor [198-200]. IL-23 [201] and IL-27 [202] were cloned by homology searches for members of the IL-6 family in DNA sequence databases [199]. IL-12, IL-23, and IL-27 are heterodimeric cytokines: IL-12 is composed of an α-chain (p35 subunit) and a β-chain (p40 subunit) [200]. IL-23 consists of the

p40 subunit of IL-12 and a novel subunit p19 [201]. The subunits of IL-27 are p28 and EBV-induced-gene (Ebi)-3 [202]. The monomeric ligands IL-12/p35, IL-23/p19, and IL-27/p28 are functionally inactive [199-202]. Hence, the heterodimers must be expressed in the same cell to generate active cytokines [199]. Nevertheless, it has been shown that transgenic overexpression of IL-23/p19 in mice can result in severe inflammation and death at 3 months of age [196, 203].

IL-12 signals through the IL-12 receptor complex that is composed of the IL-12Rβ1 and IL-12Rβ2 chains [204]. The IL-23 receptor complex consists of the IL-12Rβ1 chain and a novel receptor chain, IL-23R [205]. The receptor of IL-27 is composed of WSX-1/TCCR and gp130 [206]. The receptor complexes are expressed by macrophages, DC, NK cells, and activated T cells. In $CD4^+$ T cells the expression levels vary strongly, depending on the maturation and differentiation status of the T cells [204-206].

The structural similarity among IL-12, IL-23, and IL-27 is reflected in overlapping roles, though these cytokines are not functionally redundant [196, 199, 207, 208]. Activated monocytes, macrophages, and DC mainly produce these cytokines in response to microbial and host immune stimuli [196, 199]. They are important in regulating T cell proliferation and cytokine production, the activation of NK cells, and B cell antibody production [199, 208].

Nevertheless, there are differences: IL-12 induces IFN-γ secretion in freshly activated naïve T and NK cells and promotes the differentiation to Th1 cells [199, 209]. It is critical for the establishment of resistance to infections with viruses, intracellular mycobacteria, and parasites by inducing optimal IFN-γ secretion, expansion, and activation of T cells [210]. Its role in autoimmune diseases such as collagen-induced arthritis (CIA) or EAE is controversial [211]. IL-12 also shows potent antitumour activity in a variety of murine tumour models of established tumours and metastases [212-215]. Nevertheless, the mechanisms by which IL-12 controls tumour growth are still not fully defined, but it seems that the following processes play an important role: 1) antiangiogenesis through the induction of IFN-γ and antiangiogenic chemokines (IP-10/CXCL10, Mig/CXCL9) which might have direct effects on EC

proliferation and differentiation [181, 215-218], 2) destruction of tumour vessels by NK cell cytotoxicity or by direct lymphocyte-endothelial cell interactions, independently of IFN-γ [215, 219-221], and 3) activation of CTL, antitumour antibodies, or leukocytes which may produce proinflammatory cytokines [215, 220].

IL-23 also costimulates IFN-γ production from $CD4^+$ T and NK cells but is not as efficient as IL-12 [199, 201]. In contrast, IL-23 has the unique activity to induce strong proliferation of memory T cells [199, 222]. Thus, IL-23 is important in the later stages of Th cell development [223]. In comparison to IL-12, IL-23 is essential for the induction and maintenance of brain and joint inflammation autoimmune diseases such as CIA or EAE [169, 211] as it drives the survival of Th17 cells. Similar to IL-12, IL-23 may exert antitumour and antimetastatic activity in murine models of cancer [223-226]. However, the antitumour activity of IL-23 seems to be independent of IFN-γ as it was effective in mice depleted of IFN-γ [226]. Moreover, besides $CD8^+$ and $CD4^+$ T cells IL-23 seems to require NK cells, macrophages, and DC for its antiumour activity and it is suggested that the expression of IL-12, TNF-α, and NO contributes to the antitumour effect of IL-23 [223-226].

Like IL-12, IL-27 is able to induce proliferation of naïve T cell populations [199, 227, 228]. Thus, on the one hand, IL-27 promotes expansion of antigen-specific $CD4^+$ T cells, supports Th1 polarisation, and type I inflammation [202, 228, 229]. On the other hand, IL-27 is described as a suppressor of inflammatory responses [230-232]. IL-27 may increase antitumour activity which is mainly mediated through infiltrating $CD8^+$ T cells with enhanced tumour-specific CTL activity or NK cells [224, 233-236]. Moreover, IL-27 induces the expression of MHC class I molecules and INF-γ [224, 236]. Hence, IL-27 produces T cell-dependent and -independent antitumour effects. Moreover, it shows antiangiogenic properties due to the induction of IP-10/CXCL10 and Mig/CXCL9 and has therapeutic potential in cancer therapy similar to IL-12 [234, 237].

1.4.4.1.3 IL-17

IL-17 (IL-17A) was first identified as CTLA-8 [238] and is a member of a cytokine family consisting of IL-17A, IL-17B, IL-17C, IL-17D, IL-17E (IL-25), and IL-17F [239-241]. IL-17 acts as a proinflammatory cytokine as it stimulates endothelial, fibroblastic, and epithelial cells to secrete other inflammatory cytokines such as IL-6 and IL-8 [240, 242, 243]. It also costimulates T cells and supports T cell responses especially through the induction of the intracellular adhesion molecule-1 (ICAM-1 or CD54) which interacts with blood leukocytes [159, 161, 239]. IL-17 is critical for antibacterial immunity in mice [244] and has been associated with chronic inflammatory diseases including rheumatoid arthritis [245], bronchial asthma [167], and systemic sclerosis [246]. IL-17 also may exert antitumoural activities [170].

1.4.4.2 Role of the tumour environment in tumour rejection

To create a permissive and supportive environment for tumour development, cancer cells themselves modify their adjacent stroma by producing a variety of growth factors and proteases [91, 92, 247]. These factors induce angiogenesis and activate surrounding stromal cells such as fibroblasts and smooth muscle cells that in turn secrete further growth factors and proteases [247]. Supported by neutrophils, DC, monocytes/macrophages, eosinophils, mast cells, and lymphocytes [248, 249], intra-tumoural inflammation also promotes angiogenesis and progressive tumour growth [92, 177, 247, 250].

It has been suggested that modifying this tumour microenvironment and stimulating the infiltration of effector cells can improve T cell therapy and diminish tumour progression [171, 174, 251, 252]. In support of this idea, irradiation of transgenic mice led to tumour rejection that was mediated by lymphocytic infiltration and a proinflammatory environment [171, 174, 252]. Moreover, it has been shown that a complete tumour eradication was achieved through combination of irradiation and multiple T cell transfers, whereas treatment with tumour-specific T cells alone had no effect on tumour growth [171]. Similarly, it was demonstrated in several mouse models that previous immune suppression modifies the tumour environment and therefore improves the efficacy of transferred cells [107, 253].

1.5 Dimethylfumarate used in psoriasis treatment and its effects on endothelial cells and angiogenesis

1.5.1 Pathogenesis of Psoriasis

Psoriasis is a chronic inflammatory autoimmune disease of skin and small joints. The formation of erythematous plaques, infiltrated by IFN-γ producing Th1 cells, neutrophils, and mast cells, is a characteristic feature of psoriasis of the skin [254]. The critical role of the Th1-mediated inflammatory response in the pathogenesis of psoriasis is demonstrated through several therapies leading to clinical improvement of the disease: inhibition of T cell activation by recombinant proteins [255], reduction of activated T cells or suppression of T cell cytokine production through treatment with immunosuppressive agents including cyclosporine A [256] and methotrexate [257], or by Th2-inducing therapeutics [258]. Moreover, elevated expression of TNF-α in psoriatic skin lesions [259] and successful treatment of psoriasis with TNF-α blockers [260] suggest a central role for TNF-α in the disease. An increased expression of a variety of inflammation maintaining mediators such as IFN-γ, TNF-α, IL-17, IL-19, IL-23, IL-12, IL-8, VEGF, and others was shown in lesional skin and peripheral blood of psoriasis patients [258, 261]. Moreover, the tissue inflammation is closely associated with a strong induction of an angiogenic response, resulting in elongated, tortuous, and dilated vessels in the papillary dermis [262-265]. Elevated VEGF [266] and IL-8 [267] expression levels by hyperproliferating epidermal keratinocytes and an upregulation of VEGFR-1 and VEGFR-2 on EC of the superficial microvasculature in psoriatic skin may contribute to this neovessel formation during psoriasis [268]. Moreover, an increased expression of EC stimulating angiogenesis factor (ESAF) [266] and HIF-1α/HIF-2α [269] was demonstrated in psoriatic plaques. The EC also show an increase in αvβ3 integrin expression [270], and proliferation [265]. Moreover, reduced levels of the antiangiogenic factor TSP1 were found [267]. Together, these data suggest a critical role for angiogenesis in the pathogenesis of psoriasis.

1.5.2 Angiogenesis and reactive oxygen species

ROS are the most important class of radical species produced in the cellular metabolism [271]. The superoxide anion radical ($O_2^{\cdot-}$) has been described as the first ROS formed. It can further interact with other molecules to subsequently generate additional ROS such as hydroxyl radicals [271]. The superoxide radical is formed mostly within the cell mitochondria by reduction of molecular oxygen mediated by nicotinamide adenine dinucleotide phosphate (NADPH) oxidases [272] or non-enzymatically [271]. It is dismutated by the superoxide dismutase (SOD) to hydrogen peroxide [271, 273]. Other defence mechanisms against the accumulation of ROS include enzymatic antioxidants such as catalase [273], glutathione peroxidase (GPx)-1 [274], and non-enzymatic antioxidants such as glutathione (GSH) [275] and the synthetic N-Acetylcysteine (NAC). ROS induce cell type and stimulus specific cellular responses. At increased physiological levels, ROS are capable to cause proangiogenic responses such as EC proliferation, migration, and survival [94, 271, 276]. In contrast, high concentrations of ROS result in cell death through the induction of apoptosis or necrosis [271, 276]. Endothelial injury caused by ROS is involved in a variety of vascular diseases such as atherosclerosis, cardiomyopathy, and hypertension [271, 277-279].

1.5.3 Dimethylfumarate in the treatment of psoriasis

For the treatment of severe psoriasis, fumaric acid esters (FAE) have been used since 1959 [280] and at present FAE are approved in Germany [281]. A defined mixture of FAE containing dimethylfumarate (DMF) and the main active metabolite methylhydrogenfumarate (MHF) is used for treatment [281]. However, the mechanisms underlying of the antipsoriatic effect are not fully understood. Besides the inhibition of Th1 cytokine production [282, 283] and the upregulation of Th2 cytokines [284, 285] *in vitro* and *in vivo*, it has been shown that DMF inhibits chemokine secretion by keratinocytes and peripheral blood mononuclear cells [286]. Furthermore, the cytokine-induced expression of several adhesion molecules such as E-selectin, ICAM-1, and the vascular cell adhesion molecule-1 (VCAM-1 or CD106) that are typically found in activated endothelium of blood vessels in psoriatic skin [287, 288], is restrained [289].

Accordingly, the nuclear translocation of the vertebrate transcription factor nuclear factor (NF)κB in EC may be prevented by DMF [290]. NFκB regulates the expression of genes involved in cell growth and survival [291]. Importantly, DMF modulates the intracellular redox status by decreasing the level of GSH, a tripeptide consisting of glutamate, cysteine, and glycine (γ-Glu-CysH-Gly) [275, 282]. GSH functions as intracellular scavenger of ROS and as central redox buffer of the cell [271, 275, 292]. Moreover, additional reducing equivalents provided by both GSH and glutaredoxin are needed for DNA synthesis as DNA polymerase alpha and ribonucleotide reductase are thiol dependent enzymes [275, 292-295]. However, the mechanisms by which DMF might influence angiogenesis as a crucial component in the pathogenesis of psoriasis remain elusive.

1.6 Aims and objectives of the dissertation

1.6.1 Tumour immunotherapy

Adoptive cell transfer therapies led to an improvement in the outcomes for patients in recent clinic studies. However, little progress has been made in the description and generation of *in vivo* effective tumour-antigen specific T cells and the identification of the exact mechanisms by which these T cells eliminate large, established tumours in mice or in humans. Therefore, the following objectives have been set out:

1) Analysing mechanisms of a specific Th1 cell therapy, directed against the human tumour-associated antigen EpCAM
2) Analysing the role of cytokines, the host environment and antiangiogenic mediators
3) Optimisation of the Th1 cell therapy

1.6.2 Effects of DMF on angiogenesis

FAE therapeutics containing DMF as the main component are approved and well established for the therapy of severe psoriasis. However, the underlying mechanisms of the antipsoriatic effect are not fully understood. Since angiogenesis is supposed to be a critical component in the pathogenesis of psoriasis the following objectives have been defined:

1) Investigation of the effects of DMF regarding EC function *in vitro*
2) Identification of possible underlying signal transduction pathways
3) Analysing the effects of DMF on angiogenesis *in vivo*

2 Materials and Methods

2.1 Equipment

Table 1. Equipment used for experiments.

Instrument	Type	Company
Balances	Precision scale CP224SOCE Laboratory scale EW1500-2M	Sartorius, Göttingen Kern, Balingen-Frommern
β counter	Micro Beta Trilux	Perkin Elmer, Rodgau-Jügesheim
Cell harvester	Filter Mate	Perkin Elmer, Rodgau-Jügesheim
CO_2 humidified incubator	Hera*cell* 240	Thermo/Kendro, Dreieich/Hanau
Centrifuges	Biofuge *pico* Heraeus Biofuge *fresco* Heraeus Multifuge 3S-R Heraeus	Thermo/Kendro, Dreieich/Hanau
Cryotome	SME	Thermo Shandon, Dreieich
ELISA-Reader	Molecular Devices Emax	MWG Biotech, Ebersberg
FACS	Calibur LSRII	Becton Dickinson, Heidelberg
Gel electro-phoresis	Vertical gel: Protean II Model 45-2020i	BioRad, München Peqlab, Erlangen
	Horizontal gel: Model SUB Cell GT Model Gel XL Plus	 BioRad, München Labnet, Ried

Instrument	Type	Company
Heating blocks	Thermomixer Model Comfort Model LS2	Eppendorf, Hamburg VLM, Leipoldshöhe
Medimax	Medimax	Keul, Steinfurt
Microscopes	Axiovert25 Invers Axiovert200 Fluorescence HBO100	Zeiss, Jena
Mixer Mill	MM300	Retsch, Haan
PCR machine	Mastercycler gradient Primus 96 plus iCycler 584BR02280	Eppendorf, Hamburg MWG Biotech, Ebersberg BioRad, München
pH meter	CG842	Schott, Wertheim
Phosphoimager	Storm 860	Amersham/Pharmacia Biotech, Freiburg
Photometer	BioPhotometer 6131	Eppendorf, Hamburg
Pipettors	Model Research Model Reference Pipette boy	Eppendorf, Hamburg Eppendorf, Hamburg Hirschmann Eberstadt
Power supplies	Model EPS 300 PowerPac 300 Power Supply PowerPac Basic Power Supply	Pharmacia Biotech, Freiburg BioRad, München BioRad, München
Rotary microtom	2040	Reichert-Jung, Nußloch
Semidry Transblot	Fastblot B44	Biometra, Göttingen
Shaker	STR8 Rocking Platform	Stuart Scientific, Darmstadt

Instrument	Type	Company
Software	Cell Quest Pro	BD Bioscience, Heidelberg
	FCS Express software	DeNovoSoftware, Ontario, Canada
	Image Quant 5.1	MolecularDynamics
Tissue culture hood	HeraSafe KS18	Thermo/Kendro, Dreieich/Hanau
Tissue embedding and staining systems	Hypercenter XP	Shandon, Frankfurt/Main
	Tissue Embedding System TES99	Medite GmbH, Burgdorf
	24 Stainer	Shandon, Frankfurt/Main
	Varistain 24-4	Shandon, Frankfurt/Main
	Promounter RCM90	Medite GmbH, Burgdorf
	Automatic coverslipping machine	Medite GmbH, Burgdorf
UV trans-illuminator	RH-5.1 darkroom hood with easy 442K camera	Herolab, Wiesloch
Vortex mixer	Reax Top	Heidolph, Kelheim
Water bath	Model WB22	Funke Medingen, Freital

2.2 Materials

All sterile plastic materials for cell culture and screw-cap tubes (15 ml, 50 ml) were purchased from Greiner (Frickenhausen). FACS tubes, microcentrifuge and PCR tubes (0.2-2.0 ml) were from BD Falcon (Heidelberg).

2.3 Reagents, standards, and enzymes

Reagents used were ordered in high purity grade (puriss. p.A. or for microbiology) from the following companies, if not otherwise stated: Amersham Biosciences (Braunschweig), BD Biosciences (Heidelberg), Gibco/Invitrogen

(Karlsruhe), Merck/VWR (Darmstadt), Roth (Karlsruhe), Serva (Heidelberg), and SigmaAldrich/Fluka/RiedeldeHaen (Taufkirchen).

Cell culture products were purchased from BD Bioscience (Heidelberg), Biochrom AG (Berlin), BioWhittaker/Cambrex (Verviers, Belgium), Gibco/ Invitrogen (Karlsruhe), PAA (Cölbe), Promocell (Heidelberg), Roth (Karlsruhe), and SigmaAldrich/Fluka/RiedeldeHaen (Taufkirchen). Filter membranes with 0.22 µm pore size (Millipore, Schwalbach) were used for sterilisation purposes of cell culture reagents and Milli-Q-purified water (dH_2O) was used throughout the protocols. The following DNA ladders, protein standards (Table 2), and modified enzymes (Table 3) were used:

Table 2. DNA ladders and protein standards.

Ladder or standard	Company
Gene Ruler 100 bp DNA Ladder	Fermentas, St. Leon-Rot
Gene Ruler 1 kb DNA Ladder	Fermentas, St. Leon-Rot
Magic Mark XP Western Protein Standard	Invitrogen, Karlsruhe
SeeBlue Plus2 Pre-Stained Standard, 'High Range'	Invitrogen, Karlsruhe

Table 3. Modified enzymes.

Enzymes	Company
Accutase	PAA, Cölbe
Collagenase D	Roche, Mannheim
DNAse I, RNase free	Invitrogen, Karlsruhe
M-MLV Reverse Transcriptase (200 U/µl)	Promega, Madison, USA
Proteinase K	Roche, Mannheim

Enzymes	Company
Recombinant RNAsin Ribonuclease Inhibitor (40 U/µl)	Promega, Madison, USA
RNase A	Boehringer, Mannheim
Taq Core Kit-Taq-DNA-Polymerase	MP Biomedicals, Irvine, USA

2.4 Primary antibodies

2.4.1 For cell culture

Table 4. Primary antibodies for cell culture.

Antibody	Characteristics	Reference or company
Anti-CD4 (L3T4), anti-CD8 (Ly2), MAR (mouse anti-rat)	Hybridoma	Gift from Prof. Schmidt (IMSB, Mainz)
Anti-IFN-γ (XMG-1.2)	Purified antibody	Gift from Prof. Mocikat (GSF, Munich)
Anti-IL-4 (11B11)	Hybridoma	Gift from Prof. Schmidt (IMSB, Mainz)

2.4.2 For Fluorescence activated cell sorting (FACS) analysis

Table 5. Primary antibodies for FACS analysis.

Antibody	Characteristics	Reference or company
Anti-mouse CD4 (RM4-5)	FITC-conjugated monoclonal rat antibody	BioLegend/Biozol, Eching

Antibody	Characteristics	Reference or company
Anti-mouse CD8 (Ly2)	FITC-conjugated monoclonal rat antibody	BD Bioscience/Pharmingen Heidelberg
Anti-mouse CD11b (Mac-1 α chain)	FITC-conjugated monoclonal rat antibody	BD Bioscience/Pharmingen Heidelberg
Anti-mouse DO-11.10 TCR (KJ1-26)	FITC-conjugated monoclonal rat antibody	Caltag, Hamburg
Rat IgG_{2a} (RTK2758)	FITC-conjugated rat IgG isotyp	BioLegend/Biozol, Eching
Anti-mouse IFN-γ (XMG1.2)	PE-conjugated monoclonal rat antibody	BioLegend/Biozol, Eching
Anti-mouse IL-4 (11B11)	PE-conjugated monoclonal rat antibody	BioLegend/Biozol, Eching
Anti-mouse IL-10 (JES5-16E3)	PE-conjugated monoclonal rat antibody	BD Bioscience/Pharmingen, Heidelberg
Anti-mouse IL-17 (TC11-18H10)	PE-conjugated monoclonal rat antibody	BD Bioscience, Heidelberg
Rat IgG1 (RTK2071)	PE-conjugated rat IgG isotyp	BioLegend/Biozol, Eching
Anti-mouse CD11c (N418)	APC-conjugated monoclonal hamster antibody	Caltag, Hamburg
Hamster IgG	APC-conjugated hamster IgG isotyp	BioLegend/Biozol, Eching

2.4.3 For immunohistochemistry

Table 6. Primary antibodies for immunohistochemistry.

Antibody	Characteristics	Reference or company
Anti-mouse CD11b (Mac-1α chain)	Monoclonal rat antibody	BD Bioscience/Pharmingen, Heidelberg
Anti-mouse Ki-67 (Tec3)	Monoclonal rat antibody	DakoCytomation, Hamburg
Anti-mouse PECAM-1 CD31 (MEC 13.3)	Monoclonal rat antibody	BD Bioscience/Pharmingen, Heidelberg
Anti-mouse VEGFR-2 Flk-1 (C-1158)	Monoclonal rat antibody	Santa Cruz, Heidelberg
Anti-mouse CD4 (L3T4)	Biotin-conjugated monoclonal rat antibody	BD Bioscience/Pharmingen, Heidelberg
Anti-mouse F4/80 (BM8)	Biotin-conjugated monoclonal rat antibody	BMA Biomedicals, Augst, Switzerland
Purified rat IgG_{2a}	Monoclonal IgG isotyp	BD Bioscience, Heidelberg

2.4.4 For Western blot

Table 7. Primary antibodies for Western blot.

Antibody	Characteristics	Reference or company
Anti-p38, p-p38 (Thr180/Tyr182) MAP Kinase	Polyclonal rabbit antibody	Cell Signalling/NEB, Frankfurt/Main
Anti-p42/44, p-p42/44 (Thr202/Tyr204) MAP Kinase	Polyclonal rabbit antibody	Cell Signalling/NEB, Frankfurt/Main
Anti-mTor, p-mTor (Ser2448) Ser/Thr protein kinase	Polyclonal rabbit antibody	Cell Signalling/NEB, Frankfurt/Main

2.5 Secondary antibodies

Table 8. Secondary antibodies.

Antibody	Characteristics	Reference or company
Donkey anti-rat IgG	Cy3-conjugated antibody	MolecularProbes/Dianova, Hamburg
Goat anti-rabbit IgG	Alkaline phosphatase-conjugated goat IgG (H+L) antibody	Amersham Biosciences, Braunschweig
Goat anti-rat IgG	Biotin-conjugated goat IgG (H+L) antibody	VectorLab/Linaris, Wertheim-Bettingen
Streptavidin	PE-conjugated antibody	BD Bioscience/Pharmingen, Heidelberg
Yopro-1	Nucleus staining	MolecularProbes/Dianova, Hamburg

2.6 Mice

Female wildtype (WT) BALB/c mice and BALB/c DO11.10 TCR-transgenic mice, specific for the chicken ovalbumin (OVA) peptide ($OVA_{323-339}$), were purchased from Charles River Laboratories (Wilmington). $IL4^{-/-}$ BALB/c mice were kindly provided by Dr. M. Kopf (ETH, Zürich) [296]. The animals were maintained in the animal facilities of the Eberhard Karls University Tübingen under specific pathogen-free conditions. All experiments were performed according to the guidelines of the Institutional Animal Care and Use Committee of the Regierungspräsidium Tübingen.

2.7 Cell culture

Eukaryotic cells were cultured in appropriate cell culture media (Table 9) at 37°C in a 7.5% CO_2 humidified incubator. Adherent cells such as the colon carcinoma cell line CT26, expressing the human EpCAM (CT26-EpCAM), were grown to confluency, washed with phosphate buffered saline (PBS), and cells were dispersed by trypsin/EDTA treatment (1 ml for 75 cm^2 tissue culture flask). After washing with media (1100-1500 revolutions per minute (rpm), 5 min, room temperature (RT)) dissociated cells were reseeded into a fresh culture flask, representing a passage (p). For passaging of suspension cultures cells were pelleted, resuspended, and reseeded in a new flask. Cell suspensions were seeded in a 1:3 up to 1:15 dilution according to the growth rate of the cells. Human umbilical vein endothelial cells (HUVEC) and human lung-derived microvascular endothelial cells (HLMEC) were grown on gelatine-coated flasks and seeded in a 1:3 dilution. To determine the number of living cells in culture, cells were counted in a hemacytometer (Neubauer) using trypan blue exclusion.

Table 9. Cell culture media.

Cell line	Reference or company	Cell culture media
CT26-EpCAM	Gift from Prof. Mocikat (GSF, Munich)	Dulbecco's modified Eagles Media (DMEM, 4.5 g glucose) 10% (v/v) fetal calf serum (FCS) 1% (v/v) Pen/Strep (Stock solution: 10000 U/ml penicillin-G 10000 µg/ml streptomycin
Primary T cells	Freshly isolated	DMEM (4.5 g glucose) 10% (v/v) FCS 1% (v/v) Pen/Strep 10 µM HEPES-Buffer 1% (v/v) MEM amino acids 1 mM sodium pyruvate 40 µM 2-mercaptoethanol

Cell line	Reference or company	Cell culture medium
HUVEC	Promocell	MCDB131 media 8% (v/v) FCS 2% (v/v) human serum 1% (v/v) Pen/Strep 2.5 µg/ml amphotericin B 4 mM glutamine 10 µg/ml heparin 0.4% (v/v) endothelial cell growth supplement (ECGS)
HLMEC	Promocell	MCDB131 media 5% (v/v) FCS 5% (v/v) human serum 1% (v/v) Pen/Strep 2.5 µg/ml amphotericin B 4 mM glutamine 40 µg/ml heparin 0.4% (v/v) ECGS 2 ng/ml VEGF

2.8 Long-time storage of eukaryotic cells (Cryopreservation)

Cells to be frozen were pelleted, resuspended in FCS containing 10% (v/v) dimethyl sulfoxide (DMSO), aliquoted to cryovials, and transferred in a freezing container (Mr. Frosty, Nalgene Labware) to a −80°C freezer. For long-time storage cells were maintained in a liquid nitrogen freezer.

For reuse, cells were quickly thawed in a 37°C water bath and resuspended in prewarmed cell culture media. After centrifugation, cells were resuspended in medium and transferred to a tissue culture flask. Medium was changed the next day.

2.9 Preparation of antigen presenting cells

APC were isolated from splenocytes of WT syngeneic mice. Spleens of mice were harvested and placed in a 200 µm nylon mesh (2 spleens/mesh) in a petri dish containing 5 ml culture medium. Using the plunger of a syringe, tissue was pressed through the mash until mostly fibrous tissue remained. After washing, cells were centrifuged (1500 rpm, 5 min, RT). For removal of erythrocytes ACK lysis buffer (BioWhittaker) was added, cells were incubated for 2 min at RT, and centrifuged (1500 rpm, 5 min, RT). Afterwards, cells were washed twice with culture medium. Cells were T cell depleted by using anti-CD4, anti-CD8, and mouse anti-rat antibody (MAR) hybridomas together with rabbit complement-MA (Biozol) in FCS-free media and incubated for 45 min at 37°C. Cells were washed twice with culture medium and irradiated (30 Gy). After another washing step, living APC were counted and used for stimulation of T cell cultures.

2.10 Immunisation and *in vitro* T cell differentiation of EpCAM-reactive T helper cells

$IL4^{-/-}$ BALB/c mice were immunised subcutanously with 1.0 x 10^6 CT26-EpCAM cells dispended in 50 µl CpG1668 (200 µM, 5'-tcc atg acg ttc ctg atg ct-3', PTO oligo, MWG). After 10 days mice were boosted the same way. Spleen and lymphnodes (LN) were isolated 6 days later. Removed organs were pressed through a 200 µm nylon mash for single cell suspension and erythrocytes were lysed (see 2.9). Afterwards, cells were washed twice with culture medium. Cells were counted and $CD4^+$ T cells were islolated using mouse anti-CD4 (L3T4) magnetic beads and LS columns to reach a purity of ~ 96% according to manufacturer's instructions (MACS, Miltenyi Biotech, Bergisch Gladbach). For Th1 polarisation, 0.5 x 10^6 EpCAM-reactive $CD4^+$ T cells were stimulated with 1.0 x 10^6 APC, 1 µg/ml EpCAM protein (s17-1A, gift from Prof. Kopp, Institute of Immunology, Munich) and 0.2 µM CpG1668 in a 96-well plate. For Th17 polarisation, 10 µg/ml anti-IFN-γ (XMG-1.2) antibody was added additionally to this setup. For T cell expansion, cultures were supplemented with IL-2 (25-50 U/ml, Chiron Therapeutics) every 3-4 days.

2.11 *In vitro* T cell differentiation of OVA-specific T helper cells

For OVA T cell culture, $CD4^+$ T cells were isolated from DO11.10 transgenic mice as described above (see 2.10). For Th1 polarisation, 0.25 x 10^6 OVA $CD4^+$ T cells were stimulated with 0.5 x 10^6 APC, 0.2 µM CpG1668, 5 µg/ml OVA peptide ($OVA_{323-339}$: ISQAVHAAHAEINEAGR, EMC microcollections), and 2 µg/ml murine anti-IL-4 (11B11) antibody in a 96-well plate.

2.12 Experimental procedure of the Th1 cell therapy

CT26-EpCAM cells were harvested and washed twice with PBS. Living cells (1.5 x 10^6) dispended in 50 µl PBS were injected subcutanously in the right and left flank of WT BALB/c mice (day 0) which were narcotised with ketanest (15% (v/v) ketamin (50 mg/ml, DeltaSelect), 8% (v/v) rompun (Bayer) in PBS). The mice were irradiated (2 Gy) on day 3 to induce mild inflammation. On day 4, cultured Th1 cells (5 x 10^6 cells in 250 µl PBS) were adoptively transferred intraperitoneally into these mice. The control group received PBS. Mice were sacrificed by CO_2 asphyxiation at the indicated points in time and tumours were harvested for further analysis.

In a further approach, one group of mice received 500 µg murine anti-IFN-γ antibody intraperitoneally on day 3 after irradiation and before adoptive transfer of T cells on day 4, as indicated.

2.13 Fluorescence activated cell sorting

Fluorescence activated cell sorting (FACS) has two general applications - quantitative analysis and cell separation. Flow cytometers use one or more laser sources for scanning and excitation of fluorescent probes. Fluorescence stimulation of fluorescent-labeled antibodies is used for quantitative analysis of the expression and the density of cell surface and intracellular molecules. Moreover, characterisation of cell size, cell volume, and different cell types in heterogeneous populations is possible and the purity of subpopulations can be evaluated. Electronic cell sorting can be used to separate distinct subpopulations of cells on the basis of these measured characteristics (according to [297]).

2.13.1 Intracellular FACS staining of T cells

For polyclonal T cell stimulation, 1.0 x 10^6 T cells were activated in 1 ml culture medium with 30 ng/ml phorbol 12-myristate 13-acetate (PMA), a protein kinase C activator, and 1.5 mg/ml ionomycin, a Ca^{2+} ionophore, at 37°C in a 24-well plate. After 2 h, cells were treated with brefeldin A (concentration as instructed, BD Biosciences) which is an inhibitor of protein transport, leading to an increased accumulation of cytokine proteins within the cells. Another 2 h later, cells were washed with PBS, centrifuged (300 g, 10 min), and fixed in 2% (v/v) formaldehyde in PBS for 20 min at RT. After membranes were permeabilized by washing cells twice with flow cytometry buffer (0.5% (w/v) bovine serum albumin (BSA), 0.5% (w/v) saponin in PBS) [298, 299], 100 µl of the cell suspension were transferred to a FACS tube (2 x 10^5 cells per staining). 20 µl of diluted (1:100) antibodies were added to the suspension and cells were stained for 10 min at RT in the dark for intracellular IFN-γ (XMG-1.2), IL-4, IL-10, or IL-17 in combination with surface CD4 (RM4-5). To determine the degree of background caused by non-specific binding of the heavy chain of the antibody, cells were also stained with IgG matched isotypes. Unstained cells were used to establish levels of background autofluorescence. After incubation, cells were washed with flow cytometry buffer and resuspended in 1% (w/v) BSA in PBS for FACS analysis. 10000 cells were aquired on the FACSCalibur and analysed using Cell Quest Pro software.

2.13.2 FACS analysis of tumour tissue cells

Tumour infiltrating cells were characterised by FACS analysis. Therefore, tumours were excised on days 10, 13, and 18 after tumour cell injection. Tumours from single mice were pooled and cut with Medimax. After washing the suspension with PBS, remaining tissue was digested for 30 min at 37°C using collagenase D (1 mg/ml) with 0.6 mM $CaCl_2$ in PBS. To stop the enzyme activity, cells were washed with PBS containing 10% (v/v) FCS. The suspension was poured through a 200 µm nylon mesh which was rinsed with PBS containing 10% (v/v) FCS afterwards. The remaining single cell suspension was washed with 1% (v/v) FCS in PBS. Cells were stained using the following anti-mouse antibodies, respectively: Fluorescein isothiocyanate (FITC)-CD4 (RM4-5, 1:100), phycoerythrin (PE)-CD8 (Ly.2, 1:100), FITC-CD11b (Mac-1,

1:100), allophycocyanin (APC)-CD11c (N418, 1:200), or biotinylated anti-mouse F4/80 (1:150) with a secondary PE-labeled streptavidin antibody (1:1000) and the corresponding isotype rat IgG antibodies. After staining, cells were washed and resuspended in 1% (v/v) FCS in PBS for FACS analysis. 30000 cells were acquired on the LSRII and analysed using FCS Express software. Total living cells were gated by forward/sideward scatter and infiltrating cells were calculated on the basis of 10000 living cells.

2.13.3 Apoptosis detection in HUVEC

The early phases of the apoptotic program lead to a loss of membrane asymmetry. In apoptotic cells the membrane phospholipid phosphatidylserine (PS) is translocated from the inner to the outer plasma membrane and is therefore exposed to the external cellular environment. Thus, Annexin V, a Ca^{2+} dependent phospholipid-binding protein, is able to bind to PS as sign of an early stage of apoptosis. Through staining cells in conjunction with the vital dye propidium iodide (PI), the apoptotic state of cells can be differentiated (Table 10) according to the manufacturer's instructions (BD Biosciences).

Table 10. The apoptotic state of cells.

State of cells	Annexin V-FITC staining	PI-staining
Viable cells	negative	negative
Early apoptotic cells	positive	negative
Late apoptotic or dead cells	positive	positive

To assay apoptosis in HUVEC (p3, p4, p5) following DMF treatment, cells were seeded at 1.5 x 10^5 cells/well in a 6-well plate in triplicates. The next day medium was changed containing the given DMF concentrations. DMSO treated cells served as negative control. To detect apoptotic cells 24 h later, adherent cells were dispersed by trypsin/EDTA treatment combined with the supernatant and treated as described in the manufacturer's instructions (BD Biosciences) for subsequent FACS analysis.

2.13.4 Reactive oxygen species detection in HUVEC

Derivatives of reduced fluorescein can be used as cell-permeant indicator for ROS (OxyBURST Green, H2DCFDA, Molecular Probes/ Invitrogen). Till acetate groups are removed by intracellular esterases and oxidation occurs within the cells, the chemically reduced and acetylated forms of 2',7'-Dichloro-fluorescein are non-fluorescent. Therefore, the oxidation of the probe can be detected by monitoring the increase in fluorescence by flow cytometry according to the manufacturer's instructions (Molecular Probes/ Invitrogen).

For detection of ROS in HUVEC (p3, p4, p5), cells were grown to confluency in triplicates and incubated for 1.5 h with the appropriate concentrations of DMF and/or NAC; MCDB131 medium alone served as negative control. Cells were stained with 0.75 mM OxyBURST Green for 0.5 h. Cells were dispersed by accutase treatment, washed with PBS, and subsequent FACS analysis was performed.

2.13.5 Cell cycle analysis of HUVEC

One method for analysing cellular DNA content uses PI to reveal the distribution of cells within the major phases of the cell cycle (G_0/G_1 versus S versus G_2/M) [300]. PI intercalates into double-stranded (ds) DNA and RNA and produces a highly fluorescent adduct with excitation at 488-600 nm.

HUVEC (p3, p4, p5) were seeded at 1.5 x 10^6 cells/well in a 6-well plate in triplicates and the next day medium was changed containing different concentrations of DMF and/or NAC; MCDB131 medium alone served as negative control. After two days, cells were dispersed by accutase treatment, fixed, and permeabilized on ice for 30 min using 100% ethanol. After washing cells twice with ice cold PBS (2500 rpm, 5 min), cells were stained with 400 µl propidium iodide solution (20 µg/ml PI, 1 µg/ml RNase I in PBS). After 30 min on ice fluorescence was measured for cell cycle analysis.

2.14 RNA and DNA

2.14.1 Preparation of RNA and cDNA from tumour tissue

Total RNA was isolated from whole tumour tissue using the Mixer Mill (30 Hz, 2 x 30 sec, Retsch) and purified according to manufacturer's instructions (Macherey-Nagel). RNA was eluted in 30 µl RNA-free water. 1 µg RNA was digested with DNAse I according to manufacturer's instructions (Invitrogen) and converted to cDNA using M-MLV reverse transcriptase (RT, Table 11).

Table 11. cDNA synthesis.

Step	*Mixture*	*Treatment*
I	1 µg RNA 0.5 µM oligo dT 0.5 mM dNTPs (dATP, dTTP, dCTP, dGTP) dH_2O ad 15 µl	5 min, 70°C on ice
II	5 µl 5x buffer 3.5 µl H_2O 0.5 µl RNAsin (20 U)	2 min, 37°C
III	± 1 µl M-MLV RT (200 U)	60 min, 37°C 15 min, 70°C

2.14.2 Spectrophotometric quantitation of RNA and DNA

For quantitation of nucleic acids absorbance measurements ($A_{260\ nm}$ for RNA and DNA) were performed with a photometer. The ratio of A_{260}/A_{280} was used as an indicator of nucleic acid purity. Ratios of 1.8 to 1.9 and 1.9 to 2.0 indicate highly purified preparations of DNA and RNA, respectively. Contaminants that absorb at 280 nm (e.g. proteins) will lower this ratio (according to [301]).

The following nucleic acid concentration in water can be expected with an optical density, OD = 1 (according to R. Heidenreich):

Table 12. Nucleic acid concentration in water.

Property	Absorbance (A_{260}), OD = 1
DNA, double-stranded	50 µg/ml
DNA, single-stranded	about 30 µg/ml
RNA	40 µg/ml

2.14.3 Monitoring separation of DNA through agarose gels

Agarose gel electrophoresis is a highly effective method for separating, identifying, and purifying DNA fragments. DNA molecules exposed to an electric field (voltage: 35-135 V) migrate from the cathode toward the anode due to the negatively charged phosphates along the DNA backbone. The electrophoretic separation depends on charge and/or size of macromolecules. Fragments travel through the gel matrices at a rate that is inversely proportional to the $\log_{10}$ of their molecular weight. Therefore, the molecular weight of a fragment can be determined by using DNA standards of known molecular weight (e.g. 1 kb ladder). For visualisation of DNA fragments, ethidium bromide was used since the dye intercalates between the stacked bases of nucleic acids and when illuminated with UV light (260-360 nm), ethidium bromide gives a red-orange fluorescence (560 nm). A UV transilluminator was used for DNA visualisation and photography (according to [302]).

For gel electrophoresis concentrations of 0.5% to 2.0% (w/v) agarose in 0.5 x Tris-acetate-EDTA (TAE) electrophoresis buffer were used to separate 0.2-0.6 kb fragments. Agarose powder was melted in 0.5 x TAE buffer, cooled, and 0.5 µg/ml ethidium bromide was added into the gel. The melted agarose was poured into the gel casting platform and the gel comb inserted. After the gel has hardened, the gel comb was withdrawn, the gel was set in the electrophoresis tank, and covered with 0.5 x TAE buffer. DNA samples with

2 x loading buffer were loaded into the wells as progress of the separation can be monitored by the migration of the dyes in the loading buffer.

Table 13. Buffers used for agarose gel electrophoresis.

0.5 x TAE electrophoresis buffer	40 mM Tris 5.7% (v/v) acetic acid 0.8 mM EDTA dH_2O
2 x loading buffer	50% (v/v) glycerin 0.2% (w/v) Orange G TAE electrophoresis buffer

2.15 The polymerase chain reaction

The polymerase chain reaction (PCR) is an *in vitro* method for specifically amplifying DNA fragments enzymatically. Therefore, the standard PCR mixture (Table 14) was cycled 20-35 times through temperatures that permit denaturation (95°C), annealing (about 5°C below melting point of primers), and synthesis of the specific PCR product (72°C, elongation). PCR parameters are dependent on 1) the sequence, length, and amount of the template DNA, 2) the sequence, GC content and percent complementarity of the primers, and 3) the efficiency of the reaction. The PCR products were visualized on an appropriate agarose gel.

Table 14. PCR protocols.

Standard PCR mixture	50-100 ng template cDNA 0.2 mM dNTPs (dATP, dTTP, dCTP, dGTP) 0.5 µM primer forward 0.5 µM primer reverse 2.0 µl 10x Taq buffer 0.2 µl Taq polymerase (1-2 U) dH_2O ad 20 µl

Standard PCR protocol	94°C, 3 min (94°C, 40 sec, variable, 40 sec, 72°C, 40 sec) 20-35 x 72°C, 3 min 8°C, hold

The following primers were used for standard PCR:

Table 15. Primers used for standard PCR.

Gen	Sequence	Annea-ling	Size (bp)
GAPDH	5'-CTCACTCAAGATTGTCAGCAATG-3' (forward) 5'-GAGGGAGATGCTCAGTGTTGG-3' (reverse)	59	669
Aldolase	5'-AGCTGTCTGACATCGCTCACCG-3' (forward) 5'-CACATACTGGCAGCGCTTCAAG-3' (reverse)	59	600
Ang-1	5'-GGGGGAGGTTGGACAGTAAT-3' (forward) 5'-CGAACCACCAACCTCCTGTT-3' (reverse)	54	388
Ang-2	5'-GTCCATGAAGGAGCAGAAGG-3' (forward) 5'-GCCTTGATCTCCTCTGTGGA-3' (reverse)	51	312
CXCR3	5'-CAGCCTGAACTTTGACAGAACCT-3' (forward) 5'-GCAGCCCCAGCAAGAAGA-3' (reverse)	51	287
Mig/ CXCL9	5'-TTTTCCTTTTGGGCATCATCTT-3' (forward) 5'-AGCATCGTGCATTCCTTATCACT-3' (reverse)	59	75
PIGF	5'-CAGGTCCTAGCTGGGTTGG-3' (forward) 5'-TCACGGGTGGGGTTCC-3' (reverse)	56	441
VEGFR-2	5'-TTCTGGACTCTCCCTGCCTA-3' (forward) 5'-GACTGGTAGCCACTGGTCTG-3' (reverse)	59	354

2.16 Quantitative real-time PCR

For quantitative real-time (RT)-PCR specific amplification of a gene of interest was performed by mixing template DNA, two appropriate oligonucleotide primers (0.1-0.2 µM), and the iQ™ SYBR Green Supermix (BioRad). The mix contains thermostable iTaq™ DNA polymerase, dNTPs, buffer, and SYBR Green I, which is a fluorescent dye that directly intercalates in double-stranded (ds) DNA according to manufacturer's instructions (BioRad). The dye generates a signal that is proportional to the accumulating dsDNA concentration and can be detected using the iCycler iQ instrument. Dependent on the primers (Table 16), a standard protocol with parameters similar to standard PCR was used and multiplex reactions were run in triplicates (Table 17). For analysing the specifity of the PCR reaction a melting curve was recorded. After user defined adjustment of the threshold position to 50, crossing points (Cp) of samples were used to calculate gene expression.

Normalising the gene of interest expression values to the internal HPRT control in every sample and considering the amplification efficiency of the different primers, the arbitrary expression units were calculated as follows:

$$\text{Arbitrary expression} = \frac{X_{HPRT}^{Cp_{HPRT}}}{X_{Gen}^{Cp_{Gen}}};$$ X: tested primer efficiency

The relative expression of genes of interest is represented as fold differences of the mean of treated tumour samples to the mean of control tumour samples.

$$\text{Relative expression} = \frac{\sum AE_{treated} / n_{treated}}{\sum AE_{control} / n_{control}};$$ n: number of tumours

The following sequences were used for RT-PCR:

Table 16. Primer sequences used for RT-PCR.

Gen	Sequence	Annea-ling (°C)	Size (bp)
HPRT	5'-GTTCTTTGCTGACCTGCTGGAT-3' (forward) 5'-CTTAGGCTTTGTATTTGGCTTT-3' (reverse)	59	440
IL-23/p19	5'-CATGGAGCAACTTCACACCTC-3' (forward) 5'-GGTGATCCTCTGGCTGGA-3' (reverse)	62	63
IL-12/p35	5'-ATGACCCTGTGCCTTGGTAG-3' (forward) 5'-CAGATAGCCCATCACCCTGT-3' (reverse)	59	289
IFN-γ	5'-TCAAGTGGCATAGATGTGGAAGAA-3' (forward) 5'-TGGCTCTGCAGGATTTTCATG-3' (reverse)	59	92
ICAM	5'-CCTGTTTCCTGCCTCTGAAG-3' (forward) 5'-GTCTGCTGAGACCCCTCTTG-3' (reverse)	59	528
IL-6	5'-CCGGAGAGGAGACTTCACAG-3' (forward) 5'-CAGAATTGCCATTGCACAAC-3' (reverse)	56	120
IL-27/Ebi3	5'-GCTCCCCTGGTTACACTGAA-3' (forward) 5'-ACCGAGAAGCATGGCATT-3' (reverse)	59	72
IL-17	5'-TCAGACTACCTCAACCGTTCC-3' (forward) 5'-CTTTCCCTCCGCATTGACAC-3' (reverse)	61	126
IL-12/p40	5'-CAGTACACCTGCCACAAAGGAGGC-3' (forward) 5'-GTCCAGTGTGACCTTCTCTGCAGACA-3' (reverse)	62	264
IL-27/p28	5'-CCCAATGTTTCCCTGACTTTC-3' (forward) 5'-AGCGGAGGTGCCTGTGC-3' (reverse)	59	198
VEGF	5'-CTGCTCTCTTGGGTGCACTGG-3' (forward) 5'-CACCGCCTTGGCTTGTCACAT-3' (reverse)	59	563

Gen	Sequence	Annea-ling (°C)	Size (bp)
IP-10/ CXCL10	5'-TCCCTCTCGCAAGGACGGTC-3' (forward) 5'-GTGTGTGCGTGGCTTCACTC-3' (reverse)	59	256
VCAM	5'-TGACAAGTCCCCATCGTTGA-3' (forward) 5'-ACCTCGCGACGGCATAATT-3' (reverse)	59	110
c-Myc	5'-AGCTGTTTGAAGGCTGGATT-3' (forward) 5'-CCGCAACATAGGATGGAGAG-3' (reverse)	59	372
Cyclin D2	5'-ATTTCAAGTGCGTGCAGAAG-3' (forward) 5'-ACACTTCTGTTCCTCACAGACCT-3' (reverse)	64.5	121

Table 17. RT-PCR protocols.

Standard RT-PCR protocol	95°C, 1.5 min (95°C, 30 sec, 59°C, 30 sec, 72°C, 30 sec) 40 x (50-95°C, 30 sec, 0.5°C) 90 x 10°C, hold
Adaptation 56°C	56°C, 35 sec
Adaptation 60°C	60°C, 30 sec
Adaptation 62°C	62°C, 50 sec
Adaptation 64.5°C	64.5°C, 40 sec

2.17 Immunohistochemistry

2.17.1 Immunohistochemistry and immunofluorescence of frozen tumour tissue sections

Immunohistochemistry (IHC) is used to identify specific antigens in tissues [303]. Immunofluorescence (IF) of tissues is methodologically identical to this technique but uses a different detection and imaging system [304].

Tumours obtained from mice at day 18 after tumour cell injection were directly embedded in tissue freezing medium (Tissue tec, Jung/Leica), snap frozen in liquid nitrogen for cryosectioning, and stored at -80°C. Specimens were cut in 10 µm sections. To fix sections, slides were covered with acetone or 1:1 acetone/methanol for 10 min at -20°C. After air drying the slides for 30 min, slides were treated with 0.3% (v/v) H_2O_2 in methanol for 15 min to eliminate endogenous peroxidase activity. After washing the slides three times with PBST (0.1% (v/v) Tween 20 in PBS), the tissue sections were encircled on the glass slide with a Pap pen (water repellant wax, DakoCytomation), creating a boundary that prevented mixture of reagents. All further incubation procedures were performed in a humidified staining chamber. After blocking non-specific binding sites with specific sera for 30-60 min, the sections were incubated with diluted primary antibody in PBST for 60 min at RT or over night at 4°C. Isotype-matched IgG served as negative control in all stainings. The slides were washed three times in PBST for 10 min and the sections were stained with the secondary biotinylated antibody in PBST for 30 min at RT. After another washing step, the slides were incubated with a horseradish peroxidase (HRPO)-conjugated avidin-biotin complex (ABC, VectorLab/Linaris) for 30 min at RT [305]. 3-Amino-9-ethyl carbazole (AEC, VectorLab/Linaris) or 3,3′-diamino-benzidine (DAB, VectorLab/ Linaris) substrate solution was added to the slides after washing and specimens were incubated for 5 to 30 min till proper color development occured. AEC gives a bright red precipitate whereas DAB results in an intense brown precipitate. The slides were counterstained for 30 sec to 2 min with hematoxylin for nuclei staining (Chem Mate, DakoCytomation) and mounted with aquatex (Merck).

For immunofluorescence labeling the secondary antibody was fluorescently tagged (Cy3) and directed against the primary antibody host species. Sections were counterstained with Yopro1 for nuclei staining and mounted with moviol/DABCO (33% (v/v) glycerin, 13% (w/v) moviol, 130 mM Tris, 50 mg/ml DABCO in dH_2O).

Serial sections of eight representative tumours of Th1 cell treated and control mice from day 18 after tumour cell injection were stained (Table 18). Digital images at the magnification indicated were obtained using an Axiovert 200 Fluorescence microscope.

Table 18. Protocol for immunohistochemistry.

Antigen	Step	Characteristics
CD4 (surface marker)	Fixation	1:1 acetone/methanol, 10 min, -20°C
	Blocking	not required
	Primary antibody	1:40 dilution in PBST, 1 h, RT
	Substrate	DAB, 8-10 min
PECAM-1 (platelet endothelial cell adhesion molecule)	Fixation	acetone, 10 min, -20°C
	Blocking	1:20 donkey-serum in PBS, 1 h, RT
	Primary antibody	undiluted, 1 h, RT
	Secondary antibody	1:500 donkey α-rat Cy3 in PBST
	Nuclei staining	1:2000 Yopro1 in PBST, 5 min, RT
VEGFR-2 (endothelial receptor tyrosine kinase)	Fixation	acetone, 10 min, -20°C
	Blocking	1:20 donkey-serum in PBS, 1 h, RT
	Primary antibody	undiluted, 1 h, RT
	Secondary antibody	1:500 donkey α-rat Cy3 in PBST
	Nuclei staining	1:2000 Yopro1 in PBST, 5 min, RT

For routine histology analysis, cryosections of the same eight representative tumours of Th1 cell treated and control mice from day 18 after tumour cell injection were stained automatically with hematoxylin/eosin (H&E) using the Varistain 24-4, Promounter RCM90, and an automatic coverslipping machine. By the alkaline hematoxylin, all basophilic cell and tissue structures, particularly the chromatin of cell nuclei, are stained blue. The acidic eosin stains acidophilic cell components such as cytoplasma and most intracellularly substances red.

2.17.2 Toluidin blue staining of mast cells

Frozen tumour sections of the same eight representative Th1 cell treated and control mice from day 18 after tumour cell injection were used for the proteoglycan staining with toluidine blue to detect mast cells. Therefore, sections were fixed in acetone for 10 min at RT and air dried. Staining of specimen was carried out in toluidine blue solution (0.1% (w/v) toluidine blue in dH_2O) for 10 min at RT. Sections were washed in dH_2O short-time, air dried, and mounted with Entellan (Merck).

2.17.3 Ki-67 staining of fixed paraffin-embedded tumour sections

Tumours obtained from mice at day 18 after tumour cell injection were fixed in 1% (w/v) paraformaldehyde (PFA). Using the Hypercenter XP, specimen were washed, dehydrated through a graded ethanol series, and impregnated in paraffin wax. With the Tes99 instrument tumours were cast into blocks. Specimen of four representative tumours of Th1 cell treated and control mice were cut into 7 µm sections and dried over night at 60°C for better adherence to the slide. For immunohistochemistry, slides were deparaffinised with the 24 stainer. For unmasking Ki-67, a cell proliferation-associated nuclear antigen, specimen were heated in target-retrieval solution (DakoCytomation) in a steamer for 15 min. After washing the slides in PBST, immunohistochemistry was performed as mentioned above (2.17.1), starting with peroxidase blocking. Ki-67 primary antibody was diluted (1:25) in antibody diluent (DakoCytomation) and sections were incubated for 1 h at RT. DAB was used as substrate.

2.18 Electron microscopy of tumours

Tumour samples for electron microscopy (EM) analysis were cut into small pieces and immediately fixed by immersion in 1.5% (w/v) glutaraldehyde in 0.1 M cacodylate buffer with 5% (w/v) sucrose for 2-4 h. After washing with 0.1 M cacodylate buffer with 7.5% (w/v) sucrose, specimen were given to Prof. Dr. Wolburg (Institute of Pathology, Tübingen) for further treatment, photographing, and analysis. Briefly, specimen were postfixed in cacodylate buffer containing 1% (w/v) OsO_4 for 1 h and dehydrated in ascending series of ethanol and propyleneoxide. For contrast enhancement they were bloc-stained in uranyl-acetate in 70% ethanol for 4 h and flat-embedded in Araldite (Serva). Using an ultramicrotome (Ultracut R, Leica) semi- (1 µm) and ultrathin sections (50 nm) were cut. Ultrathin sections were stained with lead citrate, mounted on copper grids, and finally analysed with a Zeiss EM 10 Electron microscope.

2.19 Protein chemical methods

2.19.1 Cell lysis and Wessel-Fluegge precipitation

For protein analysis HUVEC (p3, p4, p5) were seeded at 2 x 10^5 cells/well in a 6-well plate, grown to 80% confluency, and medium was changed with the appropriate concentrations of DMF and/or NAC; MCDB131 medium alone served as negative control. The next day cells were serum starved (0.3% (v/v) FCS in MCDB131) for 7 h and stimulated by adding 1% (v/v) ECGS, 40 µg/ml heparin, and 20 ng/ml VEGF. Cells were scraped directly into 80 µl 6 x SDS sample buffer with disruption of cell membrans by freeze-thawing in liquid nitrogen (3 times) or into 150 µl lysis buffer per well (Table 19).

Table 19. Treatment of cells for protein preparation.

Protein	Stimulation	Scraping in
p38	7 min	80 µl 6 x SDS sample buffer
p44/42	7 min	80 µl 6 x SDS sample buffer
mTor	30 min	150 µl lysis buffer

After cell lysis, proteins were precipitated according to Wessel-Fluegge [306]. Briefly, the cell suspension was vortexed with 600 µl methanol and 150 µl chloroform. After adding 450 µl dH_2O the cell suspension was vortexed again, centrifuged (13000 rpm, 1 min), and the upper organic phase was removed. Another 450 µl methanol were added, cells were vortexed, and centrifuged (13000 rpm, 2 min). After removal of the supernatant, the pellet was air dried and resuspended in 50-80 µl 6 x SDS sample buffer for further use. Spectrophotometric quantitation of the amount of protein was performed using the Bradford method (BioRad).

To prevent proteolysis and also avoid heating artifacts specific protease inhibitors were used during protein isolation.

Table 20. Buffers used for protein sample preparation.

Lysis buffer	1 mM EDTA 0.005% (v/v) Tween 20 0.5% (v/v) Triton X 5 mM NaF 6 M urea Before use: 25 µg/ml leupeptin 25 µg/ml pepstatin 100 µM PMSF 3 µg/ml aprotinin 2 mM sodium orthovanadate
6 x SDS sample buffer (pH 6.8)	300 mM Tris 45% (v/v) glycerol 300 mM SDS 48 mM dithiothreitol (DTT) 0.15% (w/v) bromophenolblue dH_2O

2.19.2 Spectrophotometric quantitation of proteins (Bradford)

Quantitation of the amount of sample protein contained in solution was accomplished using a colorimetric method, the Bradford method [307]. This method is based upon binding of the dye Coomassie brilliant blue G-250 to an unknown protein. Quantification is possible if this binding is compared to that of different amounts of a standard protein, usually BSA. This assay can be used to quantitate solutions with protein concentrations of 125 to 1000 µg/ml and was performed according to the manufacturer's instruction manual (BioRad).

2.19.3 Electrophoretic separation of proteins

For separation of proteins, discontinuous sodium dodecyl sulfate polyacrylamide gel electrophoresis (SDS-PAGE) was performed. Proteins were denatured by heating in the presence of SDS and 2-mercaptoethanol or dithiothreitol (DTT) to reduce disulfide bonds. Proteins bind SDS in a constant weight ratio and migrate in the polyacrylamide gel according to size in response to an electrical field. Addition of ammonium persulfate initiates the polymerisation of monomeric acrylamide, leading to polyacrylamide gels. *N,N,N',N'*-Tetramethyl-ethane-1,2-diamine (TEMED) which catalyses the formation of free radicals from ammonium persulfate accelerates this reaction (according to [308]).

Electrophoresis was performed using mini gels (Protean II) and a discontinuous buffer system [309]. The separating gel was poured between a glass-plate sandwich, consisting of two clean glass plates and two 0.75-mm spacers, and covered with ethanol to form a flat interface. The desired percentage of acrylamide in the separating gel depends on the molecular size of the proteins being separated (Table 21/22).

Table 21. SDS gel concentrations used for specific proteins.

protein	acrylamide concentration and size of protein
p38	12.5%, 38 kDa
p44/42	15-18%, 42/44 kDa
mTor	7.5%, 180 kDa

Table 22. Molecular size of proteins which can be separated by SDS-PAGE [310].

Acrylamide (%)	Size of fragments separated (bp)	Size of fragments separated (kDa)
5.0	100 to 500	26 to 130
8.0	60 to 400	16 to 105
12.0	50 to 200	13 to 52
20.0	5 to 100	2 to 26

After polymerisation the ethanol layer was removed, the stacking gel was poured, and a 0.75-mm Teflon comb was inserted into the layer of stacking gel solution. After polymerisation the glass-plate sandwich was secured in an electrophoresis apparatus and the electrophoresis tank was filled with running buffer. After sample proteins were boiled in 6 x SDS sample buffer (5 min at 95°C), 25 µl of the protein solutions and 5-10 µl of specific molecular markers (visible and fluorescent) were applied to gel lanes. Gels were run at 90-120 V for 1-2 h until the desired resolution was obtained.

Table 23. Preparation of separating and stacking gel.

	Separating gel			Stacking gel
	Final acrylamide concentration (%)			
Stock solution	7.5	12.5	15	3.9
30% acrylamide/0.8% bisacrylamide (ml)	4.30	7.10	10.00	1.20
separating/stacking gel buffer (ml)	4.25	4.25	5.20	2.25
H_2O (ml)	8.20	5.40	4.60	5.30
10% (w/v) ammonium persulfate (µl)	150	150	200	100
TEMED (µl)	8.5	8.5	8.5	15.0

Table 24. Buffers used for SDS gel electrophoresis.

Separating gel buffer (pH 8.8)	1.5 M Tris 15 mM SDS dH_2O
Stacking gel buffer (pH 6.8)	0.5 M Tris 15 mM SDS dH_2O
Running buffer	24.8 mM Tris 3.5 mM SDS 0.2 M glycine dH_2O

2.19.4 Electroblotting and Western blot analysis

Proteins separated by SDS-PAGE were electroblotted onto a polyvinylidene difluoride (PVDF) membrane (Hybond P, pore size 0.2 µm, Amersham Biosciences) in a semidry transfer unit. Therefore, one sheet of a semidry buffer-soaked Whatman filter paper (Biometra) was placed on the anode, followed by the methanol-equilibrated membrane, the gel, and one more sheet of the semidry buffer-soaked filter paper. After removing air bubbles between membrane and filter paper, transfer of proteins was obtained by applying a maximum current of 0.8 mA per cm^2 of gel area according to the manufacturer's instructions (Amersham Biosciences) for 60-90 min (Table 25).

Table 25. Blotting time of specific proteins.

protein	Blotting time
p38	1 h
p44/42	1 h
mTor	1.5 h

Subsequently, transferred proteins that are bound to the surface of the membran can be analysed by immunoblotting (Western blotting) [311]. To identify specific antigens, the non-specific binding sites on the membrane were blocked by immersing the membrane in a PBST solution containing 5% (w/v) nonfat dry milk for at least 1 h at RT or over night at 4°C. Then, the membrane was stained with a specific primary antibody directed against specific antigens over night at 4°C in 5% (w/v) nonfat dry milk or BSA in PBST. The blot was washed three times with PBST. The secondary anti-IgG antibody was tagged with alkaline phosphatase enzyme (Amersham) and remained on the membrane for 1 h at RT. After washing the membrane again, the specific proteins were detected using the fluorescent substrate ECF (Amersham). Fluorescence scanning at 570 nm was performed using a phosphoimager. The image was recorded and the protein concentration was quantitated by densitometry using Image Quant.

Table 26. Buffers used for immunoblotting and western blot analysis.

Semidry buffer	48 mM Tris 39 mM glycine 1.3 mM SDS 20% (v/v) methanol dH_2O
PBS	2.6 mM KCl 1.5 mM KH_2PO_4 136.9 mM NaCl 10.1 mM Na_2HPO_4 dH_2O
PBST	0.1% (v/v) Tween 20 PBS

2.19.5 Enzyme-linked immunosorbent assay

With the Enzyme-linked immunosorbent assay (ELISA) every protein of interest can be detected in cell lysates depending on the used antibody. The ELISA is also used to measure the accumulation of a distinct cytokine secreted into a cell culture supernatant over an incubation period of 12-48 h. For detection of phosho-p38 in cell lysates, IFN-γ, and IL-4 in supernatants sandwich ELISAs were performed according to the manufacturers' instructions (R&D Systems, BD Biosciences). A 96-well microplate was coated with a capture antibody specific for the proteins to be detected. After blocking unspecific binding sites, a standard of the target protein and the samples were loaded in duplicates onto the plate. Specific proteins were detected with a biotinylated detection antibody, following Streptavidin-HRP, determination of the optical density of each well using a microplate reader set to 450 nm, and subsequent calculation of the protein content.

HUVEC (p3, p4, p5) were grown over night with appropriate concentrations of DMF. Cells were serum starved (1% (v/v) FCS in MCDB131) for 6 h. After stimulation of cells with 1% (v/v) ECGS, 40 µg/ml heparin, and 20 ng/ml VEGF for 7 min cells were scraped directly into 100 µl cell lysis buffer for analysis of the phospho-p38 content.

For IFN-γ and IL-4 ELISA LN T cells (0.1 x 10^6 cells/well) were stimulated with 1) APC alone (0.5 x 10^6 cells/well), 2) APC and EpCAM (1 µg/ml), 3) medium as negative control, and supernatants were collected after 48 h for further analysis.

2.20 *In vitro* and *in vivo* angiogenesis assays

2.20.1 Proliferation assay through BrdU incorporation

There are numerous assays for measuring cell proliferation, for example the thymidine incorporation assay and the 5-bromo-2'-deoxyuridine (BrdU) incorporation assay. The exposure of cells to the pyrimidine analogue BrdU causes proliferating cells to incorporate BrdU into their DNA. So, measuring the BrdU uptake directly correlates the amount of DNA synthesis and the number of cells in culture.

HUVEC or HLMEC were seeded at 7500 cells/well in a 96-well plate in triplicates. After 8 h, cells were stimulated by adding 1% (v/v) ECGS, 40 µg/ml heparin, and 20 ng/ml VEGF, or 100 ng/ml VEGF alone. In combination with the stimulating mixture the appropriate concentrations of DMF and/or NAC or glutathione monoethyl-glycyl ester (GSH-OEt) were added. MCDB131 medium containing 5% (v/v) FCS for HUVEC, or 2% (v/v) FCS for HLMEC served as negative control. After 12 h stimulation, BrdU was added and after 16 h of incubation the proliferation was measured by BrdU incorporation according to manufacturer's instructions (Amersham Biosciences).

2.20.2 Migration assay - Scratch-wound assay

Several assays can be used to determine the migratory response of EC to angiogenic factors, for example modified Boyden chamber experiments. Here, we used a different approach based on the idea that EC migration represents a pivotal event of wound healing *in vivo* [312].

Therefore, HUVEC were grown to confluency. A migration gap was created by introducing a scratch on the monolayer using a sterile pipette tip. For stimulation of cells 1% (v/v) ECGS, 40 µg/ml heparin, and 20 ng/ml VEGF alone or in combination with the appropriate concentrations of DMF were added. MCDB131 medium with 5% (v/v) FCS served as negative control. After an incubation period of 9 h, cells were fixed with 1% (w/v) PFA and stained with crystal violet (0.5% (w/v) crystal violet (Roth) and 20% (v/v) methanol in PBS).

After growing HMLEC to confluency they were serum starved (5% (v/v) FCS in MCDB131) for 5 h before introducing a scratch. Stimulation of HMLEC was identical to HUVEC but HMLEC were grown over night and then fixed.

Cells in the migration gap were counted microscopically in nine different areas per plate on the basis of phase-contrast micrographs at 0 h and at 9 h for HUVEC, and at 16 h for HMLEC.

2.20.3 Sprout formation assay

This angiogenesis assay allows three-dimensional neovessel formation *in vitro*. It was performed as described elsewhere [313]. Briefly, HLMEC were seeded on cytodex-3 microcarrier beads (SigmaAldrich) and embedded into a three-

dimensional fibrin gel (SigmaAldrich) containing 20 ng/ml VEGF either alone or in combination with DMF and/or NAC or GSH-OEt in triplicates. Fibrin gels without growth factors served as a negative control. Cross-linking of fibrinogen and polymerisation of fibrin was started by adding 0.65 U/ml thrombin (SigmaAldrich). Thereafter, gels were incubated in MCDB131 containing the appropriate concentrations of VEGF, DMF, and/or NAC, or GSH-OEt, 5% (v/v) FCS, 5% (v/v) human serum, and 200 U/ml trasylol (Bayer). After 24 h, the gel was fixed in 1% (w/v) PFA and the number of sprouts per 50 beads was counted microscopically.

2.20.4 Chick choreoallantoic membrane assay

Among the *in vivo* systems the chick choreoallantoic membrane (CAM) assay is a technically simple and inexpensive approach to study angiogenesis and demonstrates a functional assay to test pro- and antiangiogenic factors. The CAM assays were performed *in ovo* as described elsewhere [314, 315]. Briefly, after aspiration of 2 ml of egg white of fertilized hen's eggs to minimize adhesion of the shell membrane, a window was cut into the eggshell on embryonic day 3. The eggs were resealed with a tape and further incubated at 37°C in humidified air until day 7. Whatman filters containing the appropriate DMF concentrations were placed onto E7 CAMs and incubated for three days. Filters with DMSO alone served as a negative control. For documentation, a stereo microscope with camera adaptor was used to take photographs.

2.21 Statistical analysis

Differences between experimental groups were determined with an unpaired Mann-Whitney test using SPSS software (Chicago, Illinois). *P* values of < 0.05 were considered statistically significant.

3 Results

3.1 The effects of tumour antigen-reactive Th1 cells on tumour growth and angiogenesis

3.1.1 Adoptive transfer of tumour-reactive Th1 cells leads to an inhibition of tumour growth *in vivo*

It was previously shown that it is possible to generate IFN-γ producing Th1 cells against the tumour-associated antigen (TAA) EpCAM which is differentially expressed on human gastrointestinal tumours including colon cancer [97, 316], from immunised mice *ex vivo*. Generation of such EpCAM-reactive INF-γ producing Th1 cells required priming of $IL4^{-/-}$ BALB/c mice, and subsequent *in vitro* stimulation and expansion of the $CD4^{+}$ T cells with EpCAM protein, CpG-oligodeoxynucleotides (ODN), APC, and IL-2 [99]. Adoptive transfer of these EpCAM-reactive Th1 cells provided solid protection against intravenously injected EpCAM-expressing tumours whereas Th2 cells failed (R. Mocikat, H. Braumüller, unpublished data).

To investigate the therapeutic mechanisms underlying the Th1 cell-mediated immunotherapy, we first adapted the therapy to a subcutaneous tumour model. We injected murine colon carcinoma cells (1.5×10^6) that stably expressed EpCAM (CT26-EpCAM) into the right and left flank of syngeneic BALB/c mice on day 0 (Fig. 5). After three days, mice were irradiated to induce a mild inflammatory response and hence, to amplify the capacity of T cells to infiltrate the tumour [171]. On day 4, EpCAM-reactive Th1 cells (5×10^6) were injected intraperitoneally into the tumour bearing mice. The control group received PBS (Fig. 5).

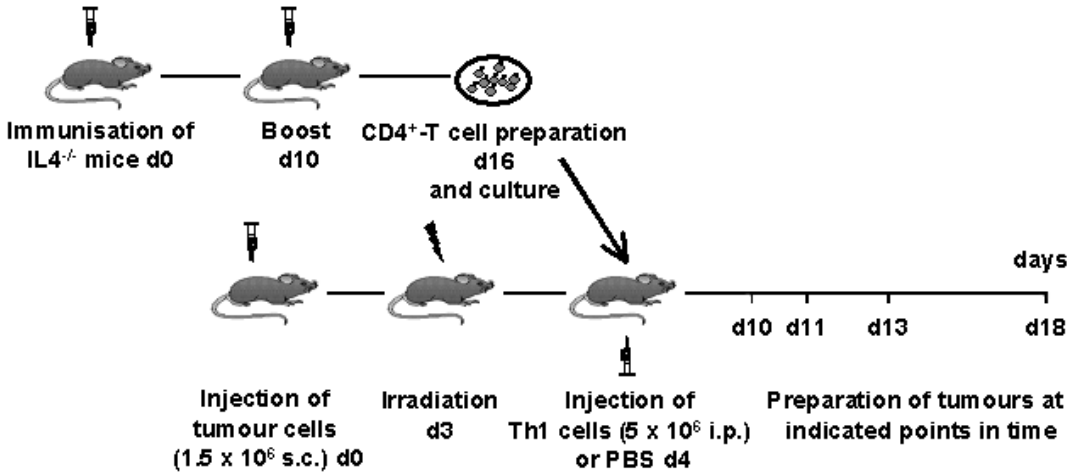

Figure 5. Schematic outline of the experimental strategy.

For generation of EpCAM-reactive Th1 cells, $CD4^+$ T cells from immunised $IL4^{-/-}$ BALB/c mice were stimulated with EpCAM protein *in vitro* in the presence of the Toll-like receptor (TLR)-9 ligand CpG1668 to enhance IL-12 production by APC [99, 317]. Cells were expanded for 14 days in medium containing IL-2 (50 U/ml) and then characterised by flow cytometry for representative Th1 and Th2 cytokines before adoptive transfer. The majority of cells was CD4 positive and about 30% of the $CD4^+$ T cell population produced IFN-γ (Fig. 6A). No IL-4 and only few IL-10 expressing cells were detectable (Fig. 6A) confirming the Th1 phenotype of the T cells. Th1 cells which were gained from lymphnodes of immunised $IL4^{-/-}$ BALB/c mice and were stimulated and expanded for 14 days *in vitro*, were used for an IFN-γ ELISA showing the reactivity of Th1 cells against EpCAM protein (Fig. 6B).

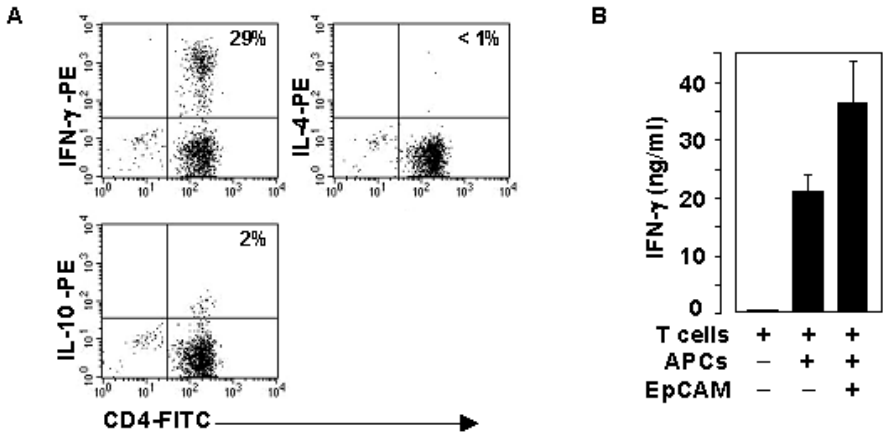

Figure 6. Characterisation of generated T cells. A, Flow cytometric analysis of generated T cells. Cultured cells were stimulated with PMA/Ionomycin, stained with surface anti-CD4 and intracellularly with anti-IFN-γ, anti-IL-4, or anti-IL-10, respectively, showing the Th1 phenotype of EpCAM-primed T cells. Representative dot plots are shown. Numbers indicate the percentage of cells in the particular fluorescence window. B, Representative IFN-γ ELISA of lymphnode-derived EpCAM-primed Th1 cells, showing the reactivity of Th1 cells against EpCAM protein.

To determine the impact of such $CD4^+$ Th1 cells on MHC-class II negative CT26-EpCAM tumours, we first measured tumour growth with a sliding calliper on days 10, 13, and 17 after tumour cell injection and calculated the tumour area. Until day 10, the Th1 cell treated and the PBS treated group showed similar tumour growth dynamics. From day 13 on, the group that had received the adoptive Th1 cell therapy showed a significant inhibition of tumour growth (Fig. 7).

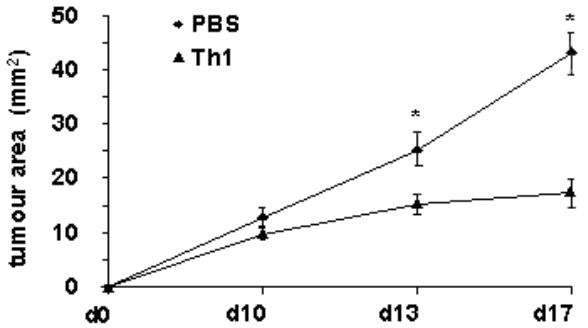

Figure 7. Determination of the therapeutic effect of adoptively transferred tumour-reactive Th1 cells on tumour growth. Tumours from Th1 cell treated (d10: n = 34; d17: n = 34; d13: n = 24) and PBS treated (d10: n = 22; d17: n = 22; d13: n = 12) mice were measured with a sliding calliper and tumour area was calculated as product of perpendicular tumour diameters (*: $p < 0.05$). Data revealed an inhibitory effect of the adoptive Th1 cell transfer on tumour growth from day 13 on. Error bars denote standard error of the mean (SEM).

To analyse the mechanisms underlying this inhibitory effect, tumours were harvested on days 10, 11, 13 and 18 after tumour cell injection. First, we determined the tumour weight and secondly, the intra-tumoural cytokine patterns were analysed. On day 18, we found a 40-84% reduction of tumour weight in the Th1 cell treated mice compared to control tumours (Fig. 8A). In contrast, on day 11, there was only a slight, non-significant decrease of tumour weight in the Th1 cell treated group (Fig. 8A). To evaluate the onset of the therapy in more detail, the tumour weight was determined on day 10 and day 13 after tumour cell injection in an independent experiment. We found a prominent decrease of tumour weight in Th1 cell treated mice compared to PBS treated mice on day 13 (Fig. 8B). On day 10, we detected a not significant increase of tumour weight in Th1 cell treated mice compared to PBS treated mice (Fig. 8B). These results indicate that the growth inhibition due to the therapy started between day 10 and day 13.

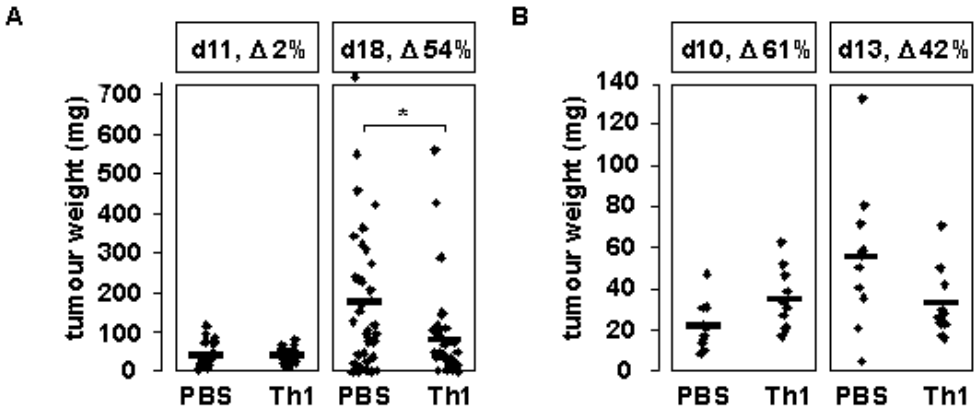

Figure 8. Adoptive transfer of tumour-reactive Th1 cells leads to inhibition of tumour growth. A, The inhibition of tumour growth is shown by analysing the tumour weight of Th1 cell and PBS treated mice on day 11 (n = 22) and day 18 (n = 34) after tumour cell injection (*: $p < 0.05$). B, The difference in tumour weight on day 10 (n = 10) and day 13 (n = 10) after tumour cell injection is shown from one experiment out of three. Δ: reduction or increase of tumour weight in Th1 cell treated mice compared to PBS treated mice.

To ensure that the tumour growth inhibition was caused by the adoptive transfer of EpCAM-reactive Th1 cells, CT26-EpCAM tumour bearing mice were treated with ovalbumin (OVA)-specific Th1 cells. Therefore, $CD4^+$ T cells were isolated from transgenic DO11.10 mice which express the TCR specific for the chicken OVA peptide. Cells were stimulated with OVA peptide and APC *in vitro* and the Th1 cell phenotype was confirmed by flow cytometry (Fig. 9A). The adoptive transfer of OVA-Th1 cells did not inhibit tumour growth (Fig. 9B), demonstrating that specific, tumour-antigen reactive Th1 cells were required for the inhibition of CT26-EpCAM tumour growth *in vivo*.

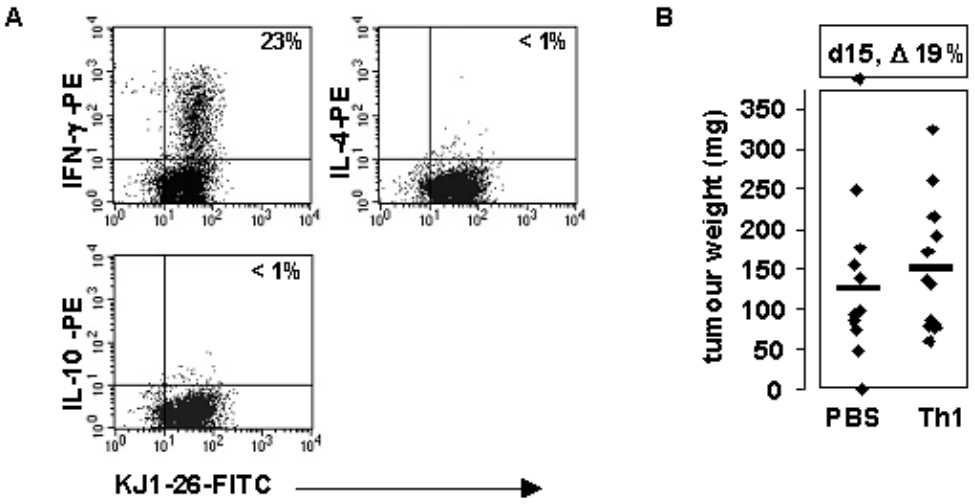

Figure 9. Adoptive transfer of OVA-primed Th1 cells shows no inhibition of tumour growth. A, Flow cytometric analysis of generated T cells. Cultured OVA-primed T cells were stimulated with PMA/Ionomycin, stained with surface anti-KJ1-26 (specific for the TCR expressed on DO11.10 mice) and intracellularly with anti-IFN-γ, anti-IL-4, or anti-IL-10, respectively, for Th1 and Th2 cytokines showing the Th1 phenotype of the OVA-primed cells. Representative dot plots are shown. Numbers indicate the percentage of cells in the particular fluorescence window. B, OVA-primed Th1 cells were injected in CT26-EpCAM tumour bearing mice. No difference in tumour weight (n = 12) was observed. Δ: increase of tumour weight in the Th1 cell treated group compared to the PBS treated group.

3.1.2 Upregulation of Th1 associated cytokines and angiogenesis regulatory genes after adoptive Th1 cell transfer

To analyse the mechanisms by which the adoptive transfer of tumour-antigen reactive Th1 cells led to the profound inhibition of tumour growth we examined the intra-tumoural gene expression profile at different points in time. Therefore, four major groups of genes were investigated that may interfere with tumour growth at different levels: 1) genes of the Th1/Th17 cytokine family, 2) genes associated with innate inflammation, 3) genes associated with angiogenesis and 4) genes associated with the cell cycle.

Since we injected IFN-γ producing Th1 cells for therapy, the first group of genes analysed were Th1/Th17 associated genes such as IFN-γ [157], IL-12, IL-23, IL-27 [199, 208], and IL-6. Moreover, IFN-γ inducible genes such as IP-10/CXCL10, Mig/CXCL9 [192, 193] and their receptor CXCR3 (CD183) which is preferentially expressed on Th1 cells but also on NK cells, DC, and macrophages were analysed [318, 319].

The second group reflected genes which are associated with innate inflammation. The adhesion molecules ICAM-1 and VCAM may contribute to the therapeutic effect as they are upregulated in EC during inflammation and are required for rolling and adhesion of leukocytes to support their infiltration [320].

Tumour growth depends on blood vessel formation. Therefore, genes associated with angiogenesis such as VEGF, PIGF, Ang-1, and Ang-2 were analysed in the third group [19, 46, 77, 321]. Moreover, IL-12, IL-27, IP-10/CXCL10, and Mig/CXCL9 are cytokines/chemokines that exhibit antiangiogenic properties [216, 234].

Markers associated with cell proliferation or growth arrest such as the oncogene c-Myc and its target gene Cyclin D2, a protein involved in cell cycle progression, were analysed in the last group [322-325].

Tumours were harvested at different points in time after tumour cell injection and total RNA was extracted from single tumours for PCR and quantitative real-time PCR analysis. First, we analysed different candidates of house keeping genes by semiquantitative PCR and found that hypoxanthine-guanine phosphoribosyl-transferase (HPRT) in contrast to glyceralehyde-3-phosphate dehydrogenase (GAPDH) and Aldolase was not regulated in our tumour model. Therefore, HPRT served as house keeping gene in our system (Fig. 10).

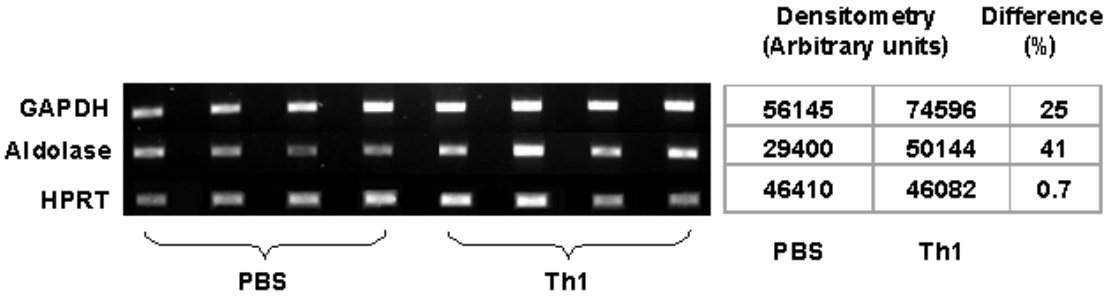

	Densitometry (Arbitrary units)		Difference (%)
GAPDH	56145	74596	25
Aldolase	29400	50144	41
HPRT	46410	46082	0.7
	PBS	Th1	

Figure 10. Analysis of different house keeping genes by semiquantitative PCR. On day 18 after tumour cell injection representative tumours (n = 4) from Th1 cell treated and PBS treated mice were analysed for different house keeping genes by PCR and gel images were densitometrically evaluated. HPRT (cycles: 20) expression in tumours compared to GAPDH (cycles: 18) and Aldolase (cycles: 20) showed no difference between Th1 cell treated and PBS treated mice by densitometry, pointing out that HPRT is not regulated in our model system.

Real-time PCR data showed that Th1-associated and immunoregulatory genes were upregulated in Th1 cell treated tumours from day 11 onwards, peaking on day 13 (Fig. 11A). The most pronounced upregulation was found for IL-23/p19 and IL-12/p35 on day 13 after tumour cell injection in Th1 cell treated tumours (Fig. 11A) whereas the expression of the corresponding subunit p40 was only slightly changed (Fig. 11B). Elevated levels of IFN-γ were found and the therapy also increased levels of ICAM-1, IL-6, and IL-27/Ebi3 (Fig. 11A) whereas the subunit IL-27/p28 remained almost unchanged (Fig. 11B). Surprisingly, we also found a very late downregulation of VCAM in Th1 cell treated tumours at day 18 after tumour cell injection (Fig. 11B). In contrast, the therapy did not influence the expression of the angiogenesis associated genes VEGF and IP-10/CXCL10 (Fig. 11B). Moreover, semiquantitative PCR data showed that the expression of Ang-1, Ang-2, PIGF, Mig/CXCL9, and CXCR3 was also similar in both groups (Fig. 11C). The expression of neither c-Myc nor Cyclin D2 was affected by the

therapy at any of the times analysed (Fig. 11B). In summary, these data suggest an important role for cytokines of the IL-6 family in tumour growth inhibition after Th1 cell transfer.

A

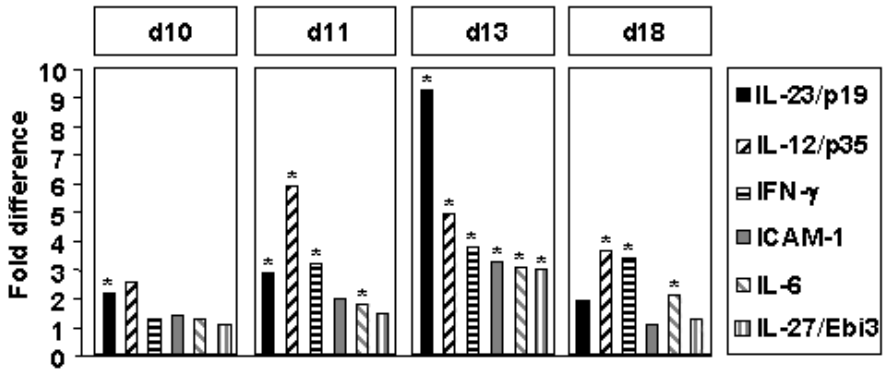

B

	d10	d11	d13	d18
IL-12/p40	n.a.	1.3	1.9	1.2
IL-27/p28	n.a.	2.1	1.8	1.8
VEGF	n.a.	1.5	n.a.	1.0
IP10	n.a.	1.5	1.0	1.3
VCAM	1.4	1.3	1.6	-2.1
c-Myc	1.1	1.2	1.3	1.2
Cyclin D2	n.a.	1.4	1.5	1.4

C

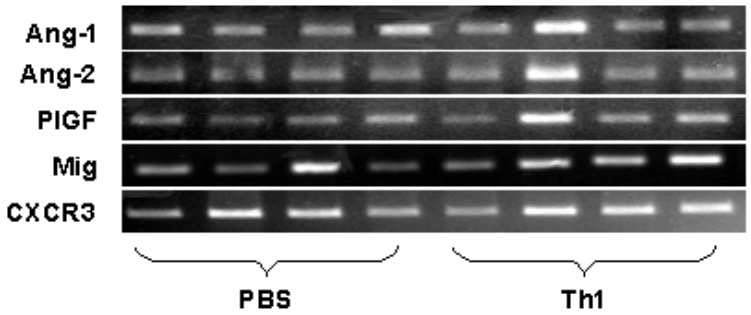

Figure 11. Gene expression analysis of tumours by PCR at different points in time. A, B, In real-time PCR analysis multiplex reactions were run in triplicates and samples were normalized to the house keeping gene HPRT. Relative expression of genes of interest is represented as fold differences of the mean of Th1 cell treated mice (d10: n = 10; d11: n = 10; d13: n = 10; d18: n = 9) over PBS controls (d10: n = 10; d11: n = 10; d13: n = 8; d18: n = 9) with highest levels on day 13 (*: $p < 0.05$). B, Genes found only slightly or not regulated by real-time PCR analysis. Fold differences of the mean of Th1 cell treated over PBS controls are shown (n.a.: not analysed). C, Semiquantitative PCR data showed that the expression of analysed genes was similar in both groups.

3.1.3 Prevention of Th1 cell suicide with anti-IFN-γ antibody further promotes tumour growth inhibition by Th1 cells

The upregulation of IFN-γ and the IFN-γ inducible cytokine IL-12 in tumours after Th1 cell transfer suggests that the therapeutic effects might be IFN-γ dependent. To block the IFN-γ mediated suicide of Th1 cells [326], we treated tumour bearing mice with 500 µg anti-IFN-γ monoclonoal antibody (mAb) one day before adoptive transfer of EpCAM-reactive Th1 cells. In agreement with the suicide hypothesis [326], we observed an even stronger reduction of tumour growth in mice receiving the combined injection of Th1 cells and anti-IFN-γ mAb (Fig. 12A) compared to mice either treated with Th1 cells alone or with PBS on day 17 after tumour cell injection. Reduced tumour growth was associated with an even stronger upregulation of IFN-γ in tumours of mice with combined Th1 cell and anti-IFN-γ therapy as compared to mice with PBS treatment (Fig. 12B). Tumours treated with Th1 cells alone also showed an upregulation of IFN-γ compared to control tumours but to a much lesser extent than the Th1 cell and anti-IFN-γ treated group. The other cytokines remained comparable between the Th1 cell and anti-IFN-γ mAb treated group and the group treated with Th1 cells alone (Fig. 12B).

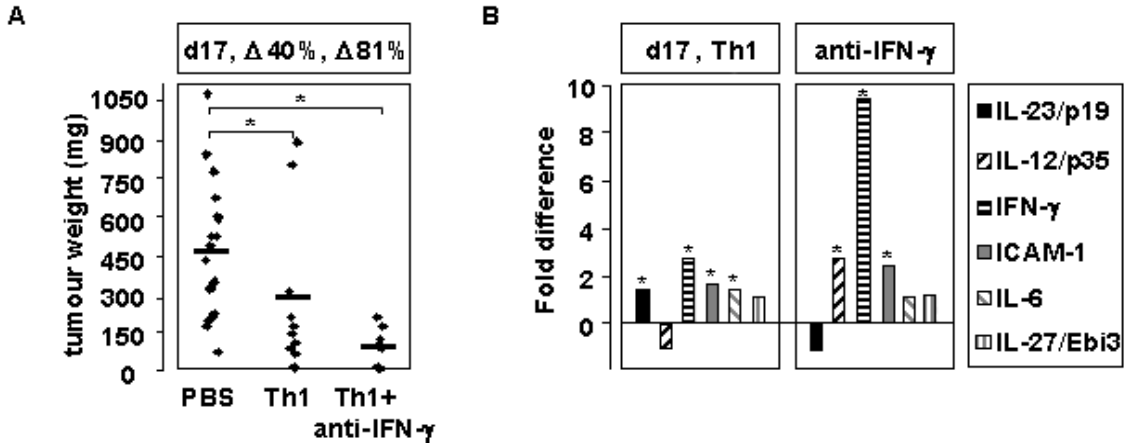

Figure 12. Combined Th1 cell and anti-IFN-γ treatment leads to further reduction of tumour growth. A, On day 3, mice were irradiated, treated with 500 µg anti-IFN-γ antibody, and on day 4, EpCAM-reactive Th1 cells were injected. Tumour weight of PBS treated (n = 18), Th1 cell treated (n = 10), and combined treated (n = 8) mice was analysed on day 17. Δ: Reduction of tumour weight of Th1 cell treated mice compared to PBS controls (*: $p < 0.05$). B, Real-time PCR data of tumours. Multiplex reactions were run in triplicates and samples were normalized to the house keeping gene HPRT. Relative expression of genes of interest is represented as fold differences of the mean of Th1 cell treated mice (n = 7) or combined treated mice (anti-IFN-γ, n = 6) over PBS controls (n = 14) on day 17 after tumour cell injection. A strong upregulation of IFN-γ was found in tumours treated with both Th1 cells and anti-IFN-γ mAb (*: $p < 0.05$).

Since we found inflammatory cytokines upregulated in tumours of Th1 cell treated mice, we further investigated the differentiation of the developing T cells into either Th1 or Th17 cells *in vitro*. Th17 cells can regulate tissue inflammation through production of IL-17, a pro-inflammatory cytokine [239, 242]. As expected from the priming protocol using CpG-ODN [327, 328], we found cells expressing IL-17 in the EpCAM-reactive Th1 cell culture. Yet, the IFN-γ producing T cells repeatedly exceeded the number of IL-17 producing cells about 3 fold (Fig. 13).

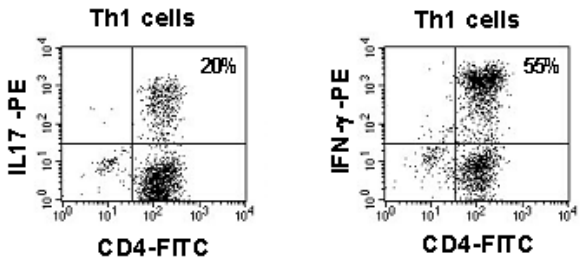

Figure 13. Further analysis of the Th1 cell population used for therapy. *In vitro* flow cytometric analysis of $CD4^+$ T cells, stimulated with PMA/Ionomycin, stained with surface anti-CD4 and intracellularly with anti-IL-17 or anti-IFN-γ, respectively, revealing IL-17 expressing cells in the EpCAM-reactive Th1 cell culture. Representative dot plots are shown.

Next, we investigated whether IL-17 expression in tumours might be relevant for therapy. Quantitative real-time PCR revealed significantly upregulated levels of IL-17 in tumours of Th1 cell treated mice compared to PBS treated mice on day 13 and day 18 after tumour cell injection (Fig. 14A), suggesting that IL-17 producing cells might be involved in the therapy. However, on day 17, the IL-17 expression was reduced in tumours of mice receiving the combined injection of Th1 cells and anti-IFN-γ mAb compared to tumours of mice treated with Th1 cells alone (Fig. 14B). This furthermore supports the suicide hypothesis [326] and argues in favour of preferential expansion of Th1 cells.

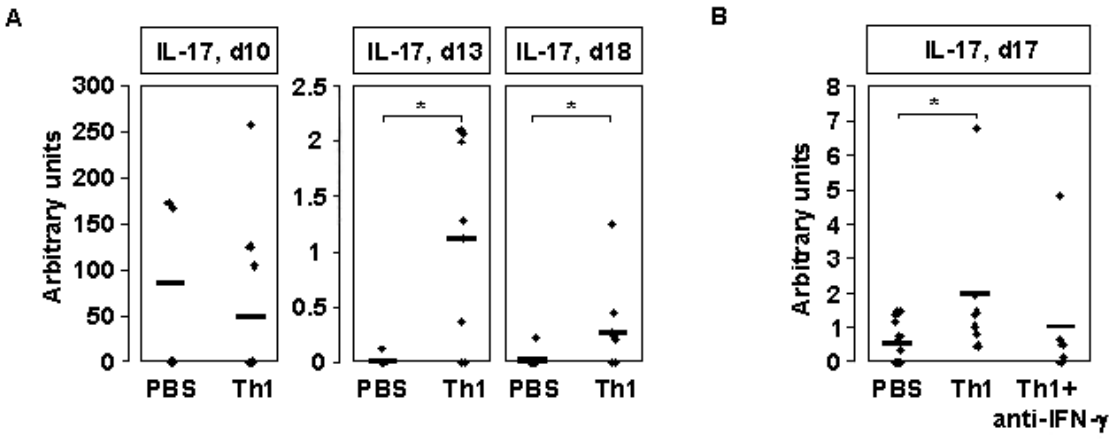

Figure 14. Real-time PCR data of tumours. A, IL-17 expression in tumours of Th1 cell treated (d10: n = 10; d13: n = 8; d18: n = 9) and control mice (d10: n = 10; d13: n = 7; d18: n = 12) on days 10, 13, and 18 showing an increase of IL-17 in tumours of Th1 cell treated mice from day 13 on (*: $p < 0.05$). B, IL-17 expression data is shown from tumours treated with Th1 cells (n = 6), Th1 cells and 500 µg anti-IFN-γ mAb (n = 7), or PBS (n = 14). Combined injection of Th1 cells and anti-IFN-γ led to a reduced IL-17 expression in tumours compared to tumours treated with Th1 cells alone.

3.1.4 Tumours are infiltrated by inflammatory cells

In our tumour model we found an upregulation of inflammatory cytokines in tumours of mice treated with Th1 cells. Therefore, we aimed to investigate which cells were responsible for the observed upregulation and characterised the cellular composition of the inflammatory infiltrate. We performed FACS analysis of tumours of Th1 cell treated and PBS treated mice on days 10, 13, and 18 after tumour cell injection. Infiltrating $CD4^+$ T cells increased over time in tumours of Th1 cell treated mice, peaking on day 18 with a 16-fold increase of $CD4^+$ T cells in tumours of Th1 cell treated mice compared to PBS controls (Table 27). Surprisingly, we found 5 times more $CD8^+$ T cells in control tumours than in tumours of Th1 cell treated mice on day 18, whereas the ratio was inverted on day 10. Interestingly, on day 18, $CD11b^+$ cells were found at a three times higher level in tumours of Th1 cell treated mice, but still neither $F4/80^+$ macrophages nor $CD11c^+$ infiltrating DC were detectable in both groups (Table 27). These data suggest that cells of the monocyte/macrophage lineage are involved in mediating the therapeutic effects. Since IL-12 and IL-23 are mainly produced by monocytes/macrophages [199, 208] and since upregulation of IL-12 and IL-23 was detected in tumours of Th1 cell treated mice, these data imply an activation of monocytes/macrophages due to Th1 cells and hence, a participation of these cells in the therapy by secreting tumour inhibiting cytokines within the tumour.

Table 27. Inflammatory infiltrate of tumours.

Tumour infiltrating hematopoetic cells (%)*	d10		d13		d18	
	control	Th1 cell treated	control	Th1 cell treated	control	Th1 cell treated
CD4	2.6	9.7	3.4	13.3	0.7	11.5
CD11b	1.0	1.4	2.1	3.1	0.7	2.2
CD8	0.1	0.4	0.9	1.3	2.7	0.5
F4/80	0.6	0.1	0.7	0.1	0.2	0.2
CD11c	1.5	1.3	1.4	0.8	1.9	0.9

Tumours (n = 10/group) from days 10, 13, and 18 after tumour cell injection were excised from mice, homogenized, and single cells were stained for different cell types. 30000 cells were acquired on the LSRII. Total living cells were gated and the percentage of infiltrating cells were calculated on the basis of 10000 cells (*).

Consistent with these findings immunohistochemical analysis of tumours of Th1 cell treated mice on day 18 after tumour cell injection showed a strong increase in $CD4^+$ T cells which were homogenously distributed throughout the tumour tissue (Fig. 15B). In contrast, in tumours of the control group only a few $CD4^+$ T cells were detectable (Fig. 15A). Otherwise, only minor differences in tumour morphology or necrosis were detectable (Fig. 15C, D). Histology of tumours revealed no obvious difference in mast cell occurrence (Fig. 15E, F), suggesting that mast cells were not involved in the therapy.

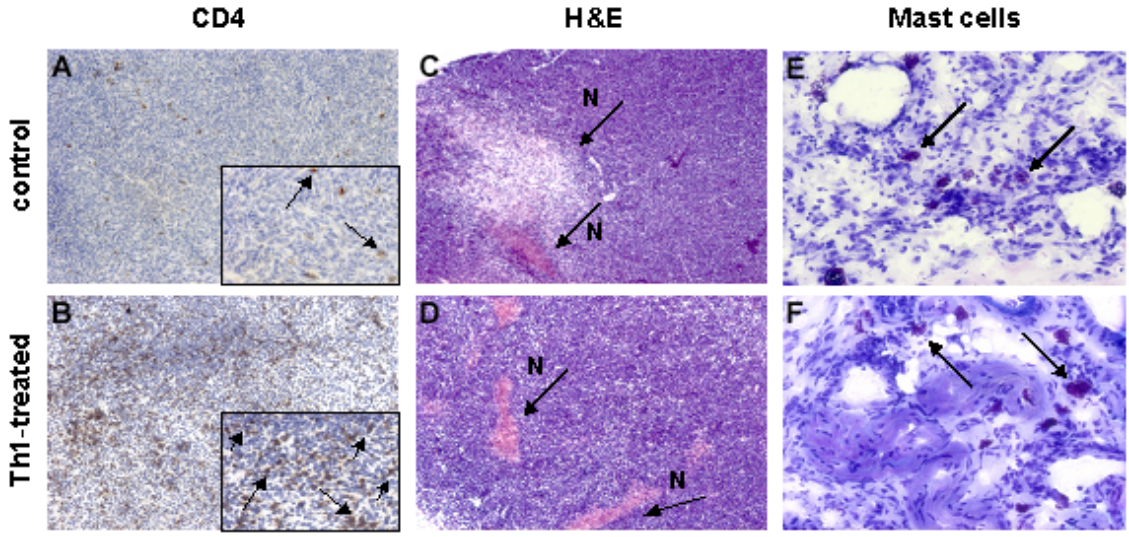

Figure 15. Immunohistochemical analysis of tumours. A-F, Serial sections of representative tumours (n = 8) of Th1 cell treated and control mice from day 18. A, B, Tumours were stained with monoclonal anti-CD4 antibody showing a strong increase in $CD4^+$ cells in tumours of Th1 cell treated mice. Arrows: $CD4^+$ cells. C, D, Staining with hematoxylin-eosin (H&E, right) showed no major differences in the morphology of the tumours. Necrosis (N) was detected in tumours of Th1 cell and PBS treated mice. E, F, Toluidin blue staining of tumours showed no difference in mast cell occurence. Arrows: Mast cells (purple). Pictures: x 100 magnification. Inlays: x 200 magnification.

Similarly, we found no differences in the proliferation rate between tumours of Th1 or PBS treated mice as determined by staining of the cell proliferation-associated nuclear antigen Ki-67 (Fig. 16).

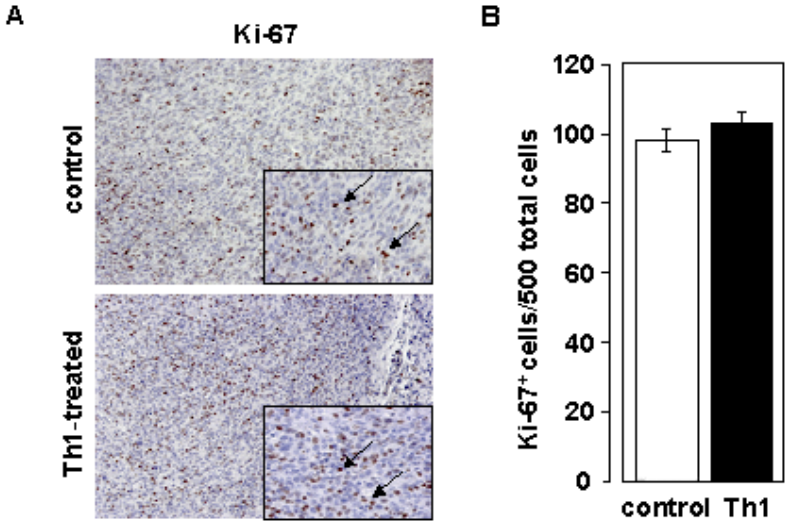

Figure 16. Immunohistochemical analysis of the proliferation rate of tumours. A, Serial sections of representative tumours (n = 8) of Th1 cell treated and control mice from day 18 were stained with monoclonal anti-Ki-67 antibody. Ki-67 staining showed no obvious differences in the proliferation rate of the tumours. Arrows: Ki-67 positive cells. Pictures: x 100 magnification. Inlays: x 200 magnification. B, Quantitative analysis of (A). Ki-67^{+} cells out of 500 total cells in tumour sections (n = 60) of Th1 cell and PBS treated mice were counted. Error bars denote standard error of the mean (SEM).

3.1.5 Tumour vessels are damaged by Th1 cell therapy

Cytokines such as IL-12 and IL-27 exert strong antiangiogenic properties not only due to IFN-γ production and subsequent induction of IP-10/CXCL10 and Mig/CXCL9 [192, 193, 218], but also by IFN-γ independent mechanisms [181, 219, 234]. As IL-12 and IL-27 were upregulated in tumours of Th1 cell treated mice and as tumour growth depends on new blood vessel formation, we investigated whether the Th1 cell therapy affected tumour angiogenesis. Immunohistological staining with a monoclonal antibody specific for the endothelial marker PECAM-1 showed no obvious differences in tumour vascularisation with homogenous vascularisation detectable in both groups (Fig. 17A-D). However, minor changes in vessel morphology such as clumpy and curved structures were observed in tumours of Th1 cell treated mice (Fig. 17B, D, arrows). The expression of the most important receptor of angiogenesis, VEGFR-2, was not restrained through the Th1 cell therapy since most of the tumour vessels were VEGFR-2 positive in both groups (Fig. 17E, F).

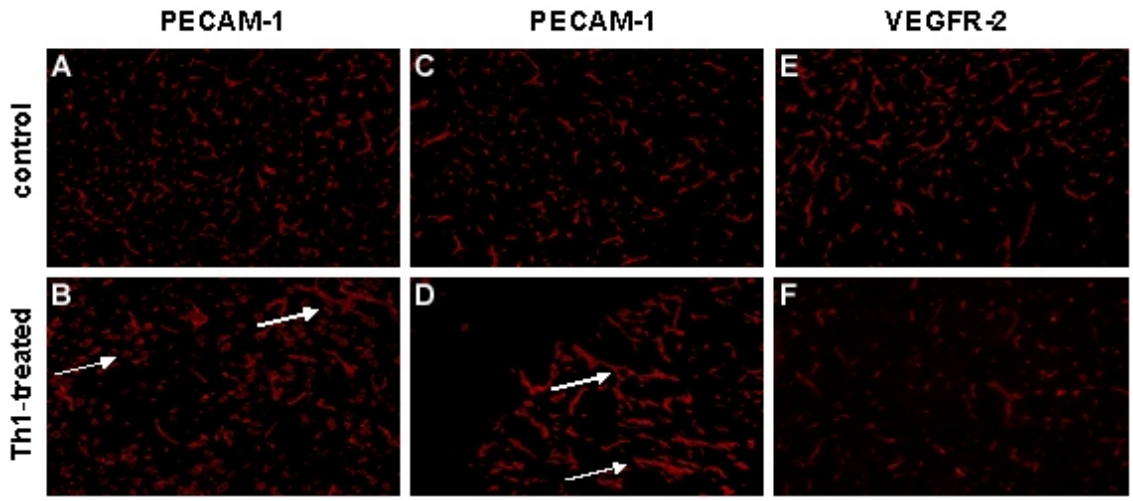

Figure 17. Tumour vessel staining. A-F, Serial sections of representative (n = 8) tumours of Th1 cell treated and control mice from day 18. A-D, Tumours were stained with monoclonal anti-PECAM-1 antibody showing homogenous vascularisation in both groups. However, minor changes in vessel morphology (arrows) and a minor decrease of tumour vessel density were detectable in tumours of Th1 cell treated mice (B, D) compared to control mice (A, C). E, F, Staining of tumours with monoclonal anti-VEGFR-2 antibody revealed no obvious change in the receptor expression pattern between both groups. Pictures: x 200 magnification.

In contrast, electron microscopy of tumours of Th1 cell treated mice revealed endothelial cell death, cytoplasma-enriched endothelia, and vessel obliteration (Fig. 18C-E), showing that tumour vessels in Th1 cell treated mice were severely impaired. In contrast, tumours in PBS treated mice (Fig. 18A, B) showed a typical tumour vascularisation [6, 13, 84]. Moreover, adjacent muscle tissue vessels remained unchanged in Th1 cell treated mice (Fig. 18F) suggesting that the Th1 cell therapy is restricted to the tumour tissue. Impaired vessel structure was associated with enhanced diapedesis in tumour tissue of Th1 cell treated mice as sign of inflammation (Fig. 18C, D).

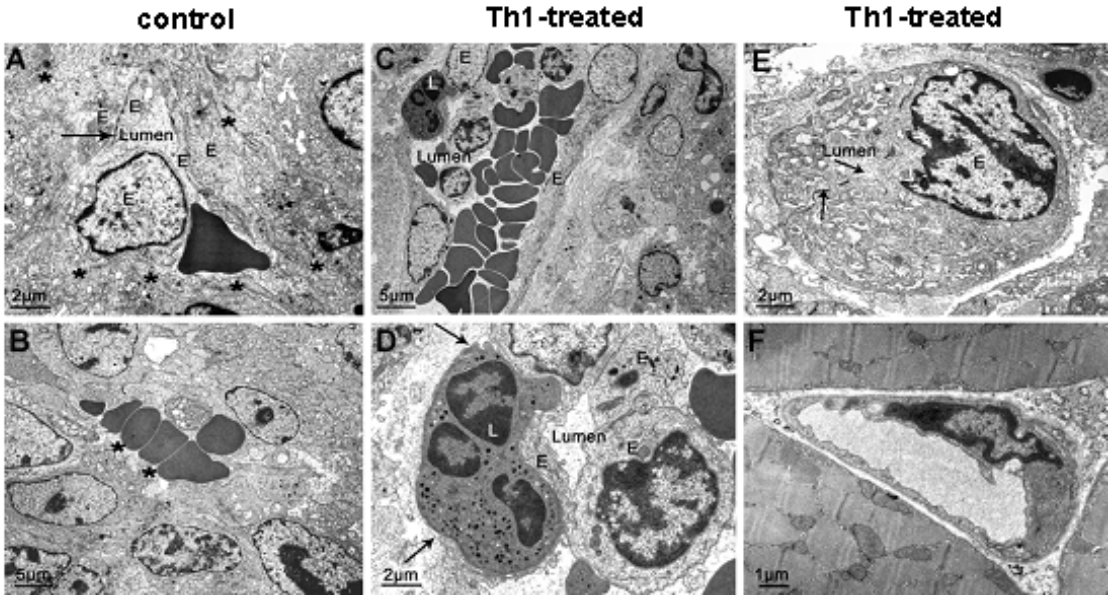

Figure 18. Electron microscopy of blood vessels. A, Blood vessels with a bulged endothelial cell body (E), tight junctions (arrow), and the basal lamina (labeled by asterisks). B, Blood lacuna without limiting endothelial cells but with extracellular matrix like collagen fibrils (asterisks) which are located between tumour cells and blood cells. C, Blood vessel with leukocyte (L) transendothelial migration. D, Higher magnification of (C) showing a transcellularly transmigrated leukocyte still covered by a basal lamina (arrow). E, Obliterated vessel. The left arrow labels a tight junction, the right arrow the rest of the lumen. F, Vessels in adjacent muscle of Th1 cell treated tumours appear normal. In summary, PBS treated (A, B) tumours showed typical tumour vascularisation. In contrast, degenerated endothelial cells were observed more frequently in tumours of Th1 cell treated mice (C-E). In addition, strong inflammatory processes (C, D) and more obliterated vessels (E) were seen in tumours of Th1 cell treated mice. Electron microscopy was kindly performed by Prof. Dr. Wolburg, Institute for Pathology, Tübingen.

3.2 Arresting angiogenesis *in vitro* and *in vivo* by increasing intracellular ROS levels with dimethylfumarate

3.2.1 Increasing intracellular ROS with DMF decreases EC proliferation and migration *in vitro*

DMF in combination with MHF is currently approved for the treatment of psoriasis [281]. The molecular basis of action of this compound is not fully understood. It has been reported that DMF covalently binds GSH [329]. This results in a depletion of GSH, an important intracellular scavenger of ROS. In consequence, DMF dose dependently diminished the intracellular GSH levels in multiple cells, including human umbilical vein endothelial cells (HUVEC) (K. Ghoreschi, R. Heidenreich, unpublished data). Antioxidants such as NAC restored intracellular GSH.

In consequence, DMF treatment of HUVEC should induce intracellular ROS levels. Quantification of intracellular ROS showed that DMF dose dependently increased intracellular ROS levels in HUVEC (Fig. 19).

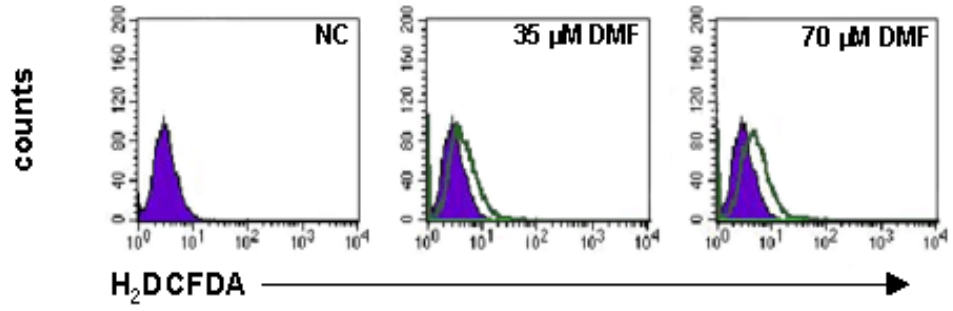

Figure 19. Intracellular ROS levels after DMF treatment. Representative flow cytometric images of intracellular ROS determination in HUVEC after DMF treatment. Untreated cells served as a negative control (NC, purple). DMF significantly induced the formation of ROS in a dose dependent manner (overlays of NC (purple) with DMF (green)).

As ROS mediate pro- and antiangiogenic effects, we investigated the influence of increasing DMF concentrations on EC proliferation and migration. Endothelial cell growth supplement (ECGS)/VEGF induced proliferation of HUVEC (Fig. 20A) and human lung-derived microvascular endothelial cells (HLMEC, Fig. 20B) was determined by BrdU incorporation and subsequent ELISA. Increasing concentrations of DMF dose dependently inhibited the proliferation of EC (Fig. 20A, B). At therapeutic doses of DMF (70 µM) EC proliferation was even down to background (Fig. 20A, B).

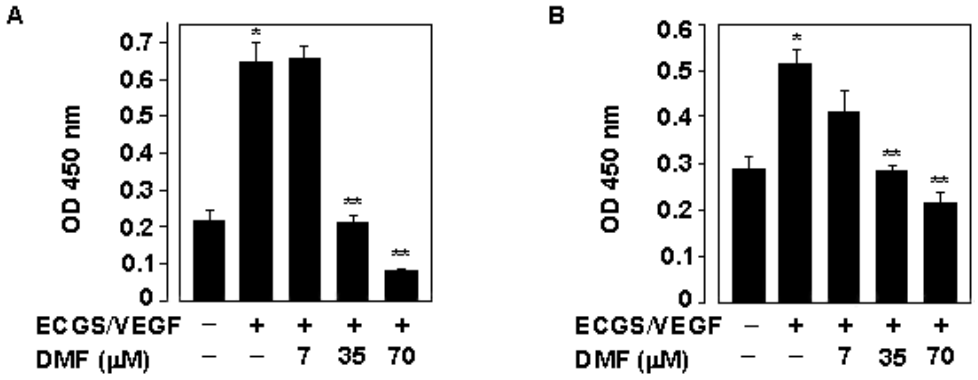

Figure 20. DMF inhibits EC proliferation *in vitro* in a dose dependent manner. EC proliferation was determined by BrdU incorporation using ELISA. A, B, DMF significantly inhibited proliferation of ECGS/VEGF stimulated HUVEC (A, n = 5) or HLMEC (B, n = 4), respectively, in a dose dependent manner. Error bars denote standard error of the mean (SEM). (*: $p < 0.05$ compared to negative control; ** compared to positive control).

Increasing levels of ROS inhibited VEGF-induced proliferation of HUVEC (Fig. 21A) and of HLMEC (Fig. 21B) to a similar extend.

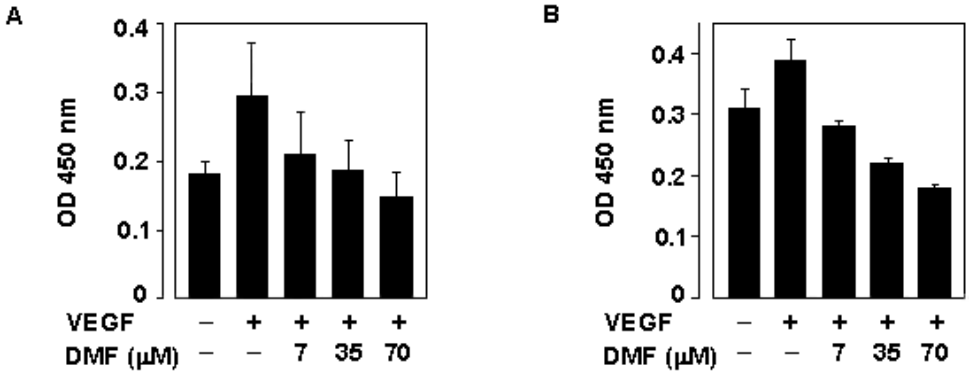

Figure 21. Inhibition of VEGF-induced EC proliferation by DMF *in vitro*. EC proliferation was determined by BrdU incorporation using ELISA. A, B, DMF inhibited proliferation of VEGF stimulated HUVEC (A) and HLMEC (B), respectively. Representative graphs are shown. Bars represent the mean of triplicates ± SD (standard deviation).

Importantly, the inhibition of EC proliferation by DMF was completely reversed by the addition of intracellular ROS scavengers such as NAC (Fig. 22A) or GSH-OEt (Fig. 22B). In contrast to GSH, GSH-OEt is transported into many cell types and is intracellularly hydrolyzed to GSH [330]. These data indicate that ROS are important mediators of DMF-induced inhibition of EC proliferation.

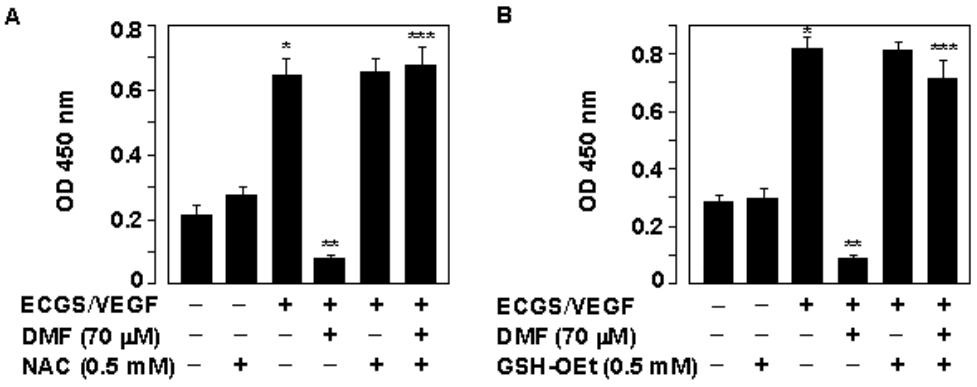

Figure 22. ROS scavengers reverse the inhibition of proliferation by DMF. Proliferation of HUVEC was determined by BrdU incorporation using ELISA. The anti-proliferative effect of DMF treatment was completely reversed by addition of NAC (A, n = 5) or GSH-OEt (B, n = 3). Error bars denote standard error of the mean (SEM). (*: $p < 0.05$ compared to negative control; ** compared to positive control; *** compared to ECGS/VEGF+70 µm DMF).

As increasing levels of ROS inhibited EC proliferation, we next analysed the effects of DMF on EC motility and migration as both are characteristic features of angiogenesis. Therefore, we used the scratch-wound assay. HUVEC or HLMEC were grown to confluency. Subsequently, a migration gap was created (point in time: 0 h). Cells were incubated with low serum as negative control or with ECGS/VEGF either alone or in combination with different concentrations of DMF. The number of cells migrating back into the migration gap was determined microscopically in several independent areas along the wound, on the basis of phase-contrast micrographs at 0 h and at 9 h (HUVEC) or 16 h (HLMEC) after stimulation (Fig. 23A). 70 µM DMF diminished the migration of HUVEC by 50% compared to untreated controls (Fig. 23B) and the migration of HLMEC by 35% (Fig. 23C) respectively.

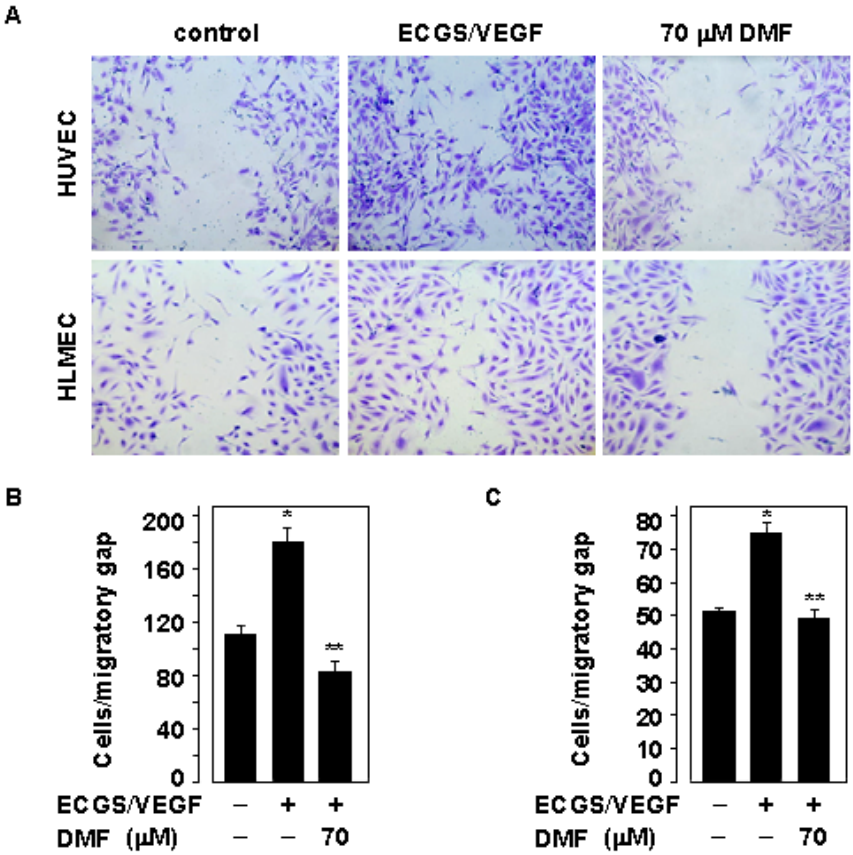

Figure 23. EC migration *in vitro* is strongly decreased by DMF. A, Microscopic view of migrating HUVEC or HLMEC in the scratch-wound assay. DMF treatment considerably inhibited the migration of ECGS/VEGF stimulated HUVEC or HLMEC as compared to the negative control. B, C, Quantitative analysis of (A). DMF significantly reduced the ECGS/VEGF induced migration of HUVEC by 50% (B, n = 3) and of HLMEC by 35% (C, n = 3). Error bars denote standard error of the mean (SEM). (*: $p < 0.05$ compared to negative control; ** compared to positive control).

3.2.2 Increasing ROS levels negatively affect EC sprout formation *in vitro*

To analyse the influence of DMF induced ROS on EC function during the complex process of angiogenesis, we performed an *in vitro* 3-dimensional spheroid based sprouting assay that reflects many features of sprouting angiogenesis *in vivo* [313]. HLMEC were stimulated to sprout from microcarrier beads and the resulting sprouts were counted microscopically. The number of sprouts was strongly reduced by DMF in a dose dependent manner (Fig. 24), indicating that sprouting angiogenesis in this model is negatively regulated by DMF.

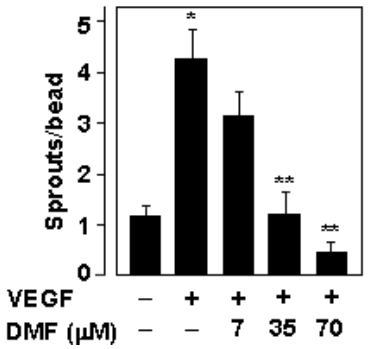

Figure 24. *In vitro* assay of sprouting angiogenesis. HMLEC were grown to confluency on cytodex-3 microcarrier beads and embedded in 3-dimensional fibrin gels. VEGF mediated strong sprout formation which was significantly inhibited by DMF in a dose dependent manner. In contrast, negative controls showed no prominent sprout-inducing activity (*: $p < 0.05$ compared to negative control; ** compared to positive control).

The sprouting capability of HLMEC was completely restored by addition of NAC to DMF treated EC (Fig. 25A). The same result was obtained by addition of GSH-OEt to DMF treated EC (Fig. 25B).

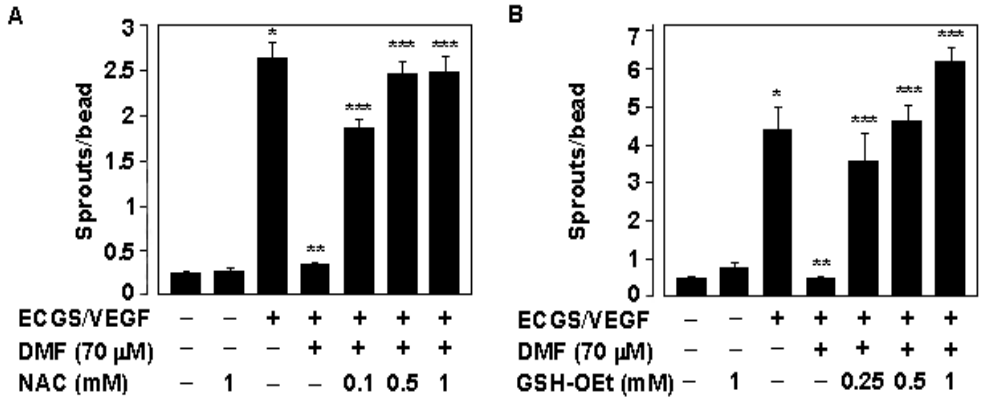

Figure 25. DMF induced inhibition of sprout formation is reversed by ROS scavengers. HMLEC were grown to confluency on cytodex-3 microcarrier beads and embedded in 3-dimensional fibrin gels. The addition of NAC (A, n = 3) or GSH-OEt (B, n = 4) completely restored the ECGS/VEGF mediated sprout formation capability of HMLEC, whereas NAC or GSH-OEt alone had no influence on the sprout formation. Error bars denote standard error of the mean (SEM). (*: $p < 0.05$ compared to negative control; ** compared to positive control; *** compared to ECGS/VEGF+70 µm DMF).

Together, these results strongly suggest that the increase in intracellular ROS concentrations plays an important role in mediating the described inhibitory effects of DMF on EC functions through inhibition of angiogenesis.

3.2.3 Increasing ROS levels prevent EC proliferation without inducing apoptosis

To address whether apoptotic cell death contributed to the DMF triggered inhibition of EC proliferation and migration, we analysed apoptosis in HUVEC and in HLMEC by Annexin-V/Propidium iodide (PI)-staining and subsequent FACS analysis (Fig. 26A, B). We did not detect increased apoptosis, even at the highest concentration of 70 µM DMF that resulted in the prominent reduction of EC functions. These data show that apoptosis was not critically involved in the growth arrest of EC. However, cell cycle analysis suggested a weak G1 arrest of EC at conditions of high ROS levels (Fig. 26C).

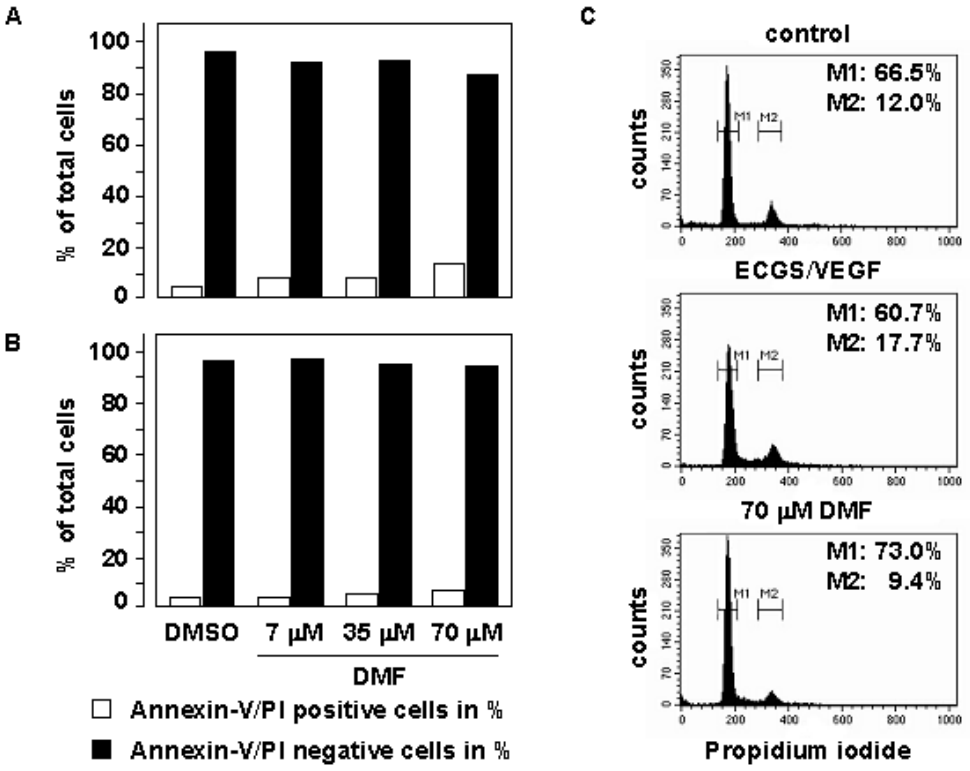

Figure 26. DMF has no significant impact on EC apoptosis. A, B, The apoptotic rate of HUVEC (A) and HLMEC (B) was determined after DMF treatment by Annexin-V/PI staining and subsequent FACS analysis. Dimethyl sulfoxide (DMSO)-treated cells served as negative control. Representative graphs out of three experiments are shown. Quantification of FACS analysis revealed only a slight increase in the number of apoptotic cells even with the highest dose of 70 µM DMF. C, Cell cycle analysis of HUVEC was performed using PI staining and subsequent FACS analysis. Data suggested a weak G1 arrest of EC due to DMF in 2 out of 4 experiments (M1: % of total cells in G0/G1 phase. M2: % of total cells in G2/M phase).

3.2.4 Mechanism underlying the inhibition of EC function

Sustained cellular proliferation is critically dependent on the coordinated action of cell cycle progression and cell growth. Furthermore, the VEGF-induced EC proliferation requires MAPK-dependent signals. The ERK1/2 MAPK and p38 SAPK signalling pathways are activated by phosphorylation. These pathways are involved in the expression of cell cycle regulated genes and control cellular responses [53-55]. Another key role in cell growth and homeostasis plays the PI3K target mTOR [56-58].

Thus, we first analysed the effect of DMF on phosphorylation of p38, ERK1/2 (p44/p42), and mTOR in HUVEC by Western blot analysis and additionally p38 by ELISA, to figure out at what point ROS interfere with the intracellular signalling cascade. We received divergent results on the phosphorylation of ERK1/2, p38, and mTOR ranging from a strong suppression to a moderate enhancement, suggesting that these factors are not critically involved in the effects of ROS on EC proliferation (Fig. 27).

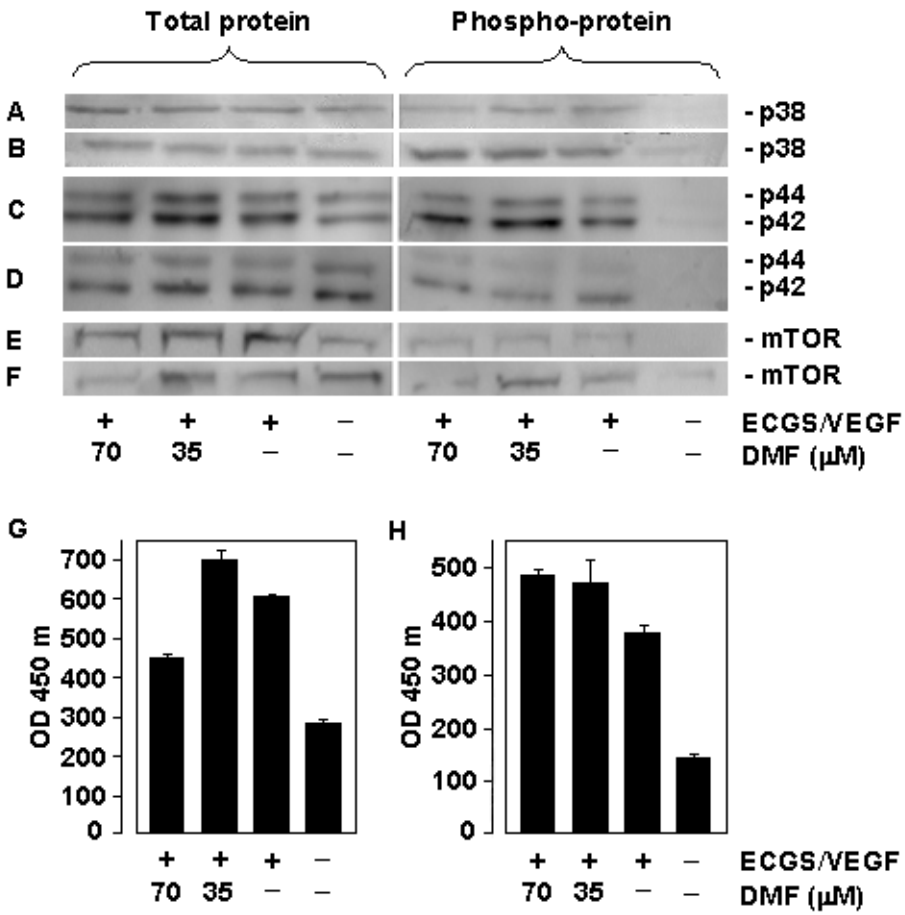

Figure 27. Analysis of the mechanism underlying the inhibition of EC function. A-D, Western blot analysis of HUVEC. Representative blots are shown. Cells showed divergent results on the phosphorylation of p38, p42/p44, and mTOR ranging from a strong suppression (A, C, E) to a moderate enhancement (B, D, F). G, H, Suppression (G) and enhancement (H) of the phosphorylation of p38 was also found with ELISA. Bars represent the mean of triplicates ± SD.

In contrast, it was shown that GSH depletion reproducibly inhibited Thr^{389} phosphorylation of S6K1, the phosphorylation site which is critical for enzyme activation (R. Heidenreich, unpublished data). The PI3K-Akt-S6 kinase pathway stimulates protein synthesis essential for endothelial cell cycle progression by activation of S6K1 which is a mitogen activated Serine/Threonine protein kinase [331, 332]. The detected inhibition was almost down to background levels of untreated EC and could be partly restored with NAC. Hence, the PI3K-Akt-S6 kinase pathway seems to be a target for DMF induced ROS.

3.2.5 Increased ROS levels inhibit VEGF-induced neovessel formation *in vivo*

Since therapeutic doses of DMF significantly inhibit EC proliferation, migration, and sprouting angiogenesis *in vitro*, we asked whether DMF also influences neovessel formation *in vivo*. Hence, we performed the chick chorioallantoic membrane (CAM) assay as a model for physiological angiogenesis [60, 314, 315]. Therefore, a window was cut into the eggshell on embryonic day 3 (E3) and the eggs were further maintained at 37°C in humidified air. On embryonic day 7 (E7) Whatman filters containing DMSO and/or the appropriate DMF concentrations were placed onto the CAMs and incubated for three days. Control eggs showed proper neovessel formation indicating that neither the experimental conditions nor the solvent DMSO affected the developing vasculature (Fig. 28A). In contrast, increasing the intracellular ROS level with DMF dose dependently prevented sprouting and branching of small capillaries and led to prominent thickening of existing vessels, finally resulting in embryonic death (Fig. 28B-E).

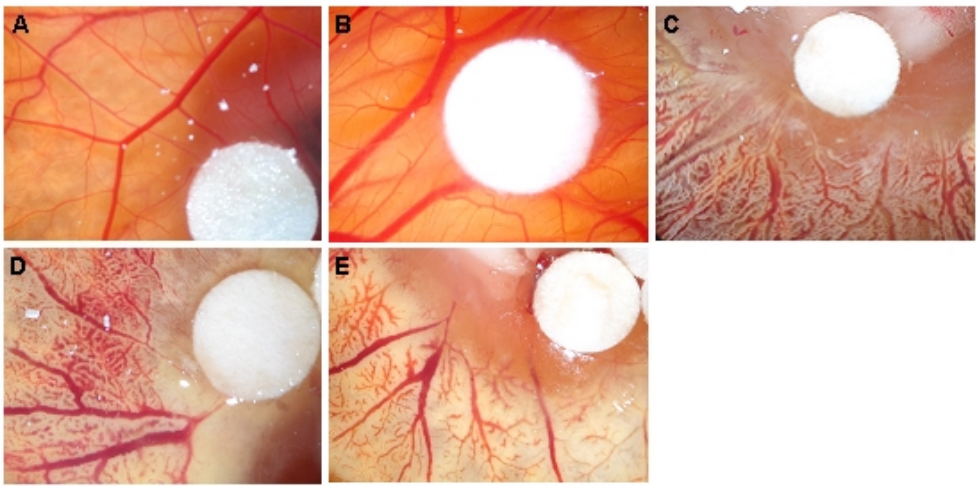

Figure 28. *In vivo* neovessel formation is strongly reduced by DMF treatment. A-E, Chorioallantoic membrane assay. Whatman filters containing DMSO and/or the indicated concentrations of DMF were placed onto E7 CAMs and incubated for three days. A, Filters containing the solvent DMSO served as negative control, showing proper angiogenesis in this assay. B, DMF concentrations up to 25 µg had no influence on vessels. C-E, Higher concentrations of DMF led to changes in blood vessel morphology and lethality of the chicken embryo (C = 50 µg DMF, D = 100 µg DMF, E = 250 µg DMF).

4 Discussion

4.1 Tumour-antigen reactive Th1 cells in tumour therapy

In the current study we investigated the potential of EpCAM-reactive Th1 cells for tumour therapy against a conventional tumour-associated antigen, the underlying cytokine-mediated, antiangiogenic mechanism, and the possible involvement of the host environment. Therefore, we generated non-transgenic EpCAM-reactive Th1 cells *in vivo*, expanded, and characterised them *in vitro*, and confirmed their therapeutic efficiency in a subcutaneous tumour model by studying the inhibition of tumour growth with CT26-EpCAM tumour cells *in vivo*. We found that Th1 cell therapy induced the expression of antitumoural IL-23 and of the antiangiogenic cytokines IL-12 and IFN-γ, all peaking at the initiation of tumour growth inhibition. Accordingly, electron microscopy of tumours revealed endothelial cell damage and vessel obliteration suggesting that tumour vessels in Th1 cell treated mice were severely impaired. Moreover, enhanced diapedesis was observed as sign of inflammation. FACS analysis of cells infiltrating the tumour suggests that $CD11b^+$ monocytes/macrophages are involved in mediating the therapeutic effects. IL-17 may be involved in the antitumour effects of the therapy as the expression increased with efficient tumour growth inhibition.

4.1.1 Design and development of an effective, tumour-antigen specific Th1 cell therapy

EpCAM, a human cell surface glycoprotein, was identified as the first human tumour-associated antigen in 1979 [333]. It is a pan-epithelial differentiation antigen which is restricted to normal epithelia in healthy individuals, but is typically overexpressed to varying degrees in most human carcinomas, making it an attractive target for tumour therapy [316]. Several clinical trials with monoclonal and bi/trispecific antibodies, vaccination strategies, and toxin-conjugated antibody fragments directed against EpCAM showed variable success in the treatment of carcinomas [97]. Hence, we investigated EpCAM as a human model TAA to study ACT. Although recent ACT therapies in the clinic

show considerably improvements in clinical outcomes for patients, a critical point remains the description and generation of tumour-antigen specific lymphocytes which are effective *in vivo* [106]. Adoptive transfer studies defined, besides $CD8^+$ T cells, an important role for tumour-specific $CD4^+$ T cells in antitumour immune responses [117, 122, 140], especially for Th1 cells [138, 139, 142]. Due to the fact that the immunostimulatory TLR9 ligand CpG-ODN promotes DC IL-12 production and the development of Th1 immunity [317, 327, 334-336], in this study we derived non-transgenic EpCAM-specific Th1 cells from BALB/c mice that were immunised with CpG1668 and CT26-EpCAM carcinoma cells. As we failed to generate Th1 cells in normal BALB/c mice, we used $IL4^{-/-}$ BALB/c mice to generate EpCAM-primed Th1 cells. Moreover, it was shown that CpG-ODN can act as an *in vitro* adjuvant by enhancing IL-12 production from APC to rapidly generate tumour-specific Th1 cells [337]. Thus, we used CpG-ODN also *in vitro* to stimulate $CD4^+$ T cells in the presence of EpCAM protein. These tumour-reactive Th1 cells had a strong ability to inhibit tumour growth of subcutaneous CT26-EpCAM tumours. We found tumour growth inhibition starting between days 10 and 13 after tumour cell injection. A similar time is required for successful treatment also in other reports of subcutaneous tumour immune rejection [99, 113, 117, 338], suggesting that this time is needed to generate efficient antitumour immunity. Our experimental design also involved irradiation of the tumour-bearing host before administration of Th1 cells as irradiation generally improves efficacy of adoptive T cell therapies [113, 171]. Moreover, it was demonstrated that irradiation induces an inflammatory response and therefore increases the ability of Th1 cells and innate cells to infiltrate solid tumours [171, 339]. In line with these reports we found an increased level of proinflammatory cytokines and ICAM-1, a strong infiltration of $CD4^+$ T cells, and diapedesis in tumours of Th1 cell treated mice. In contrast, Th1 cells reacting to OVA had no impact on tumour growth. Altogether these results demonstrate the successful development of an effective, tumour-antigen specific Th1 cell therapy.

4.1.2 Investigating a possible cytokine-mediated mechanism underlying the therapy and the involvement of the host environment

$CD4^+$ T cells also have an important role during the effector phase of an immune response which has previously been ascribed to the local release of cytokines, especially IFN-γ [142, 152]. Therefore, we analysed the cytokine milieu provided by the Th1 cell therapy that might mediate tumour rejection with specific emphasis on the role of IFN-γ and cytokines that significantly influence Th1 development, inflammation and angiogenesis. We detected an upregulation of IFN-γ in tumours of Th1 cell treated mice. IFN-γ, produced by Th1 cells, was found to be essential for T cell-mediated tumour regression following ACT in several models [99, 139, 158, 179, 213]. These findings are supported by our previous results showing that only an adoptive transfer of Th1 cells allowed long term control of A20 lymphomas whereas Th2 cells failed [99]. Similarly, many others demonstrated that neutralising IFN-γ or the responsiveness to IFN-γ diminished the therapeutic efficacy of effector cells [122, 139, 142, 152, 173, 176, 180] suggesting that the tumour protective effect primarily relies on the host immune system. In line with this, EpCAM-reactive T cells were only protective against subcutaneous tumours when they failed to produce IL-4; IL-4 producing T cells did not provide protection (H. Braumüller, unpublished data). Surprisingly, in the CT26-EpCAM tumour model injection of anti-IFN-γ mAb before adoptive transfer of Th1 cells lead to a significant inhibition of tumour growth and was even more effective than Th1 cell treatment alone. This correlated with a strong upregulation of IFN-γ mRNA in growth inhibited tumours of mice treated with anti-IFN-γ mAb and Th1 cells. In agreement with a recent manuscript [326], we assume that the anti-IFN-γ mAb protected the transferred Th1 cells from suicide. In summary, our data imply that the IFN-γ secretion of EpCAM-reactive Th1 cells is required for an effective therapy and blocking the very early IFN-γ responses in the host is able to increase the therapeutic efficacy by preventing T cell suicide.

In addition, we found highly increased levels of IL-23/p19 and an upregulation of IL-12/p35, IL-27/Ebi3, and IL-6 in tumours of Th1 cell treated mice suggesting an important role for cytokines of the IL-6 family in tumour growth inhibition.

This is in line with the findings that IL-12, IL-23, and IL-27 show potent antitumour activity in a variety of murine tumour models by further inducing the expression of IFN-γ [181, 213, 223, 225, 233]. Nevertheless, there are studies suggesting that the antitumour and antimetastatic activity of IL-23 and IL-27 act independently of IFN-γ, as these activities were not affected in mice depleted of IFN-γ [226, 234]. Moreover, an increased susceptibility to methylcholanthrene (MCA)-induced carcinogenesis was found in IL-12/p35$^{-/-}$ and IL-12/p40$^{-/-}$ mice, showing that endogenous IL-12 and IL-23 is protective for the growth of sarcomas [340].

Furthermore, the upregulation of IL-23 and IL-6 in tumours of Th1 cell treated mice promotes an environment favorable for the survival and proliferation of IL-17 producing cells [161, 162, 165, 341]. IL-17 itself induces the expression of IL-6, IL-8, TNF-α, and ICAM-1 suggesting an important role for IL-17 in localising and/or sustaining an inflammatory response [239]. We analysed the possible participation of IL-17 to the antiumoural effect of the therapy. Therefore, we first investigated the differentiation of the developing T cells *in vitro*. Analysis of the T cell culture revealed, besides IFN-γ producing cells, a population of IL-17 expressing cells. Second, correlating with the expression of IL-23/p19, IL-6, and ICAM-1, we found also a significantly increased expression of IL-17 in tumours of Th1 cell treated mice on days 13 and 18. Moreover, the levels of IL-17 in tumours of mice treated with Th1 cells correlated negatively to the levels of IFN-γ and IL-12. These data imply that IL-17 might also be involved in the antitumour effects of the therapy.

Since, besides CD4$^+$ T cells, CTL and innate effector cells such as DC and macrophages may be involved in the antitumour effects [199, 207, 223, 235], we analysed the participation of the host environment in the inhibition of tumour growth. For this purpose, we characterised the cellular composition of the tumour infiltrate. First, we found a 16-fold increase of CD4$^+$ T cells in tumours of Th1 cell treated mice compared to controls. We believe that it is unlikely that CD4$^+$ T cells themselves directly recognized and lysed the tumour cells, as *in vitro* analysis showed that CT26-EpCAM tumour cells are not able to stimulate CD4$^+$ T cells *in vitro* (H. Braumüller, unpublished data). Nevertheless, investigations regarding the involvement of apoptosis should be conducted to

analyse a potential interaction of $CD4^+$ T cells with the tumour stroma in exerting antitumoural effects. Secondly, we could detect $CD8^+$ T cells infiltrating the tumours. Surprisingly, we found 5 times more $CD8^+$ T cells in control tumours than in tumours of Th1 cell treated mice on day 18 after tumour cell injection. Consistent with this result, it has been reported that IL-23 which was found to be highly expressed by tumours of Th1 cell treated mice, is able to reduce $CD8^+$ T cell infiltration [342]. Moreover, a corresponding downregulation of VCAM which is involved in tumour leukocyte recruitment [215, 320], could be detected in tumours of Th1 cell treated mice. In summary, these data suggest that $CD8^+$ T cells are not required for tumour control in this model. Furthermore, although mast cells have been shown to contribute to tumour growth and metastasis [343, 344], histology of tumours of both groups revealed no obvious differences in mast cell numbers. These data suggest that in this model mast cells were not affected by the ACT. Moreover, we were not able to detect a change in the percentage of either $CD11c^+$ infiltrating dendritic cells or F4/80 macrophages. Yet, we found three times more $CD11b^+$ monocytes/ macrophages in tumours of Th1 cell treated mice than in PBS treated mice. Infiltrating macrophages activated by Th1 cytokines (M1 phenotype), mainly by IFN-γ, possess cytotoxic function against tumour cells and produce proinflammatory cytokines as shown in several tumour models [117, 122, 139, 143, 171]. Accordingly, we found that the inflammatory cytokines IL-23 and IL-12 were strongly upregulated within tumours of Th1 cell treated mice, cytokines that are mainly produced by cells of the monocyte/macrophage lineage [199, 208]. Moreover, IL-17 which was found to be expressed in tumours of Th1 cell treated mice, recruits cells from the monocyte/macrophage lineage into the tumour microenvironment and stimulates the secretion of IL-12 by macrophages [170, 242] which could mediate the antitumoural effects of IL-17. Therefore, summarising these data, we consider that, besides $CD4^+$ T cells, cells of the monocyte/macrophage lineage in the tumour stroma may contribute to the Th1 cell mediated antitumour effects by secreting inflammatory cytokines into the tumour stroma and consequently leading to the activation of type I polarized immune responses *in vivo*.

Furthermore, inhibition of tumour growth may result from 1) the cytotoxic ability

of macrophages toward tumour cells, by releasing high levels of toxic intermediates such as NO, ROS, and TNF-α [249, 345, 346], 2) the cytotoxic and anti-proliferative activity of IFN-γ [188], and 3) the induction of ischemic-hemorrhagic necrosis of the tumour by IL-12, through the inhibition of tumour angiogenesis [219].

Summarising these results, we conclude that the therapeutic efficiency of adoptively transferred EpCAM-reactive Th1 cells appears to be cytokine-mediated and dependent on the interaction of Th1 cells with cells of the host environment, in particular cells of the monocyte/macrophage lineage.

4.1.3 Antiangiogenic effects of the therapy

It is well known that tumours above a critical size induce the formation of new blood vessels in the tumour [70]. In consequence, inhibition of angiogenesis prevents tumour growth [347]. Hence, antibodies against VEGF [348] or VEGFR-2 [349] inhibit tumour angiogenesis in mouse models and several studies described that the $CD4^+$ T cell mediated tumour control involves antiangiogenic mechanisms [122, 132, 142]. Consistent with a previous report [122], in preliminary work we found that only 4 days after the injection of tumour cells, CT26-EpCAM tumours were well vascularised and therefore eligible to antiangiogenic treatment. Hence, we investigated whether the Th1 cell therapy had an effect on tumour angiogenesis. Surprisingly, conventional histology showed no obvious differences in tumour vascularisation and revealed only minor changes in vessel morphology in tumours of Th1 cell treated mice compared to untreated mice. In addition, we could not detect a change in the expression pattern of VEGF, the main mediator of angiogenesis. CT26-EpCAM tumour cells themselves produce high levels of VEGF *in vitro* (data not shown). This might be the reason why we were not able to reveal smaller differences in the regulation of VEGF. Moreover, the expression of VEGFR-2, the most important receptor of angiogenesis, PIGF, and the angiopoietins Ang-1 and Ang-2 were not strongly affected by the Th1 cell therapy. Supporting the idea that the therapy might have an effect on tumour angiogenesis, we found that IFN-γ, IL-12, and IL-27 were upregulated in tumours of Th1 cell treated mice. These cytokines can exert potent antiangiogenic activity by inducing the

production of the two CXC chemokines IP-10/CXCL10 and Mig/CXCL9 [152, 192, 193, 350] by monocytes/macrophages, fibroblasts, neutrophils [351], epithelial cells [352], and endothelial cells [353]. Surprisingly, we could neither detect an increased expression of IP-10/CXCL10 and Mig/CXCL9 in our therapy model nor a obvious change in the regulation of the appropriate receptor CXCR3, suggesting that IFN-γ, IL-12, and IL-27 may act through IP-10/CXCL10 and Mig/CXCL9 independent mechanims. Previously published data showed that these cytokines have also direct effects on EC proliferation and differentiation and may impair EC survival [176, 181, 217, 219, 234, 354]. In line with this, electron microscopy revealed endothelial cell death and cytoplasma-enriched endothelia augmented in tumours of Th1 cell treated mice, whereas EC in adjacent muscle tissue were not affected suggesting that the Th1 cell therapy is restricted to the tumour tissue. Together, the data suggest that IFN-γ, IL-12, and IL-27 might act directly on EC in tumour vessels causing severe damage to the endothelia. We suggest that IFN-γ, IL-12, and IL-27 exerted anti-angiogenic effects that contributed to the efficiency of the Th1 cell therapy.

4.1.4 Conclusion and perspective

The data presented here suggest that a successful ACT based on $CD4^+$ T cells will require: 1) activated tumour antigen specific Th1 lymphocytes, 2) a tumour permissive for infiltration of effector cells, 3) an appropriate proinflammatory cytokine milieu, and 4) antiangiogenic mediators. Therefore, the detailed characterisation of this network leading to tumour growth inhibition or even regression might help to develop new cancer treatment strategies which might combine active and passive immunotherapy with antiangiogenic treatments. Understanding this process should also help to predict which clinical trials will be successful in the treatment of cancer.

4.2 The antiangiogenic potential of DMF

In the present study we demonstrated the antiangiogenic potential of GSH-depletion by DMF, an antipsoriatic compound, conducting *in vitro* and *in vivo* experiments. DMF strongly influenced the intracellular redox system that ultimately resulted in the inhibition of EC function. *In vitro*, we found that DMF significantly reduced proliferation, migration, and sprouting of EC in a dose dependent manner without significantly increasing EC apoptosis or cell cycle arrest. The application of antioxidants together with DMF completely restored EC proliferation and sprout formation after DMF treatment, directly showing that ROS were central mediators of DMF induced antiangiogenesis. Detailed analysis of involved molecules was unable to show significant inhibition of mTOR, ERK1/2, and p38 phosphorylation. Subsequent work by Dr. Heidenreich unraveled that phosphorylation of S6K1 downstream of mTOR was severely affected by ROS. *In vivo*, DMF significantly reduced neovascularization in the chorioallantoic membrane assay directly proving the *in vivo* relevance of the *in vitro* findings.

4.2.1 The effects of DMF on EC function *in vitro*

Since Schweckendiek reported an improvement of psoriasis following treatment with FAE [280] much research focused on the mode of action of FAE, especially on the effects of FAE on T cell differentiation [254]. Although excessive angiogenesis significantly contributes to the pathogenesis of psoriasis [263, 264], still very little is known about the mechanisms underlying the antiangiogenic potential of antipsoriatic drugs such as cyclosporine A [257, 355], methotrexate [356], or FAE [357]. The leading compound of FAE is DMF which is hydrolysed by esterases to MHF [285, 358]. Therefore, MHF has been considered to be the active metabolite [359]. Nevertheless, other groups favor DMF as the most effective compound based on the chemical properties of DMF that is able to penetrate cellular membranes more easily than MHF [285, 360]. Moreover, MHF monotherapies had no clinical effect on psoriasis [361]. According to these results we decided to use DMF in our studies to further investigate the therapeutic action of FAE on angiogenesis. Moreover,

previous work has shown that DMF influences the redox status of cells [282], an aspect that critically contributes to the function of EC.

In several previous studies, therapeutics, established in psoriasis, such as Anthralin (the oldest topical therapy) [362], Curcumin (a natural anti-inflammatory compound) [363], and DMF [282] were shown to diminish intracellular GSH levels. One reason might be that GSH forms conjugates with a variety of compounds [275]. Accordingly, DMF is able to covalently bind intracellular GSH mediated by GSH-S-transferase [329]. As GSH functions as intracellular scavenger of ROS and as central redox buffer of the cell, decrease of GSH induces oxidative stress. In line with these previous reports, studies from our laboratory revealed that GSH depletion by DMF (K. Ghoreschi, R. Heidenreich, unpublished data) in HUVEC increased intracellular ROS levels in a dose dependent manner.

EC produce low concentrations of ROS mainly through NAD(P)H oxidase to regulate intracellular angiogenic signalling cascades for proliferation, migration, and survival [272, 364-366]. Cellular ROS production is important for endothelial cell motility as pretreatment of primary HUVEC with NAC abolishes serum-induced migration [366] and VEGF-stimulated migration and proliferation [272, 367] by rapid replenishing intracellular glutathione levels [275]. Hence, the question emerges if the increased ROS levels found in HUVEC after DMF treatment, are able to affect EC functions such as proliferation and migration and whether this may contribute to an efficient therapy. Therefore, we first analysed the effects of DMF regarding EC function *in vitro*. In our studies, we used both HUVEC and HLMEC as there are functional differences among EC populations that are related to the site of origin (large vessels versus microvasculature) [292, 368]. We found a significant inhibition of ECGS/VEGF-induced EC proliferation and migration which was dependent on increased ROS levels. Furthermore, we found that DMF inhibited the VEGF-induced proliferation of either HUVEC or HLMEC to the same extend. In addition, DMF treatment significantly inhibited sprout formation of HLMEC *in vitro.* Importantly, the DMF-induced inhibition of EC proliferation and sprouting was completely reversed through the administration of antioxidants together with DMF showing that ROS, exceeding the physiological stimulatory levels, are important

mediators of the DMF induced antiangiogenic effect. Nevertheless, the increased concentration of ROS on one side and the deficiency of ROS scavenger molecules such as GSH on the other side, may both account for the formation of oxidative stress. Hence, we cannot distinguish between signals directly derived from ROS and indirect signals mediated by ROS scavengers contributing to the inhibition of EC function.

One explanation for the decreased EC functions we found may be that depletion of GSH and subsequent exposure to high levels of ROS may induce apoptosis or even necrosis [271, 276, 369, 370]. In addition, in different studies of Sebök et al. DMF was shown to induce apoptosis in the lymphohistiocytic cell line U937 [371] and in HaCaT cells above a concentration of 12 µM [357], whereas in other studies, no cytotoxicity of FAE on keratinocytes was detected till concentrations of 200-800 µM [372]. Thus, we investigated whether apoptotic cell death contributes to the DMF triggered inhibitory effects on EC function. In contrast to the previous report [357] we could not detect increased apoptosis even at seven times higher concentrations of DMF, up to 70 µM. This result implies that apoptosis was not critically involved in the antiangiogenic effects mediated by DMF.

The participation of GSH in the regulation of cell cycle progression might represent a further mechanism to inhibit proliferation since intracellular changes in the concentration of GSH characterise the cell cycle [271]. In non-oxidant stressed cells, basal GSH levels of about 40 nmol/mg protein were detected whereas the highest levels of GSH were found in a state of proliferative growth [275, 292, 373]. Moreover, GSH provides reducing equivalents that maintain the activity of DNA polymerase alpha and ribonucleotide reductase which are both crucially involved in DNA synthesis [293-295]. Therefore, depletion of GSH by DMF might lead to a cell cycle arrest. Nevertheless, cell cycle analysis of HUVEC only suggested a weak accumulation of EC in the G1 phase due to DMF treatment suggesting that a cell cycle arrest only rarely contributes to the inhibitory effects of DMF on EC function.

In summary, we conclude that the significant dose dependent inhibition of primary EC proliferation, migration, and sprout formation observed in our *in vitro*

studies results from modulation of the intracellular redox system following GSH-depletion.

4.2.2 Investigating a possible underlying signalling transduction pathway

We analysed underlying and potentially involved signal transduction pathways which are considered to be associated with redox regulation in EC function. It is well known that EC use low concentrations of ROS as a second messenger to regulate VEGF-induced intracellular angiogenic signalling cascades for proliferation, migration, and survival [272, 364-366]. Hence, low concentrations of hydrogen peroxide are mitogenic due to the fact that growth factor signalling pathways use ROS as second messenger [276, 374]. Moreover, ligand binding to receptor tyrosine kinases is important to induce cellular responses by phosphorylation of a variety of effector proteins. Accordingly, in EC VEGF-dependent mitogenesis is mediated by VEGFR-2 activating downstream signalling enzymes including the PI3 kinase, MAP kinases (ERK, p38, cJun), and the S6 kinases [52, 364, 375-377].

Therefore, we first investigated whether DMF modulates the activation state of the MAP kinases ERK1/2 and p38. ERK and p38 subfamilies of MAPK respond to oxidative stress and are therefore able to influence cell survival [53]. The ERK1/2 MAP kinase pathway is regulating cell proliferation by controlling cell growth and cell cycle progression [53, 54]. This is based on the findings that prevention of ERK activation leads to inhibition of cell proliferation [276] and that $ERK2^{-/-}$ mice are embryonic lethal [378]. Furthermore, ERK can exert pro- and anti-apoptotic effects but it is still unclear what determines these effects [54]. The same conflicting results in regulating cell survival were found for p38 [276] which is activated by inflammatory cytokines and environmental stress [53, 276, 377]. Reflecting these facts, the analysis of the effects of increasing ROS levels on phosphorylation of p38 and ERK1/2, revealed divergent results ranging from a strong suppression to a moderate enhancement. Importantly, in most experiments we found a strong inhibition of p38 or ERK1/2 phosphorylation; yet, this was not consistently reproducible.

Nevertheless, as ERK and PI3K cooperate to activate mTOR promoting cell growth and proliferation [57], we next investigated whether phosphorylation of the protein mTOR was altered by DMF. As mTOR furthermore represents a cell cycle regulatory protein, inhibition of mTOR activity results in cell cycle arrest in the G1 phase [56, 57]. We found a weak G1 arrest in EC after DMF treatment and detected reduced phosphorylation of mTOR. Yet again, in some experiments we found enhanced activation of mTOR suggesting that unknown timing problems might hide the effects of increasing ROS levels on mTOR. We therefore analysed downstream effectors of mTOR, the ribosomal S61/2 kinases which control cell size, growth, proliferation, and G1 cell cycle progression [331, 332, 377]. Indeed, we found a strong reduction of p70 S6K1 activation in HUVEC (R. Heidenreich, unpublished data).

In summary, we could not detect an effect of ROS on mTOR or the intracellular signalling cascade of MAPK (p38, p44/42). In contrast, the S6 kinase 1 seems to be a target for ROS increases that result from GSH depletion, contributing to the antiangiogenic effects mediated by DMF.

4.2.3 The effect of DMF on angiogenesis *in vivo*

As several studies with antipsoriatic drugs such as cyclosporine A and methotrexate showed antiangiogenic effects also *in vivo* [355, 356], we investigated the influence of DMF on angiogenesis in an *in vivo* model. Therefore, we performed the CAM assay as a model for physiological angiogenesis. We could demonstrate reduced sprouting and branching of capillaries as well as blood vessel thickening, indicating that *in vivo* angiogenesis is also negatively influenced by DMF. We also observed lethality of the chicken embryos. As several fold higher doses of DMF are perfectly tolerated by humans and by mice [281, 285, 379] and as none of the doses used locally caused any toxicity in cell cultures, it is most likely that the chicken embryos died because of the local disturbance of angiogenesis.

4.2.4 Conclusion

In summary, our study suggested that the antipsoriatic molecule DMF improves the chronic inflammatory autoimmune disease psoriasis, besides the previously described effects on the immune system, through modulation of the intracellular redox system following GSH-depletion. The strong antiangiogenic potential of DMF *in vitro* and *in vivo* may provide new therapeutic options for the treatment of diseases that depend on neovessel formation such as tumour formation, aberrant wound healing, or other chronic inflammatory diseases such as rheumatoid arthritis.

5 Summary

The aim of this dissertation was to investigate the effects of immune therapies on angiogenesis in two different diseases, tumours and psoriasis.

The objectives in the tumour project were to establish a protective, tumour-antigen specific Th1 cell therapy and investigate the underlying cytokine-mediated, antiangiogenic mechanism, and the possible involvement of the host environment. Therefore, we generated non-transgenic EpCAM-reactive Th1 cells *in vivo*, expanded, and characterised them *in vitro.* We confirmed their therapeutical efficiency in a subcutaneous tumour model using EpCAM transfected CT26 carcinoma cells and reached up to 84% reduction of tumour weight by day 18 after tumour cell injection. We found significant changes in the expression patterns of IFN-γ, IL-12/p35, IL-23/p19, IL-27/Ebi3, IL-6, and IL-17, peaking at the initiation of tumour growth inhibition on day 13 after tumour cell injection. Accordingly, electron microscopy of tumours revealed endothelial cell death and vessel obliteration suggesting that tumour vessels in Th1 cell treated mice were severly impaired. Moreover, enhanced diapedesis was observed as sign of inflammation. FACS analysis of cells infiltrating the tumour suggests that $CD4^+$ and $CD11b^+$ cells are involved in mediating the therapeutic effects.

The aim of the second project was to investigate the effects of DMF, an antipsoriatic compound, on angiogenesis *in vitro* and *in vivo*, and identify possible underlying signal transduction pathways. We found that DMF influenced the intracellular redox system by increasing intracellular ROS levels. Increases in ROS resulted in the inhibition of EC function. *In vitro*, we found that DMF significantly reduced ECGS/VEGF induced proliferation, migration, and sprout formation of EC in a dose dependent manner without significantly increasing EC apoptosis or cell cycle arrest. The application of antioxidants such as NAC or GSH together with DMF completely restored EC proliferation and sprouting after DMF treatment, showing that ROS were central mediators of DMF induced antiangiogenesis. Furthermore, analysing underlying signal transduction pathways *in vitro*, we were unable to show significant effects on mTOR, ERK1/2, and p38 phosphorylation. *In vivo*, DMF significantly reduced neovascularization in the chorioallantoic membrane assay, directly proving the *in vivo* relevance of the *in vitro* findings.

Zusammenfassung

Ziel dieser Doktorarbeit war es, die Auswirkungen von Immuntherapien auf die Angiogenese zu untersuchen.

Im ersten Teil wurden Mechanismen der Tumorantigen-spezifischen Th1 Zelltherapie untersucht. Es wurde der Einfluss von Zytokinen auf die Angiogenese und die Wirtsumgebung des Tumors analysiert. Dazu wurden *in vivo* EpCAM-reaktive Th1 Zellen generiert, *in vitro* expandiert und charakterisiert. Ihr therapeutisches Potential konnte mit Hilfe einer subkutan injizierten EpCAM-exprimierenden CT26 Karzinomzelllinie gezeigt werden. Wir erzielten eine bis zu 84% Reduktion des Tumorgewichts durch die T-Zell Therapie. Es wurden signifikante Unterschiede im Expressionsmuster von IFN-γ, IL-12/p35, IL-23/p19, IL-27/Ebi3, IL-6 und IL-17 festgestellt, die an Tag 13 nach der Tumorzellinjektion ihren Höhepunkt erreichten. Dies korrelierte mit der Initiation der Tumorwachstumsinhibition. Die Elektronenmikroskopie zeigte Nekrose von Endothelzellen und Gefäßobliterationen auf. Dies lässt darauf schließen, dass die Tumorgefäße durch die Therapie stark geschädigt wurden. Auch wurde eine verstärkte Diapedese nachgewiesen. Die FACS-Analyse der infiltrierenden Zellen ergab, dass $CD4^+$ und $CD11b^+$ Zellen an der Therapie beteiligt sind.

Im zweiten Projekt wurde der Einfluss des Immunmodulators Dimethylfumarat (DMF) auf die Angiogenese *in vitro* und *in vivo* untersucht, einschließlich möglicher Signalwege. DMF erhöhte das intrazelluläre ROS Level. Dies führte zu einer Inhibition zahlreicher Endothelzellfunktionen. *In vitro*, führte die ROS Induktion zu einer signifikanten Inhibition der ECGS/VEGF induzierten Proliferation, Migration und der Aussprossung von Endothelzellen, ohne die Apoptoserate oder den Zellzyklus nachweisbar zu beeinflussen. Antioxidantien wie NAC oder GSH stellten die Proliferation und Aussprossung wieder her. Dies zeigt, dass erhöhte ROS Spiegel *in vitro* einen starken antiangiogenen Effekt besitzen. Untersuchungen der Signalkaskade führten zu keinem signifikanten Einfluss auf die Phosphorylierung von mTOR, ERK1/2 und p38. *In vivo* reduzierte DMF deutlich die Gefäßneubildung im Chorioallantois-Membran-Assay. Dies belegt die *in vivo* Relevanz der *in vitro* Befunde.

6 Bibliography

1. Risau, W. and I. Flamme, *Vasculogenesis.* Annu Rev Cell Dev Biol, 1995. **11**: p. 73-91.
2. Risau, W., *Mechanisms of angiogenesis.* Nature, 1997. **386**(6626): p. 671-674.
3. Carmeliet, P., *Mechanisms of angiogenesis and arteriogenesis.* Nat Med, 2000. **6**(4): p. 389-395.
4. Carmeliet, P., *Angiogenesis in health and disease.* Nat Med, 2003. **9**(6): p. 653-660.
5. Flamme, I., T. Frolich, and W. Risau, *Molecular mechanisms of vasculogenesis and embryonic angiogenesis.* J Cell Physiol, 1997. **173**(2): p. 206-10.
6. Carmeliet, P. and R.K. Jain, *Angiogenesis in cancer and other diseases.* Nature, 2000. **407**(6801): p. 249-257.
7. Carmeliet, P. and D. Collen, *Role of vascular endothelial growth factor and vascular endothelial growth factor receptors in vascular development.* Curr Top Microbiol Immunol, 1999. **237**: p. 133-58.
8. Folkman, J. and Y. Shing, *Angiogenesis.* J. Biol. Chem., 1992. **267**(16): p. 10931-10934.
9. Folkman, J., *Angiogenesis in cancer, vascular, rheumatoid and other disease.* Nat Med, 1995. **1**(1): p. 27-31.
10. Alessi, P., C. Ebbinghaus, and D. Neri, *Molecular targeting of angiogenesis.* Biochimica et Biophysica Acta (BBA) - Reviews on Cancer, 2004. **1654**(1): p. 39-49.
11. Hanahan, D. and J. Folkman, *Patterns and Emerging Mechanisms of the Angiogenic Switch during Tumorigenesis.* Cell, 1996. **86**(3): p. 353-364.
12. Yancopoulos, G.D., et al., *Vascular-specific growth factors and blood vessel formation.* Nature, 2000. **407**(6801): p. 242-248.
13. Bergers, G. and L.E. Benjamin, *Tumorigenesis and the angiogenic switch.* Nat Rev Cancer, 2003. **3**(6): p. 401-410.
14. Gale, N.W. and G.D. Yancopoulos, *Growth factors acting via endothelial cell-specific receptor tyrosine kinases: VEGFs, Angiopoietins, and ephrins in vascular development.* Genes Dev., 1999. **13**(9): p. 1055-1066.
15. Carmeliet, P. and D. Collen, *Vascular development and disorders: Molecular analysis and pathogenic insights.* Kidney Int, 1998. **53**(6): p. 1519-1549.
16. Carmeliet, P., et al., *Abnormal blood vessel development and lethality in embryos lacking a single VEGF allele.* Nature, 1996. **380**(6573): p. 435-439.
17. Ferrara, N., H.-P. Gerber, and J. LeCouter, *The biology of VEGF and its receptors.* Nat Med, 2003. **9**(6): p. 669-676.
18. Clauss, M., *Molecular biology of the VEGF and the VEGF receptor family.* Semin Thromb Hemost, 2000. **26**(5): p. 561-9.
19. Maisonpierre, P.C., et al., *Angiopoietin-2, a Natural Antagonist for Tie2 That Disrupts in vivo Angiogenesis.* Science, 1997. **277**(5322): p. 55-60.
20. Davis, S. and G.D. Yancopoulos, *The angiopoietins: Yin and Yang in angiogenesis.* Curr Top Microbiol Immunol, 1999. **237**: p. 173-85.
21. Suri, C., et al., *Requisite role of angiopoietin-1, a ligand for the TIE2 receptor, during embryonic angiogenesis.* Cell, 1996. **87**(7): p. 1171-80.
22. Suri, C., et al., *Increased vascularization in mice overexpressing angiopoietin-1.* Science, 1998. **282**(5388): p. 468-71.
23. Sato, T.N., et al., *Distinct roles of the receptor tyrosine kinases Tie-1 and Tie-2 in blood vessel formation.* Nature, 1995. **376**(6535): p. 70-74.

24. Ferrara, N., *Vascular endothelial growth factor.* Eur J Cancer, 1996. **32A**(14): p. 2413-22.

25. Olofsson, B., et al., *Vascular endothelial growth factor B, a novel growth factor for endothelial cells.* Proceedings of the National Academy of Sciences, 1996. **93**(6): p. 2576-2581.

26. Joukov, V., et al., *A novel vascular endothelial growth factor, VEGF-C, is a ligand for the Flt4 (VEGFR-3) and KDR (VEGFR-2) receptor tyrosine kinases.* Embo J, 1996. **15**(7): p. 1751.

27. Yamada, Y., et al., *Molecular cloning of a novel vascular endothelial growth factor, VEGF-D.* Genomics, 1997. **42**(3): p. 483-8.

28. Maglione, D., et al., *Isolation of a Human Placenta cDNA Coding for a Protein Related to the Vascular Permeability Factor.* Proceedings of the National Academy of Sciences, 1991. **88**(20): p. 9267-9271.

29. Lyttle, D.J., et al., *Homologs of vascular endothelial growth factor are encoded by the poxvirus orf virus.* J. Virol., 1994. **68**(1): p. 84-92.

30. Shibuya, M., et al., *Nucleotide sequence and expression of a novel human receptor-type tyrosine kinase gene (flt) closely related to the fms family.* Oncogene, 1990. **5**(4): p. 519-24.

31. Quinn, T.P., et al., *Fetal Liver Kinase 1 is a Receptor for Vascular Endothelial Growth Factor and is Selectively Expressed in Vascular Endothelium.* Proceedings of the National Academy of Sciences, 1993. **90**(16): p. 7533-7537.

32. Terman, B.I., et al., *Identification of the KDR tyrosine kinase as a receptor for vascular endothelial cell growth factor.* Biochem Biophys Res Commun, 1992. **187**(3): p. 1579-86.

33. Pajusola, K., et al., *FLT4 Receptor Tyrosine Kinase Contains Seven Immunoglobulin-like Loops and Is Expressed in Multiple Human Tissues and Cell Lines.* Cancer Res, 1992. **52**(20): p. 5738-5743.

34. Soker, S., et al., *Characterization of Novel Vascular Endothelial Growth Factor (VEGF) Receptors on Tumor Cells That Bind VEGF via Its Exon 7-encoded Domain.* J. Biol. Chem., 1996. **271**(10): p. 5761-5767.

35. Chen, H., et al., *Neuropilin-2, a novel member of the neuropilin family, is a high affinity receptor for the semaphorins Sema E and Sema IV but not Sema III.* Neuron, 1997. **19**(3): p. 547-59.

36. Valenzuela, D.M., et al., *Angiopoietins 3 and 4: Diverging gene counterparts in mice and humans.* Proceedings of the National Academy of Sciences, 1999. **96**(5): p. 1904-1909.

37. Partanen, J. and D.J. Dumont, *Functions of Tie1 and Tie2 receptor tyrosine kinases in vascular development.* Curr Top Microbiol Immunol, 1999. **237**: p. 159-72.

38. Esser, S., et al., *Vascular endothelial growth factor induces VE-cadherin tyrosine phosphorylation in endothelial cells.* J Cell Sci, 1998. **111**(13): p. 1853-1865.

39. Dvorak, H.F., et al., *Vascular permeability factor/vascular endothelial growth factor and the significance of microvascular hyperpermeability in angiogenesis.* Curr Top Microbiol Immunol, 1999. **237**: p. 97-132.

40. Stockinger, H., et al., *Molecular characterization and functional analysis of the leukocyte surface protein CD31.* J Immunol, 1990. **145**(11): p. 3889-3897.

41. Noel, A., et al., *Membrane associated proteases and their inhibitors in tumour angiogenesis.* J Clin Pathol, 2004. **57**(6): p. 577-584.

42. Lee, M.-H. and G. Murphy, *Matrix metalloproteinases at a glance.* J Cell Sci, 2004. **117**(18): p. 4015-4016.

43. Sottile, J., *Regulation of angiogenesis by extracellular matrix.* Biochimica et Biophysica Acta (BBA) - Reviews on Cancer, 2004. **1654**(1): p. 13-22.

44. Pepper, M.S., et al., *Vascular endothelial growth factor (VEGF) induces plasminogen activators and plasminogen activator inhibitor-1 in microvascular endothelial cells.* Biochem Biophys Res Commun, 1991. **181**(2): p. 902-6.

45. Leung, D.W., et al., *Vascular endothelial growth factor is a secreted angiogenic mitogen.* Science, 1989. **246**(4935): p. 1306-9.

46. Koblizek, T.I., et al., *Angiopoietin-1 induces sprouting angiogenesis in vitro.* Current Biology, 1998. **8**(9): p. 529-532.

47. Varner, J.A., P.C. Brooks, and D.A. Cheresh, *REVIEW: the integrin alpha V beta 3: angiogenesis and apoptosis.* Cell Adhes Commun, 1995. **3**(4): p. 367-74.

48. Brooks, P.C., R.A. Clark, and D.A. Cheresh, *Requirement of vascular integrin alpha v beta 3 for angiogenesis.* Science, 1994. **264**(5158): p. 569-571.

49. Eliceiri, B.P. and D.A. Cheresh, *Role of alpha v integrins during angiogenesis.* Cancer J, 2000. **6 Suppl 3**: p. S245-9.

50. O'Reilly, M.S., et al., *Angiostatin: a novel angiogenesis inhibitor that mediates the suppression of metastases by a Lewis lung carcinoma.* Cell, 1994. **79**(2): p. 315-28.

51. O'Reilly, M.S., et al., *Endostatin: an endogenous inhibitor of angiogenesis and tumor growth.* Cell, 1997. **88**(2): p. 277-85.

52. Veikkola, T., et al., *Regulation of Angiogenesis via Vascular Endothelial Growth Factor Receptors.* Cancer Res, 2000. **60**(2): p. 203-212.

53. Roux, P.P. and J. Blenis, *ERK and p38 MAPK-activated protein kinases: a family of protein kinases with diverse biological functions.* Microbiol Mol Biol Rev, 2004. **68**(2): p. 320-44.

54. Meloche, S. and J. Pouyssegur, *The ERK1/2 mitogen-activated protein kinase pathway as a master regulator of the G1- to S-phase transition.* Oncogene, 2007. **26**(22): p. 3227-39.

55. Raingeaud, J., et al., *Pro-inflammatory cytokines and environmental stress cause p38 mitogen-activated protein kinase activation by dual phosphorylation on tyrosine and threonine.* J Biol Chem, 1995. **270**(13): p. 7420-6.

56. Sabers, C.J., et al., *Isolation of a protein target of the FKBP12-rapamycin complex in mammalian cells.* J Biol Chem, 1995. **270**(2): p. 815-22.

57. Raught, B., A.-C. Gingras, and N. Sonenberg, *The target of rapamycin (TOR) proteins.* Proceedings of the National Academy of Sciences, 2001. **98**(13): p. 7037-7044.

58. Dennis, P.B., et al., *Mammalian TOR: a homeostatic ATP sensor.* Science, 2001. **294**(5544): p. 1102-5.

59. Hayes, A.J., et al., *Angiopoietin-1 and its receptor Tie-2 participate in the regulation of capillary-like tubule formation and survival of endothelial cells.* Microvasc Res, 1999. **58**(3): p. 224-37.

60. Patan, S., B. Haenni, and P.H. Burri, *Implementation of intussusceptive microvascular growth in the chicken chorioallantoic membrane (CAM): 1. pillar formation by folding of the capillary wall.* Microvasc Res, 1996. **51**(1): p. 80-98.

61. Burri, P.H. and M.R. Tarek, *A novel mechanism of capillary growth in the rat pulmonary microcirculation.* Anat Rec, 1990. **228**(1): p. 35-45.

62. Grant, D.S., H.K. Kleinman, and G.R. Martin, *The role of basement membranes in vascular development.* Ann N Y Acad Sci, 1990. **588**: p. 61-72.

63. Hobson, B. and J. Denekamp, *Endothelial proliferation in tumours and normal tissues: continuous labelling studies.* Br J Cancer, 1984. **49**(4): p. 405-13.

64. Engerman, R.L., D. Pfaffenbach, and M.D. Davis, *Cell turnover of capillaries.* Lab Invest, 1967. **17**(6): p. 738-43.

65. Dimmeler, S. and A.M. Zeiher, *Endothelial Cell Apoptosis in Angiogenesis and Vessel Regression.* Circ Res, 2000. **87**(6): p. 434-439.

66. Carmeliet, P., et al., *Targeted deficiency or cytosolic truncation of the VE-cadherin gene in mice impairs VEGF-mediated endothelial survival and angiogenesis.* Cell, 1999. **98**(2): p. 147-57.

67. Brooks, P.C., et al., *Integrin [alpha]v[beta]3 antagonists promote tumor regression by inducing apoptosis of angiogenic blood vessels.* Cell, 1994. **79**(7): p. 1157-1164.

68. Goldman, E., *The growth of malignant disease in man and the lower animals with special reference to the vascular system.* Lancet, 1907. **2**: p. 1236-1240.

69. Ide, A.G., N.H. Baker, and S.L. Warren, *Vascularization of the Brown-Pearce rabbit epithelioma transplant as seen in a transparent ear chamber.* Am. J. Radiol. , 1939. **42**: p. 891-899.

70. Folkman, J., *The role of angiogenesis in tumor growth.* Semin Cancer Biol, 1992. **3**(2): p. 65-71.

71. Bouck, N., V. Stellmach, and S.C. Hsu, *How tumors become angiogenic.* Adv Cancer Res, 1996. **69**: p. 135-74.

72. Folkman, J., *Tumor angiogenesis: therapeutic implications.* N Engl J Med, 1971. **285**(21): p. 1182-6.

73. Vajkoczy, P., et al., *Microtumor growth initiates angiogenic sprouting with simultaneous expression of VEGF, VEGF receptor-2, and angiopoietin-2.* J. Clin. Invest., 2002. **109**(6): p. 777-785.

74. Gimbrone, M.A., Jr., et al., *Tumor dormancy in vivo by prevention of neovascularization.* J Exp Med, 1972. **136**(2): p. 261-76.

75. Fukumura, D., et al., *Tumor induction of VEGF promoter activity in stromal cells.* Cell, 1998. **94**(6): p. 715-25.

76. Ferrara, N., *VEGF and the quest for tumour angiogenesis factors.* Nat Rev Cancer, 2002. **2**(10): p. 795-803.

77. Ferrara, N., *Role of vascular endothelial growth factor in the regulation of angiogenesis.* Kidney Int, 1999. **56**(3): p. 794-814.

78. Plate, K.H., et al., *Vascular endothelial growth factor is a potential tumour angiogenesis factor in human gliomas in vivo.* Nature, 1992. **359**(6398): p. 845-8.

79. Holash, J., et al., *Vessel cooption, regression, and growth in tumors mediated by angiopoietins and VEGF.* Science, 1999. **284**(5422): p. 1994-8.

80. Holash, J., S.J. Wiegand, and G.D. Yancopoulos, *New model of tumor angiogenesis: dynamic balance between vessel regression and growth mediated by angiopoietins and VEGF.* Oncogene, 1999. **18**(38): p. 5356-62.

81. Ehrmann, R.L. and M. Knoth, *Choriocarcinoma. Transfilter stimulation of vasoproliferation in the hamster cheek pouch. Studied by light and electron microscopy.* J Natl Cancer Inst, 1968. **41**(6): p. 1329-41.

82. Greenblatt, M. and P. Shubi, *Tumor angiogenesis: transfilter diffusion studies in the hamster by the transparent chamber technique.* J Natl Cancer Inst, 1968. **41**(1): p. 111-24.

83. Kerbel, R. and J. Folkman, *Clinical translation of angiogenesis inhibitors.* Nat Rev Cancer, 2002. **2**(10): p. 727-739.

84. Shchors, K. and G. Evan, *Tumor Angiogenesis: Cause or Consequence of Cancer?* Cancer Res, 2007. **67**(15): p. 7059-7061.

85. Hashizume, H., et al., *Openings between Defective Endothelial Cells Explain Tumor Vessel Leakiness.* Am J Pathol, 2000. **156**(4): p. 1363-1380.

86. Folberg, R., M.J.C. Hendrix, and A.J. Maniotis, *Vasculogenic Mimicry and Tumor Angiogenesis.* Am J Pathol, 2000. **156**(2): p. 361-381.

87. Maniotis, A.J., et al., *Vascular Channel Formation by Human Melanoma Cells in Vivo and in Vitro: Vasculogenic Mimicry.* Am J Pathol, 1999. **155**(3): p. 739-752.

88. Zhang, S., D. Zhang, and B. Sun, *Vasculogenic mimicry: Current status and future prospects.* Cancer Letters, 2007. **254**(2): p. 157-164.

89. di Tomaso, E., et al., *Mosaic Tumor Vessels: Cellular Basis and Ultrastructure of Focal Regions Lacking Endothelial Cell Markers.* Cancer Res, 2005. **65**(13): p. 5740-5749.

90. Pugh, C.W. and P.J. Ratcliffe, *Regulation of angiogenesis by hypoxia: role of the HIF system.* Nat Med, 2003. **9**(6): p. 677-84.

91. Jackson, J.R., et al., *The codependence of angiogenesis and chronic inflammation.* FASEB J., 1997. **11**(6): p. 457-465.

92. Coussens, L.M. and Z. Werb, *Inflammation and cancer.* Nature, 2002. **420**(6917): p. 860-867.

93. Sunderkotter, C., et al., *Macrophages and angiogenesis.* J Leukoc Biol, 1994. **55**(3): p. 410-422.

94. Maulik, N., *Redox signaling of angiogenesis.* Antioxid Redox Signal, 2002. **4**(5): p. 805-15.

95. Ho, W.Y., C. Yee, and P.D. Greenberg, *Adoptive therapy with CD8+ T cells: it may get by with a little help from its friends.* J. Clin. Invest., 2002. **110**(10): p. 1415-1417.

96. June, C.H., *Principles of adoptive T cell cancer therapy.* J. Clin. Invest., 2007. **117**(5): p. 1204-1212.

97. Trzpis, M., et al., *Epithelial Cell Adhesion Molecule: More than a Carcinoma Marker and Adhesion Molecule.* Am J Pathol, 2007. **171**(2): p. 386-395.

98. Bodey, B., S.E. Siegel, and H.E. Kaiser, *Human cancer detection and immunotherapy with conjugated and non-conjugated monoclonal antibodies.* Anticancer Res, 1996. **16**(2): p. 661-74.

99. Egeter, O., et al., *Eradication of Disseminated Lymphomas with CpG-DNA Activated T Helper Type 1 Cells from Nontransgenic Mice.* Cancer Res, 2000. **60**(6): p. 1515-1520.

100. Pardoll, D.M., *Cancer vaccines.* Nat Med, 1998. **4**(5 Suppl): p. 525-31.

101. Overwijk, W.W., et al., *Vaccination with a recombinant vaccinia virus encoding a "self" antigen induces autoimmune vitiligo and tumor cell destruction in mice: Requirement for CD4+ T lymphocytes.* Proceedings of the National Academy of Sciences, 1999. **96**(6): p. 2982-2987.

102. Gilboa, E., *DC-based cancer vaccines.* J Clin Invest, 2007. **117**(5): p. 1195-203.

103. Tey, S.-K., C.M. Bollard, and H.E. Heslop, *Adoptive T-cell transfer in cancer immunotherapy.* Immunol Cell Biol, 2006. **84**(3): p. 281-289.

104. Bristol, J.A., J. Schlom, and S.I. Abrams, *Persistence, immune specificity, and functional ability of murine mutant ras epitope-specific CD4(+) and CD8(+) T lymphocytes following in vivo adoptive transfer.* Cell Immunol, 1999. **194**(1): p. 78-89.

105. Rooney, C.M., et al., *Infusion of Cytotoxic T Cells for the Prevention and Treatment of Epstein-Barr Virus-Induced Lymphoma in Allogeneic Transplant Recipients.* Blood, 1998. **92**(5): p. 1549-1555.

106. Dudley, M.E. and S.A. Rosenberg, *Adoptive-cell-transfer therapy for the treatment of patients with cancer.* Nat Rev Cancer, 2003. **3**(9): p. 666-675.

107. Dudley, M.E., et al., *Cancer regression and autoimmunity in patients after clonal repopulation with antitumor lymphocytes.* Science, 2002. **298**(5594): p. 850-4.

108. Warren, E.H., P.D. Greenberg, and S.R. Riddell, *Cytotoxic T-Lymphocyte-Defined Human Minor Histocompatibility Antigens With a Restricted Tissue Distribution.* Blood, 1998. **91**(6): p. 2197-2207.

109. Mackinnon, S., et al., *Adoptive cellular therapy for cytomegalovirus infection following allogeneic stem cell transplantation using virus-specific T cells.* Blood Cells Mol Dis, 2007.

110. Brodie, S.J., et al., *In vivo migration and function of transferred HIV-1-specific cytotoxic T cells.* Nat Med, 1999. **5**(1): p. 34-41.

111. Yee, C., et al., *Adoptive T cell therapy using antigen-specific CD8+ T cell clones for the treatment of patients with metastatic melanoma: In vivo persistence, migration, and antitumor effect of transferred T cells.* Proceedings of the National Academy of Sciences, 2002. **99**(25): p. 16168-16173.

112. Ohno, K., et al., *Adoptive immunotherapy with tumor-specific T lymphocytes generated from cytokine gene-modified tumor-primed lymph node cells.* J Immunol, 1996. **156**(10): p. 3875-3881.

113. Greenberg, P.D., *Adoptive T cell therapy of tumors: mechanisms operative in the recognition and elimination of tumor cells.* Adv Immunol, 1991. **49**: p. 281-355.

114. Gattinoni, L., et al., *Adoptive immunotherapy for cancer: building on success.* Nat Rev Immunol, 2006. **6**(5): p. 383-393.

115. Daniel, D., et al., *CD4+ T Cell-Mediated Antigen-Specific Immunotherapy in a Mouse Model of Cervical Cancer.* Cancer Res, 2005. **65**(5): p. 2018-2025.

116. Leen, A.M., C.M. Rooney, and A.E. Foster, *Improving T Cell Therapy for Cancer.* Annual Review of Immunology, 2007. **25**(1): p. 243-265.

117. Corthay, A., et al., *Primary antitumor immune response mediated by CD4+ T cells.* Immunity, 2005. **22**(3): p. 371-83.

118. Boon, T., et al., *Tumor Antigens Recognized by T Lymphocytes.* Annual Review of Immunology, 1994. **12**(1): p. 337-365.

119. Hanahan, D. and R.A. Weinberg, *The hallmarks of cancer.* Cell, 2000. **100**(1): p. 57-70.

120. Janeway, C.A., et al., *Immunologie*. Vol. 5. 2002: Spektrum Akademischer Verlag GmbH. p. 317-363.

121. Jung, G., *T-Zell Funktion.* Einführung in die Immunologie, Vorlesung, 2007.

122. Qin, Z. and T. Blankenstein, *CD4+ T cell--mediated tumor rejection involves inhibition of angiogenesis that is dependent on IFN gamma receptor expression by nonhematopoietic cells.* Immunity, 2000. **12**(6): p. 677-86.

123. Huang, A.Y., et al., *Role of bone marrow-derived cells in presenting MHC class I-restricted tumor antigens.* Science, 1994. **264**(5161): p. 961-5.

124. Knuth, A., et al., *Cytolytic T-Cell Clones against an Autologous Human Melanoma: Specificity Study and Definition of Three Antigens by Immunoselection.* Proceedings of the National Academy of Sciences, 1989. **86**(8): p. 2804-2808.

125. Gattinoni, L., et al., *Acquisition of full effector function in vitro paradoxically impairs the in vivo antitumor efficacy of adoptively transferred CD8+ T cells.* J. Clin. Invest., 2005. **115**(6): p. 1616-1626.

126. Hanson, H.L., et al., *Eradication of established tumors by CD8+ T cell adoptive immunotherapy.* Immunity, 2000. **13**(2): p. 265-76.

127. Adam, C., et al., *DC-NK cell cross talk as a novel CD4+ T-cell-independent pathway for antitumor CTL induction.* Blood, 2005. **106**(1): p. 338-344.

128. Prevost-Blondel, A., et al., *Tumor-Infiltrating Lymphocytes Exhibiting High Ex Vivo Cytolytic Activity Fail to Prevent Murine Melanoma Tumor Growth In Vivo.* J Immunol, 1998. **161**(5): p. 2187-2194.

129. Perez-Diez, A., et al., *CD4 cells can be more efficient at tumor rejection than CD8 cells.* Blood, 2007. **109**(12): p. 5346-5354.

130. Prevost-Blondel, A., et al., *Differential requirement of perforin and IFN-gamma in CD8 T cell-mediated immune responses against B16.F10 melanoma cells expressing a viral antigen.* Eur J Immunol, 2000. **30**(9): p. 2507-15.

131. Schuler, T. and T. Blankenstein, *Cutting Edge: CD8+ Effector T Cells Reject Tumors by Direct Antigen Recognition but Indirect Action on Host Cells.* J Immunol, 2003. **170**(9): p. 4427-4431.

132. Qin, Z., et al., *A Critical Requirement of Interferon {gamma}-mediated Angiostasis for Tumor Rejection by CD8+ T Cells.* Cancer Res, 2003. **63**(14): p. 4095-4100.

133. Monach, P.A., et al., *A unique tumor antigen produced by a single amino acid substitution.* Immunity, 1995. **2**(1): p. 45-59.

134. Dengjel, J., et al., *Unexpected Abundance of HLA Class II Presented Peptides in Primary Renal Cell Carcinomas.* Clin Cancer Res, 2006. **12**(14): p. 4163-4170.

135. Pieper, R., et al., *Biochemical Identification of a Mutated Human Melanoma Antigen Recognized by CD4+ T Cells.* J. Exp. Med., 1999. **189**(5): p. 757-766.

136. Manici, S., et al., *Melanoma cells present a MAGE-3 epitope to CD4(+) cytotoxic T cells in association with histocompatibility leukocyte antigen DR11.* J Exp Med, 1999. **189**(5): p. 871-6.

137. Echchakir, H., et al., *Cutaneous T Cell Lymphoma Reactive CD4+ Cytotoxic T Lymphocyte Clones Display a Th1 Cytokine Profile and Use a Fas-Independent Pathway for Specific Tumor Cell Lysis.* 2000. **115**(1): p. 74-80.

138. Greenberg, P.D., D.E. Kern, and M.A. Cheever, *Therapy of disseminated murine leukemia with cyclophosphamide and immune Lyt-1+,2- T cells. Tumor eradication does not require participation of cytotoxic T cells.* J Exp Med, 1985. **161**(5): p. 1122-34.

139. Hung, K., et al., *The Central Role of CD4+ T Cells in the Antitumor Immune Response.* J. Exp. Med., 1998. **188**(12): p. 2357-2368.

140. Toes, R.E.M., et al., *CD4 T Cells and Their Role in Antitumor Immune Responses.* J. Exp. Med., 1999. **189**(5): p. 753-756.

141. Hong, C., et al., *CD4+ T Cells in the Absence of the CD8+ Cytotoxic T Cells Are Critical and Sufficient for NKT Cell-Dependent Tumor Rejection.* J Immunol, 2006. **177**(10): p. 6747-6757.

142. Mumberg, D., et al., *CD4+ T cells eliminate MHC class II-negative cancer cells in vivo by indirect effects of IFN-gamma.* Proceedings of the National Academy of Sciences, 1999. **96**(15): p. 8633-8638.

143. Dace, D.S., P.W. Chen, and J.Y. Niederkorn, *CD4+ T-cell-dependent tumour rejection in an immune-privileged environment requires macrophages.* Immunology, 2008. **123**(3): p. 367-77.

144. Moeller, M., et al., *Adoptive transfer of gene-engineered CD4+ helper T cells induces potent primary and secondary tumor rejection.* Blood, 2005. **106**(9): p. 2995-3003.

145. Ossendorp, F., et al., *Specific T Helper Cell Requirement for Optimal Induction of Cytotoxic T Lymphocytes against Major Histocompatibility Complex Class II Negative Tumors.* J. Exp. Med., 1998. **187**(5): p. 693-702.

146. Bennett, S.R.M., et al., *Help for cytotoxic-T-cell responses is mediated by CD40 signalling.* Nature, 1998. **393**(6684): p. 478-480.

147. Dembic, Z., K. Schenck, and B. Bogen, *Dendritic cells purified from myeloma are primed with tumor-specific antigen (idiotype) and activate CD4+ T cells.* Proceedings of the National Academy of Sciences, 2000. **97**(6): p. 2697-2702.

148. Mosmann, T.R. and R.L. Coffman, *TH1 and TH2 Cells: Different Patterns of Lymphokine Secretion Lead to Different Functional Properties.* Annual Review of Immunology, 1989. **7**(1): p. 145-173.

149. Marzo, A.L., et al., *Tumor-Specific CD4+ T Cells Have a Major "Post-Licensing" Role in CTL Mediated Anti-Tumor Immunity.* J Immunol, 2000. **165**(11): p. 6047-6055.

150. Cheever, M.A., et al., *Augmentation of the anti-tumor therapeutic efficacy of long-term cultured T lymphocytes by in vivo administration of purified interleukin 2.* J Exp Med, 1982. **155**(4): p. 968-80.

151. Hunziker, L., et al., *Exhaustion of cytotoxic T cells during adoptive immunotherapy of virus carrier mice can be prevented by B cells or CD4+ T cells.* European Journal of Immunology, 2002. **32**(2): p. 374-382.

152. Beatty, G.L. and Y. Paterson, *IFN-{{gamma}}-Dependent Inhibition of Tumor Angiogenesis by Tumor-Infiltrating CD4+ T Cells Requires Tumor Responsiveness to IFN-{{gamma}}.* J Immunol, 2001. **166**(4): p. 2276-2282.

153. Rocken, M., et al., *Central role for TCR/CD3 ligation in the differentiation of CD4+ T cells toward A Th1 or Th2 functional phenotype.* J Immunol, 1992. **148**(1): p. 47-54.

154. Cherwinski, H.M., et al., *Two types of mouse helper T cell clone. III. Further differences in lymphokine synthesis between Th1 and Th2 clones revealed by RNA hybridization, functionally monospecific bioassays, and monoclonal antibodies.* J Exp Med, 1987. **166**(5): p. 1229-44.

155. Knutson, K.L. and M.L. Disis, *Tumor antigen-specific T helper cells in cancer immunity and immunotherapy.* Cancer Immunology, Immunotherapy, 2005. **54**(8): p. 721-728.

156. Rocken, M., J.H. Saurat, and C. Hauser, *A common precursor for CD4+ T cells producing IL-2 or IL-4.* J Immunol, 1992. **148**(4): p. 1031-6.

157. Szabo, S.J., et al., *Molecular Mechanisms Regulating TH1 Immune Responses.* Annual Review of Immunology, 2003. **21**(1): p. 713-758.

158. Nishimura, T., et al., *Distinct Role of Antigen-specific T Helper Type 1 (Th1) and Th2 Cells in Tumor Eradication In Vivo.* J. Exp. Med., 1999. **190**(5): p. 617-628.

159. Bettelli, E., M. Oukka, and V.K. Kuchroo, *TH-17 cells in the circle of immunity and autoimmunity.* Nat Immunol, 2007. **8**(4): p. 345-350.

160. Mangan, P.R., et al., *Transforming growth factor-[beta] induces development of the TH17 lineage.* Nature, 2006. **441**(7090): p. 231-234.

161. Aggarwal, S., et al., *Interleukin-23 Promotes a Distinct CD4 T Cell Activation State Characterized by the Production of Interleukin-17.* J. Biol. Chem., 2003. **278**(3): p. 1910-1914.

162. Harrington, L.E., et al., *Interleukin 17-producing CD4+ effector T cells develop via a lineage distinct from the T helper type 1 and 2 lineages.* Nat Immunol, 2005. **6**(11): p. 1123-32.

163. Zhou, L., et al., *IL-6 programs TH-17 cell differentiation by promoting sequential engagement of the IL-21 and IL-23 pathways.* Nat Immunol, 2007. **8**(9): p. 967-974.

164. Bettelli, E., et al., *Reciprocal developmental pathways for the generation of pathogenic effector TH17 and regulatory T cells.* Nature, 2006. **441**(7090): p. 235-238.

165. Veldhoen, M., et al., *TGFbeta in the context of an inflammatory cytokine milieu supports de novo differentiation of IL-17-producing T cells.* Immunity, 2006. **24**(2): p. 179-89.

166. Ivanov, II, et al., *The orphan nuclear receptor RORgammat directs the differentiation program of proinflammatory IL-17+ T helper cells.* Cell, 2006. **126**(6): p. 1121-33.

167. Linden, A., *Role of interleukin-17 and the neutrophil in asthma.* Int Arch Allergy Immunol, 2001. **126**(3): p. 179-84.

168. Teunissen, M.B., et al., *Interleukin-17 and interferon-gamma synergize in the enhancement of proinflammatory cytokine production by human keratinocytes.* J Invest Dermatol, 1998. **111**(4): p. 645-9.

169. Langrish, C.L., et al., *IL-23 drives a pathogenic T cell population that induces autoimmune inflammation.* J. Exp. Med., 2005. **201**(2): p. 233-240.

170. Benchetrit, F., et al., *Interleukin-17 inhibits tumor cell growth by means of a T-cell-dependent mechanism.* Blood, 2002. **99**(6): p. 2114-2121.

171. Ganss, R., et al., *Combination of T-Cell Therapy and Trigger of Inflammation Induces Remodeling of the Vasculature and Tumor Eradication.* Cancer Res, 2002. **62**(5): p. 1462-1470.

172. Dranoff, G., *Cytokines in cancer pathogenesis and cancer therapy.* Nat Rev Cancer, 2004. **4**(1): p. 11-22.

173. Li, Z., et al., *Cross-Talk between T Cells and Innate Immune Cells Is Crucial for IFN-{gamma}-Dependent Tumor Rejection.* J Immunol, 2007. **179**(3): p. 1568-1576.

174. Ganss, R. and D. Hanahan, *Tumor Microenvironment Can Restrict the Effectiveness of Activated Antitumor Lymphocytes.* Cancer Res, 1998. **58**(20): p. 4673-4681.

175. Cuadros, C., et al., *Cooperative Effect between Immunotherapy and Antiangiogenic Therapy Leads to Effective Tumor Rejection in Tolerant Her-2/neu Mice.* Cancer Res, 2003. **63**(18): p. 5895-5901.

176. Ibe, S., et al., *Tumor Rejection by Disturbing Tumor Stroma Cell Interactions.* J. Exp. Med., 2001. **194**(11): p. 1549-1560.

177. Nelson, D. and R. Ganss, *Tumor growth or regression: powered by inflammation.* J Leukoc Biol, 2006. **80**(4): p. 685-690.

178. Lin, W.-W. and M. Karin, *A cytokine-mediated link between innate immunity, inflammation, and cancer.* J. Clin. Invest., 2007. **117**(5): p. 1175-1183.

179. Becker, C., et al., *Adoptive tumor therapy with T lymphocytes enriched through an IFN-[gamma] capture assay.* Nat Med, 2001. **7**(10): p. 1159-1162.

180. Dighe, A.S., et al., *Enhanced in vivo growth and resistance to rejection of tumor cells expressing dominant negative IFN gamma receptors.* Immunity, 1994. **1**(6): p. 447-56.

181. Hess, S.D., et al., *Human CD4+ T Cells Present Within the Microenvironment of Human Lung Tumors Are Mobilized by the Local and Sustained Release of IL-12 to Kill Tumors In Situ by Indirect Effects of IFN-{gamma}.* J Immunol, 2003. **170**(1): p. 400-412.

182. Ikeda, H., L.J. Old, and R.D. Schreiber, *The roles of IFN[gamma] in protection against tumor development and cancer immunoediting.* Cytokine & Growth Factor Reviews, 2002. **13**(2): p. 95-109.

183. Boehm, U., et al., *Cellular responses to interferon-gamma.* Annual Review of Immunology, 1997. **15**(1): p. 749-795.

184. Dalton, D.K., et al., *Multiple defects of immune cell function in mice with disrupted interferon-gamma genes.* Science, 1993. **259**(5102): p. 1739-1742.

185. Bradley, L.M., D.K. Dalton, and M. Croft, *A direct role for IFN-gamma in regulation of Th1 cell development.* J Immunol, 1996. **157**(4): p. 1350-1358.

186. Farrar, M.A. and R.D. Schreiber, *The Molecular Cell Biology of Interferon-gamma and its Receptor.* Annual Review of Immunology, 1993. **11**(1): p. 571-611.

187. Fransen, L., et al., *Recombinant tumor necrosis factor: its effect and its synergism with interferon-gamma on a variety of normal and transformed human cell lines.* Eur J Cancer Clin Oncol, 1986. **22**(4): p. 419-26.

188. Pfizenmaier, K., et al., *Differential {gamma}-Interferon Response of Human Colon Carcinoma Cells: Inhibition of Proliferation and Modulation of Immunogenicity as Independent Effects of {gamma}-Interferon on Tumor Cell Growth.* Cancer Res, 1985. **45**(8): p. 3503-3509.

189. Weber, J.S. and S.A. Rosenberg, *Modulation of Murine Tumor Major Histocompatibility Antigens by Cytokines in Vivo and in Vitro.* Cancer Res, 1988. **48**(20): p. 5818-5824.

190. Beatty, G.L. and Y. Paterson, *IFN-{gamma} Can Promote Tumor Evasion of the Immune System In Vivo by Down-Regulating Cellular Levels of an Endogenous Tumor Antigen.* J Immunol, 2000. **165**(10): p. 5502-5508.

191. Mocikat, R., et al., *Natural killer cells activated by MHC class I(low) targets prime dendritic cells to induce protective CD8 T cell responses.* Immunity, 2003. **19**(4): p. 561-9.

192. Sgadari, C., et al., *Interferon-inducible protein-10 identified as a mediator of tumor necrosis in vivo.* Proceedings of the National Academy of Sciences, 1996. **93**(24): p. 13791-13796.

193. Sgadari, C., et al., *Mig, the Monokine Induced By Interferon-gamma , Promotes Tumor Necrosis In Vivo.* Blood, 1997. **89**(8): p. 2635-2643.

194. Yao, L., et al., *Anti-tumor activities of the angiogenesis inhibitors interferon-inducible protein-10 and the calreticulin fragment vasostatin.* Cancer Immunology, Immunotherapy, 2002. **51**(7): p. 358-366.

195. Fathallah-Shaykh, H.M., et al., *Gene Transfer of IFN-{gamma} into Established Brain Tumors Represses Growth by Antiangiogenesis.* J Immunol, 2000. **164**(1): p. 217-222.

196. Hunter, C.A., *New IL-12-family members: IL-23 and IL-27, cytokines with divergent functions.* Nat Rev Immunol, 2005. **5**(7): p. 521-531.

197. Kobayashi, M., et al., *Identification and purification of natural killer cell stimulatory factor (NKSF), a cytokine with multiple biologic effects on human lymphocytes.* J Exp Med, 1989. **170**(3): p. 827-45.

198. Stern, A.S., et al., *Purification to homogeneity and partial characterization of cytotoxic lymphocyte maturation factor from human B-lymphoblastoid cells.* Proc Natl Acad Sci U S A, 1990. **87**(17): p. 6808-12.

199. Beadling, C. and M. Slifka, *Regulation of innate and adaptive immune responses by the related cytokines IL-12, IL-23, and IL-27.* Archivum Immunologiae et Therapiae Experimentalis, 2006. **54**(1): p. 15-24.

200. Schoenhaut, D.S., et al., *Cloning and expression of murine IL-12.* J Immunol, 1992. **148**(11): p. 3433-40.

201. Oppmann, B., et al., *Novel p19 protein engages IL-12p40 to form a cytokine, IL-23, with biological activities similar as well as distinct from IL-12.* Immunity, 2000. **13**(5): p. 715-25.

202. Pflanz, S., et al., *IL-27, a heterodimeric cytokine composed of EBI3 and p28 protein, induces proliferation of naive CD4(+) T cells.* Immunity, 2002. **16**(6): p. 779-90.

203. Wiekowski, M.T., et al., *Ubiquitous transgenic expression of the IL-23 subunit p19 induces multiorgan inflammation, runting, infertility, and premature death.* J Immunol, 2001. **166**(12): p. 7563-70.

204. Presky, D.H., et al., *A functional interleukin 12 receptor complex is composed of two beta-type cytokine receptor subunits.* Proc Natl Acad Sci U S A, 1996. **93**(24): p. 14002-7.

205. Parham, C., et al., *A receptor for the heterodimeric cytokine IL-23 is composed of IL-12Rbeta1 and a novel cytokine receptor subunit, IL-23R.* J Immunol, 2002. **168**(11): p. 5699-708.

206. Pflanz, S., et al., *WSX-1 and glycoprotein 130 constitute a signal-transducing receptor for IL-27.* J Immunol, 2004. **172**(4): p. 2225-31.

207. Belladonna, M.L., et al., *IL-23 and IL-12 Have Overlapping, but Distinct, Effects on Murine Dendritic Cells.* J Immunol, 2002. **168**(11): p. 5448-5454.

208. Trinchieri, G., S. Pflanz, and R.A. Kastelein, *The IL-12 family of heterodimeric cytokines: new players in the regulation of T cell responses.* Immunity, 2003. **19**(5): p. 641-4.

209. McKnight, A.J., et al., *Effects of IL-12 on helper T cell-dependent immune responses in vivo.* J Immunol, 1994. **152**(5): p. 2172-2179.

210. Langrish, C.L., et al., *IL-12 and IL-23: master regulators of innate and adaptive immunity.* Immunol Rev, 2004. **202**: p. 96-105.

211. Murphy, C.A., et al., *Divergent Pro- and Antiinflammatory Roles for IL-23 and IL-12 in Joint Autoimmune Inflammation.* J. Exp. Med., 2003. **198**(12): p. 1951-1957.

212. Brunda, M.J., et al., *Antitumor and antimetastatic activity of interleukin 12 against murine tumors.* J Exp Med, 1993. **178**(4): p. 1223-30.

213. Nastala, C.L., et al., *Recombinant IL-12 administration induces tumor regression in association with IFN-gamma production.* J Immunol, 1994. **153**(4): p. 1697-1706.

214. Boggio, K., et al., *Interleukin 12-mediated prevention of spontaneous mammary adenocarcinomas in two lines of Her-2/neu transgenic mice.* J Exp Med, 1998. **188**(3): p. 589-96.

215. Cavallo, F., et al., *Immune Events Associated with the Cure of Established Tumors and Spontaneous Metastases by Local and Systemic Interleukin 12.* Cancer Res, 1999. **59**(2): p. 414-421.

216. Kanegane, C., et al., *Contribution of the CXC chemokines IP-10 and Mig to the antitumor effects of IL-12.* J Leukoc Biol, 1998. **64**(3): p. 384-392.

217. Friesel, R., A. Komoriya, and T. Maciag, *Inhibition of endothelial cell proliferation by gamma-interferon.* J. Cell Biol., 1987. **104**(3): p. 689-696.

218. Sgadari, C., A.L. Angiolillo, and G. Tosato, *Inhibition of angiogenesis by interleukin-12 is mediated by the interferon-inducible protein 10.* Blood, 1996. **87**(9): p. 3877-3882.

219. Strasly, M., et al., *IL-12 Inhibition of Endothelial Cell Functions and Angiogenesis Depends on Lymphocyte-Endothelial Cell Cross-Talk.* J Immunol, 2001. **166**(6): p. 3890-3899.

220. Colombo, M.P. and G. Trinchieri, *Interleukin-12 in anti-tumor immunity and immunotherapy.* Cytokine Growth Factor Rev, 2002. **13**(2): p. 155-68.

221. Coughlin, C.M., et al., *Interleukin-12 and interleukin-18 synergistically induce murine tumor regression which involves inhibition of angiogenesis.* J Clin Invest, 1998. **101**(6): p. 1441-52.

222. Lankford, C.S.R. and D.M. Frucht, *A unique role for IL-23 in promoting cellular immunity.* J Leukoc Biol, 2003. **73**(1): p. 49-56.

223. Hao, J.-S. and B.-E. Shan, *Immune enhancement and anti-tumour activity of IL-23.* Cancer Immunology, Immunotherapy, 2006. **55**(11): p. 1426-1431.

224. Oniki, S., et al., *Interleukin-23 and Interleukin-27 Exert Quite Different Antitumor and Vaccine Effects on Poorly Immunogenic Melanoma.* Cancer Res, 2006. **66**(12): p. 6395-6404.

225. Kaiga, T., et al., *Systemic Administration of IL-23 Induces Potent Antitumor Immunity Primarily Mediated through Th1-Type Response in Association with the Endogenously Expressed IL-12.* J Immunol, 2007. **178**(12): p. 7571-7580.

226. Lo, C.-H., et al., *Antitumor and Antimetastatic Activity of IL-23.* J Immunol, 2003. **171**(2): p. 600-607.

227. Lucas, S., et al., *IL-27 regulates IL-12 responsiveness of naive CD4+ T cells through Stat1-dependent and -independent mechanisms.* Proceedings of the National Academy of Sciences, 2003. **100**(25): p. 15047-15052.

228. Owaki, T., et al., *A Role for IL-27 in Early Regulation of Th1 Differentiation.* J Immunol, 2005. **175**(4): p. 2191-2200.

229. Goldberg, R., et al., *Suppression of Ongoing Experimental Autoimmune Encephalomyelitis by Neutralizing the Function of the p28 Subunit of IL-27.* J Immunol, 2004. **173**(10): p. 6465-6471.

230. Villarino, A.V., E. Huang, and C.A. Hunter, *Understanding the pro- and anti-inflammatory properties of IL-27.* J Immunol, 2004. **173**(2): p. 715-20.

231. Colgan, J. and P. Rothman, *All in the family: IL-27 suppression of TH-17 cells.* Nat Immunol, 2006. **7**(9): p. 899-901.

232. Batten, M., et al., *Interleukin 27 limits autoimmune encephalomyelitis by suppressing the development of interleukin 17-producing T cells.* Nat Immunol, 2006. **7**(9): p. 929-936.

233. Hisada, M., et al., *Potent Antitumor Activity of Interleukin-27.* Cancer Res, 2004. **64**(3): p. 1152-1156.

234. Shimizu, M., et al., *Antiangiogenic and antitumor activities of IL-27.* J Immunol, 2006. **176**(12): p. 7317-24.

235. Morishima, N., et al., *Augmentation of Effector CD8+ T Cell Generation with Enhanced Granzyme B Expression by IL-27.* J Immunol, 2005. **175**(3): p. 1686-1693.

236. Salcedo, R., et al., *IL-27 mediates complete regression of orthotopic primary and metastatic murine neuroblastoma tumors: role for CD8+ T cells.* J Immunol, 2004. **173**(12): p. 7170-82.

237. Chiyo, M., et al., *Expression of IL-27 in murine carcinoma cells produces antitumor effects and induces protective immunity in inoculated host animals.* Int J Cancer, 2005. **115**(3): p. 437-42.

238. Rouvier, E., et al., *CTLA-8, cloned from an activated T cell, bearing AU-rich messenger RNA instability sequences, and homologous to a herpesvirus saimiri gene.* J Immunol, 1993. **150**(12): p. 5445-56.

239. Kolls, J.K. and A. Linden, *Interleukin-17 family members and inflammation.* Immunity, 2004. **21**(4): p. 467-76.

240. Aggarwal, S. and A.L. Gurney, *IL-17: prototype member of an emerging cytokine family.* J Leukoc Biol, 2002. **71**(1): p. 1-8.

241. Fossiez, F., et al., *Interleukin-17.* Int Rev Immunol, 1998. **16**(5-6): p. 541-51.

242. Park, H., et al., *A distinct lineage of CD4 T cells regulates tissue inflammation by producing interleukin 17.* Nat Immunol, 2005. **6**(11): p. 1133-41.

243. Fossiez, F., et al., *T cell interleukin-17 induces stromal cells to produce proinflammatory and hematopoietic cytokines.* J Exp Med, 1996. **183**(6): p. 2593-603.

244. Dong, C., *Diversification of T-helper-cell lineages: finding the family root of IL-17-producing cells.* Nat Rev Immunol, 2006. **6**(4): p. 329-334.

245. Chabaud, M., et al., *Human interleukin-17: A T cell-derived proinflammatory cytokine produced by the rheumatoid synovium.* Arthritis Rheum, 1999. **42**(5): p. 963-70.

246. Kurasawa, K., et al., *Increased interleukin-17 production in patients with systemic sclerosis.* Arthritis Rheum, 2000. **43**(11): p. 2455-63.

247. Mueller, M.M. and N.E. Fusenig, *Friends or foes - bipolar effects of the tumour stroma in cancer.* Nat Rev Cancer, 2004. **4**(11): p. 839-849.

248. Matzinger, P., *Friendly and dangerous signals: is the tissue in control?* Nat Immunol, 2007. **8**(1): p. 11-13.

249. Allavena, P., et al., *The inflammatory micro-environment in tumor progression: The role of tumor-associated macrophages.* Critical Reviews in Oncology/Hematology. **In Press, Corrected Proof**.

250. Mor, F., F.J. Quintana, and I.R. Cohen, *Angiogenesis-Inflammation Cross-Talk: Vascular Endothelial Growth Factor Is Secreted by Activated T Cells and Induces Th1 Polarization.* J Immunol, 2004. **172**(7): p. 4618-4623.

251. Reits, E.A., et al., *Radiation modulates the peptide repertoire, enhances MHC class I expression, and induces successful antitumor immunotherapy.* J. Exp. Med., 2006. **203**(5): p. 1259-1271.

252. Zhang, B., et al., *Induced sensitization of tumor stroma leads to eradication of established cancer by T cells.* J. Exp. Med., 2007. **204**(1): p. 49-55.

253. Cheever, M.A., P.D. Greenberg, and A. Fefer, *Specificity of adoptive chemoimmunotherapy of established syngeneic tumors.* J Immunol, 1980. **125**(2): p. 711-714.

254. Ghoreschi, K., C. Weigert, and M. Rocken, *Immunopathogenesis and role of T cells in psoriasis.* Clin Dermatol, 2007. **25**(6): p. 574-80.

255. Ellis, C.N. and G.G. Krueger, *Treatment of chronic plaque psoriasis by selective targeting of memory effector T lymphocytes.* N Engl J Med, 2001. **345**(4): p. 248-55.

256. Gottlieb, S.L., et al., *Short-contact anthralin treatment augments therapeutic efficacy of cyclosporine in psoriasis: a clinical and pathologic study.* J Am Acad Dermatol, 1995. **33**(4): p. 637-45.

257. Yamasaki, E., et al., *Methotrexate inhibits proliferation and regulation of the expression of intercellular adhesion molecule-1 and vascular cell adhesion molecule-1 by cultured human umbilical vein endothelial cells.* British Journal of Dermatology, 2003. **149**(1): p. 30-38.

258. Ghoreschi, K., et al., *Interleukin-4 therapy of psoriasis induces Th2 responses and improves human autoimmune disease.* Nat Med, 2003. **9**(1): p. 40-6.

259. Ettehadi, P., et al., *Elevated tumour necrosis factor-alpha (TNF-alpha) biological activity in psoriatic skin lesions.* Clin Exp Immunol, 1994. **96**(1): p. 146-51.

260. Chaudhari, U., et al., *Efficacy and safety of infliximab monotherapy for plaque-type psoriasis: a randomised trial.* Lancet, 2001. **357**(9271): p. 1842-7.

261. Austin, L.M., et al., *The majority of epidermal T cells in Psoriasis vulgaris lesions can produce type 1 cytokines, interferon-gamma, interleukin-2, and tumor necrosis factor-alpha, defining TC1 (cytotoxic T lymphocyte) and TH1 effector populations: a type 1 differentiation bias is also measured in circulating blood T cells in psoriatic patients.* J Invest Dermatol, 1999. **113**(5): p. 752-9.

262. Barker, J.N., *The pathophysiology of psoriasis.* Lancet, 1991. **338**(8761): p. 227-30.

263. Wolf, J.E., Jr., *Angiogenesis in normal and psoriatic skin.* Lab Invest, 1989. **61**(2): p. 139-42.

264. Folkman, J., *Angiogenesis in psoriasis: therapeutic implications.* J Invest Dermatol, 1972. **59**(1): p. 40-3.

265. Creamer, D., et al., *Localization of endothelial proliferation and microvascular expansion in active plaque psoriasis.* Br J Dermatol, 1997. **136**(6): p. 859-65.

266. Bhushan, M., et al., *Levels of endothelial cell stimulating angiogenesis factor and vascular endothelial growth factor are elevated in psoriasis.* Br J Dermatol, 1999. **141**(6): p. 1054-60.

267. Nickoloff, B.J., et al., *Aberrant production of interleukin-8 and thrombospondin-1 by psoriatic keratinocytes mediates angiogenesis.* Am J Pathol, 1994. **144**(4): p. 820-8.

268. Detmar, M., et al., *Overexpression of vascular permeability factor/vascular endothelial growth factor and its receptors in psoriasis.* J Exp Med, 1994. **180**(3): p. 1141-6.

269. Rosenberger, C., et al., *Upregulation of hypoxia-inducible factors in normal and psoriatic skin.* J Invest Dermatol, 2007. **127**(10): p. 2445-52.

270. Creamer, D., et al., *Altered vascular endothelium integrin expression in psoriasis.* Am J Pathol, 1995. **147**(6): p. 1661-7.

271. Valko, M., et al., *Free radicals and antioxidants in normal physiological functions and human disease.* Int J Biochem Cell Biol, 2007. **39**(1): p. 44-84.

272. Ushio-Fukai, M., et al., *Novel Role of gp91phox-Containing NAD(P)H Oxidase in Vascular Endothelial Growth Factor-Induced Signaling and Angiogenesis.* Circ Res, 2002. **91**(12): p. 1160-1167.

273. Vives-Bauza, C., A. Starkov, and E. Garcia-Arumi, *Measurements of the antioxidant enzyme activities of superoxide dismutase, catalase, and glutathione peroxidase.* Methods Cell Biol, 2007. **80**: p. 379-93.

274. Raes, M., C. Michiels, and J. Remacle, *Comparative study of the enzymatic defense systems against oxygen-derived free radicals: the key role of glutathione peroxidase.* Free Radic Biol Med, 1987. **3**(1): p. 3-7.

275. Meister, A., *Glutathione metabolism and its selective modification.* J Biol Chem, 1988. **263**(33): p. 17205-8.

276. Martindale, J.L. and N.J. Holbrook, *Cellular response to oxidative stress: signaling for suicide and survival.* J Cell Physiol, 2002. **192**(1): p. 1-15.

277. Tosaki, A., et al., *Effects of SOD, catalase, and a novel antiarrhythmic drug, EGB 761, on reperfusion-induced arrhythmias in isolated rat hearts.* Free Radic Biol Med, 1993. **14**(4): p. 361-70.

278. Cordis, G.A., et al., *Detection of Oxidative DNA Damage to Ischemic Reperfused Rat Hearts by 8-Hydroxydeoxyguanosine Formation.* Journal of Molecular and Cellular Cardiology, 1998. **30**(10): p. 1939-1944.

279. Finkel, T. and N.J. Holbrook, *Oxidants, oxidative stress and the biology of ageing.* Nature, 2000. **408**(6809): p. 239-47.

280. Schweckendiek, W., *[Treatment of psoriasis vulgaris.].* Med Monatsschr, 1959. **13**(2): p. 103-4.

281. Altmeyer, P.J., et al., *Antipsoriatic effect of fumaric acid derivatives. Results of a multicenter double-blind study in 100 patients.* J Am Acad Dermatol, 1994. **30**(6): p. 977-81.

282. Lehmann, J.C., et al., *Dimethylfumarate induces immunosuppression via glutathione depletion and subsequent induction of heme oxygenase 1.* J Invest Dermatol, 2007. **127**(4): p. 835-45.

283. Ockenfels, H.M., et al., *The antipsoriatic agent dimethylfumarate immunomodulates T-cell cytokine secretion and inhibits cytokines of the psoriatic cytokine network.* Br J Dermatol, 1998. **139**(3): p. 390-5.

284. de Jong, R., et al., *Selective stimulation of T helper 2 cytokine responses by the anti-psoriasis agent monomethylfumarate.* Eur J Immunol, 1996. **26**(9): p. 2067-74.

285. Mrowietz, Christophers, and C. Altmeyer For The German Fumaric Acid Ester Consensus, *Treatment of severe psoriasis with fumaric acid esters: scientific background and guidelines for therapeutic use.* British Journal of Dermatology, 1999. **141**(3): p. 424-429.

286. Stoof, T.J., et al., *The antipsoriatic drug dimethylfumarate strongly suppresses chemokine production in human keratinocytes and peripheral blood mononuclear cells.* Br J Dermatol, 2001. **144**(6): p. 1114-20.

287. Horrocks, C., et al., *Adhesion molecule expression in psoriatic skin lesions and the influence of cyclosporin A.* Clin Exp Immunol, 1991. **84**(1): p. 157-62.

288. Terajima, S., et al., *An important role of tumor necrosis factor-alpha in the induction of adhesion molecules in psoriasis.* Arch Dermatol Res, 1998. **290**(5): p. 246-52.

289. Vandermeeren, M., et al., *Dimethylfumarate is an inhibitor of cytokine-induced E-selectin, VCAM-1, and ICAM-1 expression in human endothelial cells.* Biochem Biophys Res Commun, 1997. **234**(1): p. 19-23.

290. Loewe, R., et al., *Dimethylfumarate inhibits TNF-induced nuclear entry of NF-kappa B/p65 in human endothelial cells.* J Immunol, 2002. **168**(9): p. 4781-7.

291. Pahl, H.L., *Activators and target genes of Rel/NF-kappaB transcription factors.* Oncogene, 1999. **18**(49): p. 6853-66.

292. Mallery, S.R., et al., *Modulation of human microvascular endothelial cell bioenergetic status and glutathione levels during proliferative and differentiated growth.* J Cell Biochem, 1993. **53**(4): p. 360-72.

293. Engstrom, Y., et al., *Cell cycle-dependent expression of mammalian ribonucleotide reductase. Differential regulation of the two subunits.* J. Biol. Chem., 1985. **260**(16): p. 9114-9116.

294. Foster, K.A. and J.M. Collins, *The interrelation between DNA synthesis rates and DNA polymerases bound to the nuclear matrix in synchronized HeLa cells.* J. Biol. Chem., 1985. **260**(7): p. 4229-4235.

295. Holmgren, A., *Glutathione-dependent synthesis of deoxyribonucleotides. Characterization of the enzymatic mechanism of Escherichia coli glutaredoxin.* J Biol Chem, 1979. **254**(9): p. 3672-8.

296. Kopf, M., et al., *Disruption of the murine IL-4 gene blocks Th2 cytokine responses.* Nature, 1993. **362**(6417): p. 245-8.

297. Sharrow, S.O., *Flow Cytometry*, in *Current Protocols in Immunology*, J.E. Coligan, et al., Editors. 2002, John Wiley & Sons.

298. Sander, B., J. Andersson, and U. Andersson, *Assessment of cytokines by immunofluorescence and the paraformaldehyde-saponin procedure.* Immunol Rev, 1991. **119**: p. 65-93.

299. Jacob, M.C., M. Favre, and J.C. Bensa, *Membrane cell permeabilization with saponin and multiparametric analysis by flow cytometry.* Cytometry, 1991. **12**(6): p. 550-8.

300. Rabinovitch, P.S., *Practical considerations for DNA content and cell cycle analysis.* In Clinical Flow Cytometry. Principles and Applications. (K.E. Bauer, R.E. Duque, T.V. Shankey, eds.) Williams & Wilkins, Baltimore, 1993: p. 117-142.

301. Gallagher, S.R., *Quantitation of DNA and RNA with Absorption and Fluorescence Spectroscopy*, in *Protocols in Molecular Biology*, F.M. Ausubel, et al., Editors. 2004, John Wiley & Sons.

302. Voytas, D., *Agarose Gel Electrophoresis*, in *Current Protocols in Molecular Biology*, F.M. Ausubel, et al., Editors. 2001, John Wiley & Sons.

303. Taylor, C.R. and R.J. Cote, *Immunomicroscopy: A Diagnostic Tool for the Surgical Pathologist.* W.B. Saunders, Philadelphia, 1994: p. 1-70.

304. Coons, A.H. and H.J.J. Creech, R.N. , *Immunological properties of an antibody containing a fluorescent group.* Proc. Soc. Exp. Biol. Med., 1941. **47**: p. 200-202

305. Hsu, S.M., L. Raine, and H. Fanger, *The use of avidin-biotin peroxidase complex (ABC) in immunoperoxidase technique: A comparison between ABC and unlabeled antibody (PAP) procedures.* J. Histochem. Cytochem. , 1981. **29**: p. 577-580.

306. Wessel, D. and U.I. Fluegge, Anal. Biochem., 1984. **138**: p. 141-143.

307. Bradford, M.M., *A rapid and sensitive method for the quantitation of microgram quantities of protein utilizing the principle of protein dye binding.* Anal. Biochem. , 1976. **72**: p. 248-254.

308. Gallagher, S.R., *One-Dimensional SDS Gel Electrophoresis of Proteins*, in *Current Protocols in Molecular Biology*, F.M. Ausubel, et al., Editors. 2001, John Wiley & Sons.

309. Laemmli, U.K., *Cleavage of structural proteins during the assembly of the head of bacteriophage T4.* Nature, 1970. **227**: p. 680-685.

310. Maniatis, T., A. Jeffrey, and H. van deSande, *Chain length determination of small double- and single-stranded DNA molecules by polyacrylamide gel electrophoresis.* Biochemistry 1975. **14**: p. 3787-3794.

311. Gallagher, S., et al., *Immunoblotting and Immunodetection*, in *Current Protocols in Molecular Biology*, F.M. Ausubel, et al., Editors. 2004, John Wiley & Sons, Inc.

312. Staton, C.A., et al., *Current methods for assaying angiogenesis in vitro and in vivo.* International Journal of Experimental Pathology, 2004. **85**(5): p. 233-248.

313. Nehls, V. and D. Drenckhahn, *A Novel, Microcarrier-Based in Vitro Assay for Rapid and Reliable Quantification of Three-Dimensional Cell Migration and Angiogenesis.* Microvascular Research, 1995. **50**(3): p. 311-322.

314. Ribatti, D., et al., *The chick embryo chorioallantoic membrane as a model for in vivo research on angiogenesis.* Int. J. Dev. Biol., 1996. **40**: p. 1189-1197.

315. Norrby, K., *In vivo models of angiogenesis.* Journal of Cellular and Molecular Medicine, 2006. **10**(3): p. 588-612.

316. Chaudry, M.A., et al., *EpCAM an immunotherapeutic target for gastrointestinal malignancy: current experience and future challenges.* Br J Cancer, 2007. **96**(7): p. 1013-9.

317. Chu, R.S., et al., *CpG oligodeoxynucleotides act as adjuvants that switch on T helper 1 (Th1) immunity.* J Exp Med, 1997. **186**(10): p. 1623-31.

318. Lasagni, L., et al., *An Alternatively Spliced Variant of CXCR3 Mediates the Inhibition of Endothelial Cell Growth Induced by IP-10, Mig, and I-TAC, and Acts as Functional Receptor for Platelet Factor 4.* J. Exp. Med., 2003. **197**(11): p. 1537-1549.

319. Piali, L., et al., *The chemokine receptor CXCR3 mediates rapid and shear-resistant adhesion-induction of effector T lymphocytes by the chemokines IP10 and Mig.* European Journal of Immunology, 1998. **28**(3): p. 961-972.

320. Kobayashi, H., K.C. Boelte, and P.C. Lin, *Endothelial cell adhesion molecules and cancer progression.* Curr Med Chem, 2007. **14**(4): p. 377-86.

321. Luttun, A., et al., *Genetic dissection of tumor angiogenesis: are PlGF and VEGFR-1 novel anti-cancer targets?* Biochimica et Biophysica Acta (BBA) - Reviews on Cancer, 2004. **1654**(1): p. 79-94.

322. Sherr, C.J., *Growth factor-regulated G1 cyclins.* Stem Cells, 1994. **12 Suppl 1**: p. 47-55; discussion 55-7.

323. Bouchard, C., et al., *Direct induction of cyclin D2 by Myc contributes to cell cycle progression and sequestration of p27.* Embo J, 1999. **18**(19): p. 5321-33.

324. Coller, H.A., et al., *Expression analysis with oligonucleotide microarrays reveals that MYC regulates genes involved in growth, cell cycle, signaling, and adhesion.* Proc Natl Acad Sci U S A, 2000. **97**(7): p. 3260-5.

325. Adhikary, S. and M. Eilers, *Transcriptional regulation and transformation by Myc proteins.* Nat Rev Mol Cell Biol, 2005. **6**(8): p. 635-645.

326. Berner, V., et al., *IFN-[gamma] mediates CD4+ T-cell loss and impairs secondary antitumor responses after successful initial immunotherapy.* Nat Med, 2007. **13**(3): p. 354-360.

327. Krieg, A.M., *Development of TLR9 agonists for cancer therapy.* J. Clin. Invest., 2007. **117**(5): p. 1184-1194.

328. Infante-Duarte, C., et al., *Microbial Lipopeptides Induce the Production of IL-17 in Th Cells.* J Immunol, 2000. **165**(11): p. 6107-6115.

329. Held, K.D., et al., *Effect of dimethyl fumarate on the radiation sensitivity of mammalian cells in vitro.* Radiat Res, 1988. **115**(3): p. 495-502.

330. Anderson, M.E., et al., *Glutathione monoethyl ester: preparation, uptake by tissues, and conversion to glutathione.* Arch Biochem Biophys, 1985. **239**(2): p. 538-48.

331. Dufner, A. and G. Thomas, *Ribosomal S6 kinase signaling and the control of translation.* Exp Cell Res, 1999. **253**(1): p. 100-9.

332. Vinals, F., J.C. Chambard, and J. Pouyssegur, *p70 S6 kinase-mediated protein synthesis is a critical step for vascular endothelial cell proliferation.* J Biol Chem, 1999. **274**(38): p. 26776-82.

333. Koprowski, H., et al., *Colorectal carcinoma antigens detected by hybridoma antibodies.* Somatic Cell Genet, 1979. **5**(6): p. 957-71.

334. Zimmermann, S., et al., *CpG oligodeoxynucleotides trigger protective and curative Th1 responses in lethal murine leishmaniasis.* J Immunol, 1998. **160**(8): p. 3627-30.

335. Stern, B.V., B.O. Boehm, and M. Tary-Lehmann, *Vaccination with Tumor Peptide in CpG Adjuvant Protects Via IFN-{gamma}-Dependent CD4 Cell Immunity.* J Immunol, 2002. **168**(12): p. 6099-6105.

336. Heckelsmiller, K., et al., *Combined dendritic cell- and CpG oligonucleotide-based immune therapy cures large murine tumors that resist chemotherapy.* Eur J Immunol, 2002. **32**(11): p. 3235-45.

337. Weeratna, R.D., et al., *CpG DNA induces stronger immune responses with less toxicity than other adjuvants.* Vaccine, 2000. **18**(17): p. 1755-62.

338. Shen, Y. and S. Fujimoto, *A tumor-specific Th2 clone initiating tumor rejection via primed CD8+ cytotoxic T-lymphocyte activation in mice.* Cancer Res, 1996. **56**(21): p. 5005-11.

339. Mukai, S., et al., *Infiltration of Tumors by Systemically Transferred Tumor-Reactive T Lymphocytes Is Required for Antitumor Efficacy.* Cancer Res, 1999. **59**(20): p. 5245-5249.

340. Swann, J.B. and M.J. Smyth, *Immune surveillance of tumors.* J. Clin. Invest., 2007. **117**(5): p. 1137-1146.

341. Kimura, A., T. Naka, and T. Kishimoto, *IL-6-dependent and -independent pathways in the development of interleukin 17-producing T helper cells.* Proceedings of the National Academy of Sciences, 2007. **104**(29): p. 12099-12104.

342. Langowski, J.L., et al., *IL-23 promotes tumour incidence and growth.* Nature, 2006. **442**(7101): p. 461-465.

343. Ribatti, D., et al., *Mast cell contribution to angiogenesis related to tumour progression.* Clin Exp Allergy, 2004. **34**(11): p. 1660-4.

344. Ch'ng, S., et al., *Mast cells and cutaneous malignancies.* Mod Pathol, 2006. **19**(1): p. 149-59.

345. Sica, A., et al., *Targeting tumour-associated macrophages.* Expert Opinion on Therapeutic Targets, 2007. **11**(9): p. 1219-1229.

346. Mantovani, A., A. Sica, and M. Locati, *Macrophage polarization comes of age.* Immunity, 2005. **23**(4): p. 344-6.

347. Folkman, J., *Antiangiogenic gene therapy.* Proceedings of the National Academy of Sciences, 1998. **95**(16): p. 9064-9066.

348. Borgstrom, P., et al., *Complete inhibition of angiogenesis and growth of microtumors by anti-vascular endothelial growth factor neutralizing antibody: novel concepts of angiostatic therapy from intravital videomicroscopy.* Cancer Res, 1996. **56**(17): p. 4032-9.

349. Prewett, M., et al., *Antivascular endothelial growth factor receptor (fetal liver kinase 1) monoclonal antibody inhibits tumor angiogenesis and growth of several mouse and human tumors.* Cancer Res, 1999. **59**(20): p. 5209-18.

350. Strieter, R.M., et al., *CXC chemokines in angiogenesis.* Cytokine & Growth Factor Reviews, 2005. **16**(6): p. 593-609.

351. Gasperini, S., et al., *Gene expression and production of the monokine induced by IFN-gamma (MIG), IFN-inducible T cell alpha chemoattractant (I-TAC), and IFN-gamma-inducible protein-10 (IP-10) chemokines by human neutrophils.* J Immunol, 1999. **162**(8): p. 4928-37.

352. Sauty, A., et al., *The T cell-specific CXC chemokines IP-10, Mig, and I-TAC are expressed by activated human bronchial epithelial cells.* J Immunol, 1999. **162**(6): p. 3549-58.

353. Ebnet, K., M.M. Simon, and S. Shaw, *Regulation of chemokine gene expression in human endothelial cells by proinflammatory cytokines and Borrelia burgdorferi.* Ann N Y Acad Sci, 1996. **797**: p. 107-17.

354. Ruegg, C., et al., *Evidence for the involvement of endothelial cell integrin alphaVbeta3 in the disruption of the tumor vasculature induced by TNF and IFN-gamma.* Nat Med, 1998. **4**(4): p. 408-14.

355. Hernandez, G.L., et al., *Selective Inhibition of Vascular Endothelial Growth Factor-mediated Angiogenesis by Cyclosporin A: Roles of the Nuclear Factor of Activated T Cells and Cyclooxygenase 2.* J. Exp. Med., 2001. **193**(5): p. 607-620.

356. Hirata, S., et al., *Inhibition of in vitro vascular endothelial cell proliferation and in vivo neovascularization by low-dose methotrexate.* Arthritis Rheum, 1989. **32**(9): p. 1065-73.

357. Sebok, B., et al., *Antiproliferative and cytotoxic profiles of antipsoriatic fumaric acid derivatives in keratinocyte cultures.* Eur J Pharmacol, 1994. **270**(1): p. 79-87.

358. Litjens, N.H., et al., *In vitro pharmacokinetics of anti-psoriatic fumaric acid esters.* BMC Pharmacol, 2004. **4**: p. 22.

359. Nibbering, P.H., et al., *Effects of monomethylfumarate on human granulocytes.* J Invest Dermatol, 1993. **101**(1): p. 37-42.

360. Zhu, K. and U. Mrowietz, *Inhibition of Dendritic Cell Differentiation by Fumaric Acid Esters.* 2001. **116**(2): p. 203-208.

361. Nieboer, C., et al., *Systemic therapy with fumaric acid derivates: new possibilities in the treatment of psoriasis.* J Am Acad Dermatol, 1989. **20**(4): p. 601-8.

362. Muller, K., *Current status and recent developments in anthracenone antipsoriatics.* Curr Pharm Des, 2000. **6**(9): p. 901-18.

363. Donatus, I.A., Sardjoko, and N.P. Vermeulen, *Cytotoxic and cytoprotective activities of curcumin. Effects on paracetamol-induced cytotoxicity, lipid peroxidation and glutathione depletion in rat hepatocytes.* Biochem Pharmacol, 1990. **39**(12): p. 1869-75.

364. Colavitti, R., et al., *Reactive oxygen species as downstream mediators of angiogenic signaling by vascular endothelial growth factor receptor-2/KDR.* J Biol Chem, 2002. **277**(5): p. 3101-8.

365. Gonzalez-Pacheco, F.R., et al., *Mechanisms of endothelial response to oxidative aggression: protective role of autologous VEGF and induction of VEGFR2 by H2O2.* Am J Physiol Heart Circ Physiol, 2006. **291**(3): p. H1395-401.

366. van Wetering, S., et al., *Reactive oxygen species mediate Rac-induced loss of cell-cell adhesion in primary human endothelial cells.* J Cell Sci, 2002. **115**(9): p. 1837-1846.

367. Cai, T., et al., *N-acetylcysteine inhibits endothelial cell invasion and angiogenesis.* Lab Invest, 1999. **79**(9): p. 1151-9.

368. Fajardo, L.F., *The complexity of endothelial cells. A review.* Am J Clin Pathol, 1989. **92**(2): p. 241-50.

369. Beaver, J.P. and P. Waring, *A decrease in intracellular glutathione concentration precedes the onset of apoptosis in murine thymocytes.* Eur J Cell Biol, 1995. **68**(1): p. 47-54.

370. Lum, H. and K.A. Roebuck, *Oxidant stress and endothelial cell dysfunction.* Am J Physiol Cell Physiol, 2001. **280**(4): p. C719-41.

371. Sebök, B., et al., *Dimethylfumarat ist unter den Fumaderm-Inhaltsstoffen der stärkste Induktor von Apoptose-Phänomenen in lympho-histiozytären U-937-Zellen.* Z. Hautkr., 2000. **75**: p. 1-5.

372. Thio, H.B., et al., *Fumaric acid derivatives evoke a transient increase in intracellular free calcium concentration and inhibit the proliferation of human keratinocytes.* Br J Dermatol, 1994. **131**(6): p. 856-61.

373. Shaw, J.P. and I.N. Chou, *Elevation of intracellular glutathione content associated with mitogenic stimulation of quiescent fibroblasts.* J Cell Physiol, 1986. **129**(2): p. 193-8.

374. Burdon, R.H., *Superoxide and hydrogen peroxide in relation to mammalian cell proliferation.* Free Radic Biol Med, 1995. **18**(4): p. 775-94.

375. Rousseau, S., et al., *p38 MAP kinase activation by vascular endothelial growth factor mediates actin reorganization and cell migration in human endothelial cells.* Oncogene, 1997. **15**(18): p. 2169-77.

376. Seetharam, L., et al., *A unique signal transduction from FLT tyrosine kinase, a receptor for vascular endothelial growth factor VEGF.* Oncogene, 1995. **10**(1): p. 135-47.

377. Yu, Y. and J.D. Sato, *MAP kinases, phosphatidylinositol 3-kinase, and p70 S6 kinase mediate the mitogenic response of human endothelial cells to vascular endothelial growth factor.* Journal of Cellular Physiology, 1999. **178**(2): p. 235-246.

378. Hatano, N., et al., *Essential role for ERK2 mitogen-activated protein kinase in placental development.* Genes Cells, 2003. **8**(11): p. 847-56.

379. Hoefnagel, J.J., et al., *Long-term safety aspects of systemic therapy with fumaric acid esters in severe psoriasis.* Br J Dermatol, 2003. **149**(2): p. 363-9.

7 Publications

Sprung, I., **Ziegler, A.**, Flitsch, S. L. 2002. Enzymatic synthesis of β-mannosyl phosphates on solid support. *Chem. Commun.,* 2676-2677

8 List of academic teachers

Becker, Bertagnolli, Binder, Effenberger, Hashmi, Jäger, Jung, Kaim, Klein, Müller, Mundt, Rammensee, Röcken, Schleid, Schmid, Schwarz, Siegemund, Steinle, Stevanovic, Stoll, Weitkamp, Werner, Wolf, Zabel.